

**Regulation of hepatic stellate cell
phenotype and cytoglobin expression by
extracellular matrix proteins**

By

Louise Catherine Stone

A thesis submitted to
The University of Birmingham
for the degree of
DOCTOR OF PHILOSOPHY

School of Biosciences
The University of Birmingham

October 2014

UNIVERSITY OF
BIRMINGHAM

University of Birmingham Research Archive

e-theses repository

This unpublished thesis/dissertation is copyright of the author and/or third parties. The intellectual property rights of the author or third parties in respect of this work are as defined by The Copyright Designs and Patents Act 1988 or as modified by any successor legislation.

Any use made of information contained in this thesis/dissertation must be in accordance with that legislation and must be properly acknowledged. Further distribution or reproduction in any format is prohibited without the permission of the copyright holder.

Abstract

All chronic liver diseases can induce fibrosis and lead to liver cirrhosis. Within liver disease, hepatic stellate cells (HSC) are accepted as the major effectors of fibrogenesis and changes in the extracellular matrix (ECM). Cytoglobin (CYGB), a hexacoordinated globin, is upregulated in liver disease, and expression has been reported to be specific to HSCs in the liver, though this is disputed. Data presented in Chapter 3 of this thesis confirm upregulation of *Cygb* in murine models of liver disease and diseased human liver tissue. Chapter 4 shows how ECM can effect HSC morphology, behaviour and phenotype with collagen I, an important component of the hepatic scar conferring an activated HSC phenotype, and laminin, a basal protein in a normal liver, inducing a more quiescent phenotype in HSC cell lines HSC-T6 and LX-2. Chapter 5 demonstrates the novel observation of collagen I-induced downregulation, and laminin-induced upregulation, of *Cygb* in HSC-T6s. Chapter 6 explores the role of cell signalling through membrane receptors and regulation of *Cygb* expression, identifying phosphorylated focal adhesion kinase as a mechanism of signal transduction through integrin activation. These findings suggest that *Cygb* expression is modulated by 'outside-in signalling' and this is important in the activation status of HSCs.

Acknowledgements

I would like to thank Nik Hodges for supporting and guiding me throughout this process. I would also like to thank Mark Graham and Kevin Chipman for their advice, and Chris Weston for his assistance, with many aspects of this project. I would also like to express my gratitude to the BBSRC and Astra Zeneca for providing funding for the research and also to attend conferences, which has allowed me to develop my skills.

The advice and support of the many members of the 4th floor has been invaluable, and special thanks must go to Nadine Taylor, Leda Mirbahai, Lorna Thorne, Bob Harris, Nicola Cumley, Rachael Kershaw, Chibuzor Uchea, Fiona McRonald, Tim Williams and Shrikant Jondhale.

My family have been of great help over the last four years, my parents, Julie and Nigel Stone my sister Helen Stone and my fiancé Marc Lloyd providing love, support and a shoulder to cry on, as well as pride in my achievements.

My Ph.D. would not have been possible without these people, and I thank them for helping me through it.

Table of Contents

Chapter 1

Introduction	1
1.1 Cytoglobin	2
1.1.1 Discovery	2
1.1.2 The globin family	3
1.1.2.1 Evolutionary history of CYGB	5
1.1.2.2 CYGB in comparison with other globins	5
1.1.3 The structure of CYGB	6
1.1.4 Genetics of <i>Cygb</i>	12
1.1.4.1 Regulation of <i>Cygb</i> expression	13
1.1.5 Localisation of CYGB	15
1.1.6 Putative functions of CYGB	17
1.1.6.1 CYGB and O ₂	17
1.1.6.2 CYGB, reactive oxygen species and reactive nitrogen species	19
1.1.6.3 CYGB in hypoxia	21
1.1.6.4 Enzymatic activity of CYGB	23
1.1.7 CYGB and collagen I synthesis	23
1.1.8 CYGB in disease	25
1.1.8.1 CYGB in cancer	25

1.1.8.2 CYGB in fibrosis	27
1.2 Hepatic Stellate Cells	29
1.2.1 HSC function.....	30
1.2.1.1 HSCs in a normal liver	30
1.2.1.2 Function on liver injury	31
1.2.1.3 Senescence of HSCs	33
1.2.1.4 Transcription factors involved in the regulation of HSC activation and quiescence in the context of <i>Cygb</i> regulatory elements.....	37
1.2.2 Liver fibrosis	41
1.2.3 Changes in ECM	42
1.2.4 The reversibility of liver fibrosis.....	43
1.3 Liver disease.....	44
1.3.1 Overview of liver disease	45
1.3.2 Types of liver disease	45
1.4 Hypothesis, Aims and Objectives.....	51
1.4.1 Hypothesis	51
1.4.2 Aims and Objectives.....	51
Chapter 2	
Materials and Methods	52
2.1 Chemicals and consumables	53

2.2 Cell lines	53
2.2.1 HSC-T6 cell line.....	53
2.2.2 LX-2 cell line	54
2.2.3 Primary rat HSCs	55
2.3 Continual Cell Culture	55
2.3.1 Cell Cryopreservation.....	56
2.4 Culture on different ECM proteins	56
2.4.1 Collagen coating procedure	57
2.4.2 Laminin coating procedure	58
2.4.3 Mixed matrix effects on HSC-T6 cells	58
2.5 Cell imaging using Light Microscopy.....	58
2.6 Retinoic Acid uptake on different culture surfaces	59
2.7 Ribonucleic acid Isolation	59
2.8 Complementary DNA synthesis	60
2.9 Quantitative RT-PCR.....	61
2.10 Proliferation Assay	61
2.10.1 HSC-T6 manual count time-course	61
2.10.2 Cell IQ analysis for HSC-T6 cells and LX-2 cells	62
2.11 Whole Cell Protein Isolation	64
2.11.1 Buffers.....	64

2.11.2 Procedure.....	64
2.11.3 Bradford assay for protein quantification	65
2.12 Western Blot for Cygb and Phosphorylated FAK.....	65
2.12.1 Buffers.....	65
2.12.2 Gels	65
2.12.3 Assay procedure	66
2.13 Exploration if the effects of collagen I	67
2.14 pFAK expression and pFAK Inhibition Assays	68
2. 14.1 4 3-(4,5-Dimethyl-2-thiazolyl)-2,5-diphenyl-2H-tetrazolium bromide (MTT) reduction assay	68
2.14.2 Assay procedure	68
2.14.3 Flow cytometry for pFAK and FAKI	69
2.14.4 Confocal microscopy for pFAK and FAKI.....	70
2.15 Intracellular ROS assay with 2',7'-dichlorodihydrofluorescein diacetate (H ₂ DCF- DA)	71
2.16 RNA inhibition (RNAi) of FAK	71
2.16.1 Optimisation of RNAi	71
2.16.2 Optimised RNAi.....	72
2.17 <i>In vivo</i> mouse models of liver disease	73
2.17.1 CCl ₄ -induced liver fibrosis in murine models.....	73

2.17.2 Murine models of steatohepatitis	74
2.18 Protein and RNA extraction from liver tissue	74
2.19 Human tissue section staining	76
2.20 Statistical Analysis.....	77

Chapter 3

Cygb expression in liver disease	78
3.1 Introduction	79
3.2 Results.....	79
3.2.1 <i>Cygb</i> RNA expression in murine models of liver disease.....	79
3.2.2 CYGB expression in different disease pathologies in human liver	80
3.3 Discussion.....	85

Chapter 4

Effect ECM on HSC phenotype	87
4.1 Introduction	88
4.2 Results.....	89
4.2.1 Different ECM proteins affect the morphology and proliferation of HSC-T6 cells.....	89
4.2.1.1 Culture on mixed collagen I and laminin matrices alters the observed morphology in HSC-T6 cells	89
4.2.2 Proliferation of HSC-T6 cells is affected by ECM	92
4.2.2.1 Endpoint cell counts of HSC-T6 after 48 hrs of culture	92
4.2.2.2 Cell-IQ analysis of HSC-T6 proliferation.....	94

4.2.3 The morphology of human LX-2 cells and rat primary HSC is not affected ECM	95
4.2.4 Different ECM proteins do not significantly affect the proliferation of LX-2 cells at passage end point, but proliferation is affected by laminin over a passage.....	96
4.2.4.1 End point cell counts of LX-2s after 48 hrs of culture	96
4.2.4.2 Cell-IQ analysis of LX-2 proliferation.	102
4.2.5 Culture on laminin increases All trans Retinoic Acid (ATRA) uptake in HSC-T6 cells and LX-2 cells	104
4.3 Discussion.....	106

Chapter 5

Regulation of <i>Cygb</i> by ECM.....	111
5.1 Introduction	112
5.2 Results.....	112
5.2.1 ECM proteins affect the expression of <i>Cygb</i> and α SMA.....	112
5.2.2 Time dependant expression of <i>Cygb</i> on collagen I.....	114
5.2.3 Surface coated collagen is required for regulation of <i>Cygb</i>	119
5.2.4 Intracellular ROS in HSC-T6s cultured on collagen I, laminin and non-coated plastic.....	121
5.3 Discussion.....	123

Chapter 6

Signalling between ECM and <i>Cygb</i>	128
6.1 Introduction	129

6.1.1 The structure of integrins	130
6.1.2 Integrins, focal adhesions and focal adhesion kinase (FAK)	130
6.1.3 Integrins associated with HSC.....	134
6.2 Results.....	136
6.2.1 Cell Surface ECM protein receptors are differently expressed in HSC-T6 cells cultured on different ECM proteins.....	136
6.2.2 ECM affects FAK phosphorylation in HSC-T6s	137
6.2.3 RNAi of <i>FAK</i> was unsuccessful and had no effect on <i>Cygb</i> expression in HSC-T6 cells.	141
6.2.4 Inhibition of FAK with FAK Inhibitor 14	141
6.2.5 The effect of FAKI on <i>Cygb</i> expression is inconclusive	147
6.3 Discussion.....	149
Chapter 7	154
General Discussion	154
7.1 General Discussion.....	155
7.2 Future work.....	163
Chapter 8	166
References	166
Appendices	179

List of Figures

Chapter 1

Figure 1.1: An example of an eight helices globin fold and a porphyrin ring.....4

Figure 1.2: Illustration of the distal and proximal regions of the CYGB haem binding site.....9

Figure 1.3: The crystal protein structure of homodimer of CYGB.....10

Figure 1.4: Changes in the sinusoid and Space of Disse on liver injury and development of fibrosis.....35

Figure 1.5: The process of HSC activation through initiation, perpetuation and possible resolution.....36

Figure 1.6: Transcription factors important in hepatic stellate cell (HSC) activation that are also important in the context of regulatory elements present in the promoter region of cytoglobin (Cyg b).....40

Chapter 3

Figure 3.1: Fold change in *Cygb* gene expression by RT-PCR analysis of RNA extractions from whole mouse liver from models of liver disease.....82

Figure 3.2: Investigation of *CYGB* expression in human liver diseases.....83

Figure 3.3: Immunohistochemistry analysis of frozen liver sections with CYGB antibody 1:200.....84

Chapter 4

Figure 4.1: HSC-T6 cell morphology on different ECM proteins.....	90
Figure 4.2: Images of HSC-T6 cells cultured on mixed matrix surfaces of collagen I and laminin in differing concentrations.....	91
Figure 4.3: Mean (+/- SEM) number of HSC-T6 cells on different ECM proteins.....	93
Figure 4.4: Affect of ECM on cell number per T25 across a passage.....	97
Figure 4.5: Estimated cell number per well across 70 hrs for HSCs cultured on non-coated plastic, collagen I and laminin.....	98
Figure 4.6: LX-2 cell morphology on different ECM proteins.....	99
Figure 4.7: Primary rat HSC cell morphology on different ECM proteins.....	100
Figure 4.8 Mean number (+/- SEM) of LX-2 cells seeded at 300,000 cells/ml on different ECM proteins.....	101
Figure 4.9: Estimated cell number per well across 45 hrs for HSCs cultured on non-coated plastic, collagen I and laminin.....	103
Figure 4.10: A-F) Confocal images of HSC-T6 cells seeded at 100,000 cells/ml on Glass, collagen I and laminin coverslips 48hrs post seeding, looking at retinoid auto-fluorescence.....	105

Chapter 5

Figure 5.1: Mean (+/- SEM) expression of <i>Cygb</i> and α <i>SMA</i> in HSC-T6 cells cultured on different ECM proteins analysed by RT-qPCR calibrated to expression on non-coated flasks.....	115
Figure 5.2: Expression <i>Cygb</i> of in HSC-T6 cells cultured on laminin, collagen I and non-coated plastic analysed by western blot.....	116
Figure 5.3: Mean expression (+/- SEM) expression of <i>CYGB</i> in LX-2 cells cultured on collagen I and laminin proteins analysed by RT-qPCR calibrated to expression on non-coated flasks.....	117

Figure 5.4: Mean (+/- SEM) expression of *Cygb* across a passage (48hr) on non-coated and collagen I coated flasks relative to 0hr time point on a confluent non-coated plastic.....118

Figure 5.5: Mean (+/- SEM) expression of *Cygb* in HSC-T6 in the presence of collagen I 48 hrs after seeding.....120

Figure 5.6: Mean (+/- SEM) relative levels of intracellular ROS in HSC-T6 cells cultured on non-coated plastic, collagen I laminin.....122

Chapter 6

Figure 6.1: A simplified schematic of the structure of an integrin heterodimer showing the transmembrane region and the α and β subunits.....132

Figure 6.2: A simplified schematic of integrin clustering, focal adhesion formation and FAK autophosphorylation leading to downstream signalling.....133

Figure 6.3: RT-PCR expression of A) $\alpha 2$ N=5 and B) $\beta 4$ integrin subunit ECM receptors across laminin, collagen I and gelatin ECM proteins in HSC-T6 cells relative to the expression levels of those grown on non-coated T25 culture flasks.....138

Figure 6.4: Expression data for $\alpha 5$ integrin subunit ECM receptor across laminin, collagen I and gelatin ECM proteins in HSC-T6 cells relative to the expression levels of those grown on non-coated T25 culture flasks.....139

Figure 6.5: pFAK expression in HSC-T6 cells cultured on non-coated plastic and collagen I.....140

Figure 6.6: FAK expression after RNAi treatment with *PKt2* (*FAK*) in HSC-T6 cells.....143

Figure 6.7: *Cygb* expression after RNAi treatment with *PKt2* (*FAK*) in HSC-T6 cells.....144

Figure 6.8: Results of MTT viability assay for HSC-T6 treated for 48hrs with FAKI.....145

Figure 6.9: Results of pFAK inhibition in HSC-T6 cells.....146

Figure 6.10: The effect of pFAK inhibition on *Cygb* expression in HSC-T6s.....148

Chapter 7

Figure 7.1: Signalling pathways from focal adhesion kinase (FAK) phosphorylation (P) to transcription factors known to have binding motifs present in the cytoglobin promoter region.....160

Figure 7.2: Simplified signalling pathways.....161

Figure 7.3: Possible signalling pathway between ECM and *Cygb* expression through integrin activation.....162

List of Tables

Chapter 1

Table 1.1: Diseases of the liver.....47

Chapter 2

Table 2.1: Details Of TaqMan Style Primer-Probes used in this Study.....63

Chapter 6

Table 6.1: Integrin subunits associated with HSCs.....134

List of Abbreviations

4-HNE	4-hydroxy-2-nonenal
Ab	Antibody
AKT	RAC-alpha serine/threonine-protein kinase
ALD	Alcoholic Liver Disease
ANOVA	Analysis of variance
AP	Activator protein
APS	Ammonium persulphate
ASH	Alcoholic Steatohepatitis
ATRA	All <i>trans</i> Retinoic Acid
BDL	Bile duct ligation
bp	Base pair
C/EBP	CCAAT-enhancer-binding protein
CC	Collagen I coated
CCl ₄	Carbon tetrachloride
cDNA	Complimentary deoxyribonucleic acid
c-Ets-1	Cellular erythroblastosis virus E26 oncogene homolog 1
cm	Centimetre
CO	Carbon monoxide
CYGB/Cygb	Cytoglobin
CYP2E1	Cytochrome P450 2E1
Cys	Cysteine
DDR	Discoidin Domain Receptor
DEN	N,N-diethylnitrosamine
DMEM	Dulbeco's modified eagles medium
DMSO	Dimethyl sulphoxide
DNA	Deoxyribonucleic acid
dNTP	deoxynucleotide triphosphates
DPX	Distrene 80 Plasticizer and Xylene

ECL	Enhanced Chemiluminescence
ECM	Extracellular matrix
EGF	Epidermal growth factor
EHS	Engelbreth-Holm-Swarm
EPO	Erythropoietin
ERK	Extracellular signal-regulated kinase 1
Ets1	E26 transformation-specific transcription factor
FAKI	FAK Inhibitor 14
FBS	Foetal Bovine Serum
Fe	Iron
FITC	Fluorescein isothiocyanate
FOS B	FBJ murine osteosarcoma viral oncogene homolog B
Fra	Fos-related antigen
H2DCF-DA	2',7'-dichlorodihydrofluorescein diacetate
H ₂ O ₂	Hydrogen peroxide
HAV	Hepatitis A
Hb	Haemoglobin
HBV	Hepatitis B
HCl	Hydrochloric acid
HCV	Hepatitis C
HDV	Hepatitis D
HEV	Hepatitis E
HFE	High Iron
HIF1	Hypoxia inducible factor 1
HIPBS	Hypoxia inducible protein binding site
His	Histidine
HK1	Hexokinase 1
hr	Hour
HRE	Hypoxia regulatory elements
HSC	Hepatic Stellate Cells

hxHb	Hexacoordinate haemoglobin
iHSCs	Inactivated HSCs
IKB	NF-kappa-B inhibitor
IKK α	Inhibitor of nuclear factor kappa-B kinase alpha
kDa	Kilodaltons
MALLS	Multi-Angle Laser Light Scattering
Mb	Myoglobin
MCD	Methionine choline deficient diet
MDA	Malondialdehyde
MEM	Modified eagles medium
ml	Microlitre
mM	Millimolar
MMP	Matrix metalloproteinase
mRNA	Messenger ribonucleic acid
MTT	3-(4,5-Dimethyl-2-thiazolyl)-2,5-diphenyl-2H-tetrazolium bromide
NaCl	Sodium Chloride
NAFLD	Non-Alcoholic Fatty Liver Disease
NASH	Non-Alcoholic Steatohepatitis
NC	Normal chow
NC	Non-coated
NF-1	Nuclear factor 1
NFAT	Nuclear factor of activated T-cells
NF κ B	Nuclear factor kappa-light-chain-enhancer of activated B cells
Ngb	Neuroglobin
nm	nanometre
NO	Nitric oxide
NT	Non-targeting
O ₂	Oxygen
PAGE	Polyacrylamide gel electrophoresis
PBC	Primary Biliary Cirrhosis

PBS	Phosphate buffered saline
PDGF	Platelet derived growth factor
PDK	Pyruvate dehydrogenase kinase
pFAK	Phosphorylated Focal Adhesion Kinase
Phe	Phenylalanine
PIP	Phosphatidylinositol 4-phosphate
PPAR- γ	Proliferator-activated receptor gamma
PSC	Primary Sclerosing Cholangitis
Ptk2	Focal Adhesion Kinase
PVDF	Polyvinylidene difluoride
pY397	Phosphorylated tyrosine 397
RA	Retinoic acid
RAC	Ras-related C3 botulinum toxin substrate
RNA	Ribonucleic acid
RNAi	Ribonucleic acid inhibition
RNS	Reactive nitrogen species
ROS	Reactive oxygen species
RT-PCR	Real-time polymerase chain reaction
SDS	Sodium dodecyl sulfate
SEM	Standard error of the mean
siRNA	Short-interfering ribonucleic acid
Sp1	Stimulatory protein 1
STAP	Stellate cell activation protein
STAT	Signal transducer and activator of transcription
TBS	Tris-buffered Saline
TEMED	N,N,N,N-tetramethylethylenediamine
TGF β 1	Transforming growth factor beta
TIMP	Tissue inhibitors of metalloproteinase
TOC	Tylosis with oesophageal cancer
WLM	Western lifestyle model of liver disease

$\alpha 11$	Integrin alpha 11
$\alpha 2$	Integrin alpha 2
$\alpha 5$	Integrin alpha 5
$\alpha 6$	Integrin alpha 6
α SMA	Alpha smooth muscle actin
$\beta 1$	Integrin Beta 1
$\beta 3$	Integrin Beta 3
$\beta 4$	Integrin Beta 4

Chapter 1

Introduction

1.1 Cytoglobin

1.1.1 Discovery

Cytoglobin (Cygb) was discovered in a proteomic screen as a protein that was upregulated on *in vivo* activation of Hepatic Stellate Cells (HSCs), achieved by carbon tetrachloride (CCl₄) injection (Kristensen *et al.*, 2000). HSCs, hepatocytes, endothelial cells and kupffer cells were isolated from normal and fibrotic rat livers and subjected to proteomic analysis, which identified 17 novel, upregulated proteins between quiescent and activated HSCs. Further analysis by Kawada *et al.* (2001), investigating HSCs activated *in vitro* and *in vivo*, showed that one protein spot, previously identified by Kristensen *et al.*, was notably upregulated both *in vitro* and *in vivo* on HSC activation. The DNA sequence of this protein was used as a probe, and a screen of an activated HSC complimentary DNA (cDNA) library of rat origin was conducted. A 2028bp (base pair) cDNA clone was found, with an open reading frame of 570bp coding for 190 amino acids with a molecular weight of 21,496daltons. The amino acid sequence showed between 30% to 40% homology with myoglobin and there was evidence of cytoplasmic location according to Reinhardt's criterion (Reinhardt and Hubbard, 1998, Kawada *et al.*, 2001). This novel protein was named stellate cell activation protein or 'STAP', as it was discovered to be time independently induced when HSC were activated *in vitro* and *in vivo*. Homologues to rat STAP cDNA in human and mouse cDNA libraries were identified, sharing 94% and 97% amino acid sequence identity to rat STAP respectively. Human and rat STAP were found to contain two histidine residues at positions 81 and 113 from the N-terminus and it was suggested these residues could be involved in haem binding sites. Analysis revealed that the human STAP gene comprised four exons on chromosome 17q and that its mRNA is expressed in the normal adult brain, heart, kidney, lung, trachea, liver and

placenta. In culture HSCs and HepG2 (a human hepatocellular carcinoma cell line) cells express human STAP mRNA and STAP positive cells have occasionally observed around bile ducts (Kawada and Le, 2011). STAP was renamed cytoglobin (CYGB) by Burmester *et al.*(2002) after several reports showed ubiquitous expression in human tissue and in a wide range murine tissue and organs, Trent and Hargrove (2002) named CYGB 'Histoglobin' as it is expressed in a wide range of tissues, however CYGB has become the recognised nomenclature for this globin in the scientific literature.

1.1.2 The globin family

Proteins containing a haem group are generally referred to as globins, and globins in general bind gaseous diatomic ligands using an iron containing porphyrin ring. Globins have been identified in archea, bacteria, protists, plants, fungi and animals (Hardison, 1996, Hardison, 1998). There are four main types of vertebrate globin, which have different tissue distribution and function, haemoglobin (HB), myoglobin (MB), neuroglobin (NGB) and CYGB (Schmidt *et al.*, 2004), but it has recently been reported that the vertebrate globin family contains at least eight constituents, all with distinct features (Shivapurkar *et al.*, 2008). Globin proteins are characterised by a fold of six to eight α helices (Figure 1.1 A) and a haem group comprised of Fe^{2+} -protoporphyrin IX (Figure 1.1 B)(Murzin *et al.*, 1995) and the globin fold is highly evolutionarily conserved (Bashford *et al.*, 1987). The structure of the globin fold seen in CYGB is indistinguishable from the globin folds of Hb and Mb, despite their low overall amino acid sequence identities (Makino *et al.*, 2011).

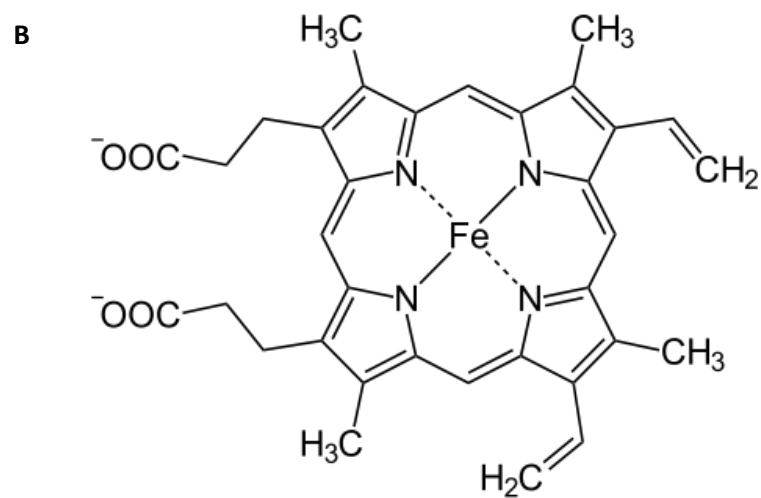
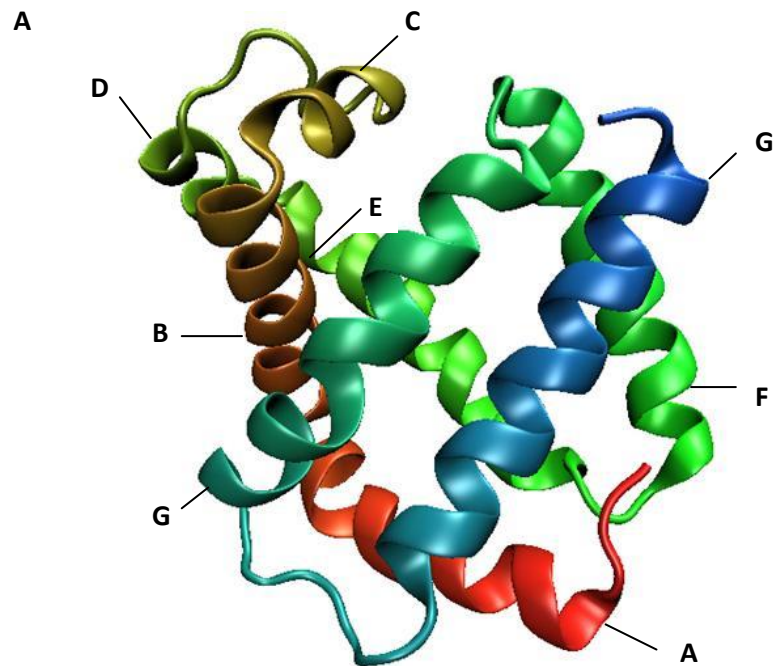


Figure 1.1: A): An example of an eight helices globin fold showing helices A-H, image available under the Creative Commons Attribution-Share Alike license 3.0 <http://creativecommons.org/licenses/by-sa/3.0/deed.en>, attribution : [Opabinia regalis](#), source: Wikicommons. **B)** A representation of Fe^{2+} protoporphyrin IX haem group. Image in public domain, source: Wikicommons.

1.1.2.1 Evolutionary history of CYGB

Much debate and discussion exists around the evolution of CYGB, it has been found in all vertebrates studied so far, and some reports suggest that it is an ancestral globin (Pesce *et al.*, 2002, Shivapurkar *et al.*, 2008), indicating a primitive and vital function (Fago *et al.*, 2004). There are many reports analysing the evolution of CYGB and new data are frequently being published; however, currently there is no consensus on CYGB's phylogenetic relationship with other globins within the vertebrate phylogenetic tree (Goodman *et al.*, 1987, Benton, 1990, Burmester *et al.*, 2002, Pesca *et al.*, 2002, Hankeln *et al.*, 2005, Shivapurkar *et al.*, 2008).

1.1.2.2 CYGB in comparison with other globins

Globins are typically thought of as respiratory proteins involved in respiratory chain metabolism, but they can also have enzymatic functions and undergo redox reactions (for example Hb undergoes redox reactions forming ferric $[\text{Fe}^{+3}]$ and ferryl $[\text{Fe}^{+4}]$ Hb) they are also involved in and oxygen transport (Dickerson and Geis, 1983, Bunn and Forget, 1986, Brunori, 1999, Minning *et al.*, 1999, Merx *et al.*, 2001). CYGB shares common sequence structures with the other human globins; such as the invariant proximal His^{F8} and Phe^{CD1}, and the distal His^{E7}, and is most closely related to Mb amongst the human globins, with similar haem pocket amino acid sequence and O₂ and CO affinities —the association of ligands in CYGB is faster than MB, but ligand dissociation slower, and therefore the overall equilibrium constants for O₂ and CO in MB and CYGB are similar. Spectroscopic analysis of reduced deoxygenated CYGB

distinguishes it from MB though. Ligand association rates for CYGB are slower than that of NGB for both oxygen and histidine (Makino *et al.*, 2011).

1.1.3 The structure of CYGB

The mammalian CYGB protein is longer than mammalian HB, MB and NGB at 190 amino acids, compared with the 140 – 160 amino acids, which is typical of the other human globins — MB and HB are approximately 150 amino acids long. CYGB is 190 amino acids due to the unusually long N- and C- termini. These termini extensions change the hydrodynamic properties of CYGB compared with other globins by increasing its hydrodynamic diameter to that of a dimer whilst retaining the mass of a monomer, they also contribute to interactions with neighbouring molecules of the protein crystal of CYGB (Makino *et al.*, 2006, Lechauve *et al.*, 2010). Similar extensions at the N- and C- termini have been observed in some invertebrate globins like *Caenorhabditis elegans* (Neuwald *et al.*, 1997) but their functional relevance is not known. The N- terminus extension in murine and human CYGB might have been caused by a direct duplication of 21 nucleotides at the 5' end of the coding region and the C- terminus extension could be due to the recruitment of an additional exon. Many globins, including vertebrate HB, MB and NGB contain the B12-2 (meaning, helix B, 12th amino acid, between codon positions 2 and 3) and G7-0 introns present in CYGB, and are considered to be ancient in phylogenetic terms (Dixon and Pohajdak, 1992, Burmester *et al.*, 2000). The identification of the most 3' intron of the murine and human CYGB at the C- terminal position HC11-2 had not been seen in previous globin

structures, and the function of the 10 amino acid long exon sequence at the 3' end, which is not present in chicken and fish, is uncertain, however, it has speculated that the C- and N- termini extensions may be involved in lipid binding (Burmester *et al.*, 2002, Burmester, 2004 #26, Reeder, 2011 #25). Between amino acid residues 18 to 71, which form the core of its structure, CYGB displays the 3-over-3 α helical sandwich common in other globins, the protoporphyrin IX prosthetic group is coordinated to the polypeptide chain by His 113 and His 81, proximally and distally, and sits between the E and F α helices (de Sanctis *et al.*, 2004).

Recombinant CYGB is a hexacoordinate haemoglobin (hxHb) in the deoxy form (Kawada *et al.*, 2001, Asahina *et al.*, 2002, Trent and Hargrove, 2002), and hxHbs have been discovered in animals, protists, cyanobacteria and plants (Arredondo-Peter *et al.*, 1998, Burmester *et al.*, 2000, Scott and Lecomte, 2000, Awenius *et al.*, 2001, Hvitved *et al.*, 2001). Hexacoordinate haemoglobins potentially differ in physiological function from pentacoordinate haemoglobins like Hb and Mb, and use a different ligand binding mechanism which involves reversible intramolecular coordination of the haem iron, contrary to the previous belief that an open binding site is required for reversible ligand binding. hxHbs reversibly bind Oxygen (O_2) as well as other haem ligands with relatively high affinities despite the apparent impediment (Hargrove, 2000).

One of the two histidine side chains, which coordinate hxHb haem groups, is able to reversibly dissociate and, therefore, exogenous ligands can bind stably. The binding time, speed of association/dissociation of the coordinating histidine from the haem iron, and the equilibrium fraction of protein in the hexacoordinate state are influenced

by the distal histidine coordination (Hamdane *et al.*, 2003, Smagghe *et al.*, 2008). The affinity constant for histidine coordination is directly related to the effect of hexacoordination on equilibrium constants in h_xHb binding (Trent *et al.*, 2001, Trent and Hargrove, 2002).

In the haem pocket of CYGB, His113 (F8) and His81 (E7) bind to the iron atom as fifth and sixth axial ligands respectively, before ligand binding in CYGB there needs to be dissociation of His81 and the binding of CO seems to be competitive with His81. CYGB has been shown to be able to form an intraprotein disulfide bridge, which affects the position of the E-helix, therefore modifies affinity for the distal histidine. O₂ affinity is dependent on histidine binding, so disulfide bond formation affects O₂ binding affinity. In CYGB the Cys E9 and His E7 are on opposite sides of the E-helix and the formation of a disulfide bond between Cys83(E9) and Cys38(B2) bond theoretically directly pulls on His E7, causing a conformational change and affect the molecular dynamics, influencing ligand binding (Lechauve *et al.*, 2010). Recent research by Astudillo *et al.* (2013) has indicated that this disulfide bond between the B and E helices does indeed adjust the conformational dynamics of CYGB. The helices' conformation alters depending on the oxidation state of the Cys 38 and Cys 83 side chains, and disulfide bridge formation changes the migration pathway of ligands. Figure 1.2 shows the shift from hexacoordinate to pentacoordinate form in the haem pocket of CYGB.

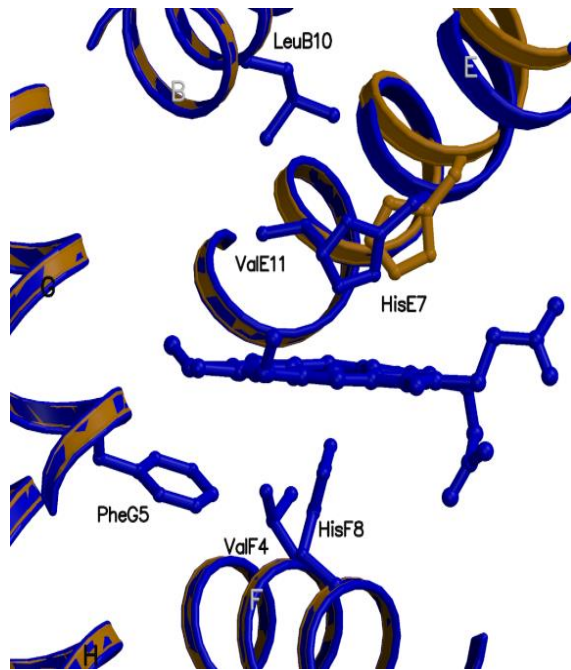


Figure 1.2: Illustration of the distal and proximal regions of the CYGB haem binding site, overlaying the closed hexacoordinated form (blue haem and ribbons), and the open pentacoordinated form (ochre colour). From de Sanctis *et al.*(2004) with permission from Elsevier (license number 3527240919479).

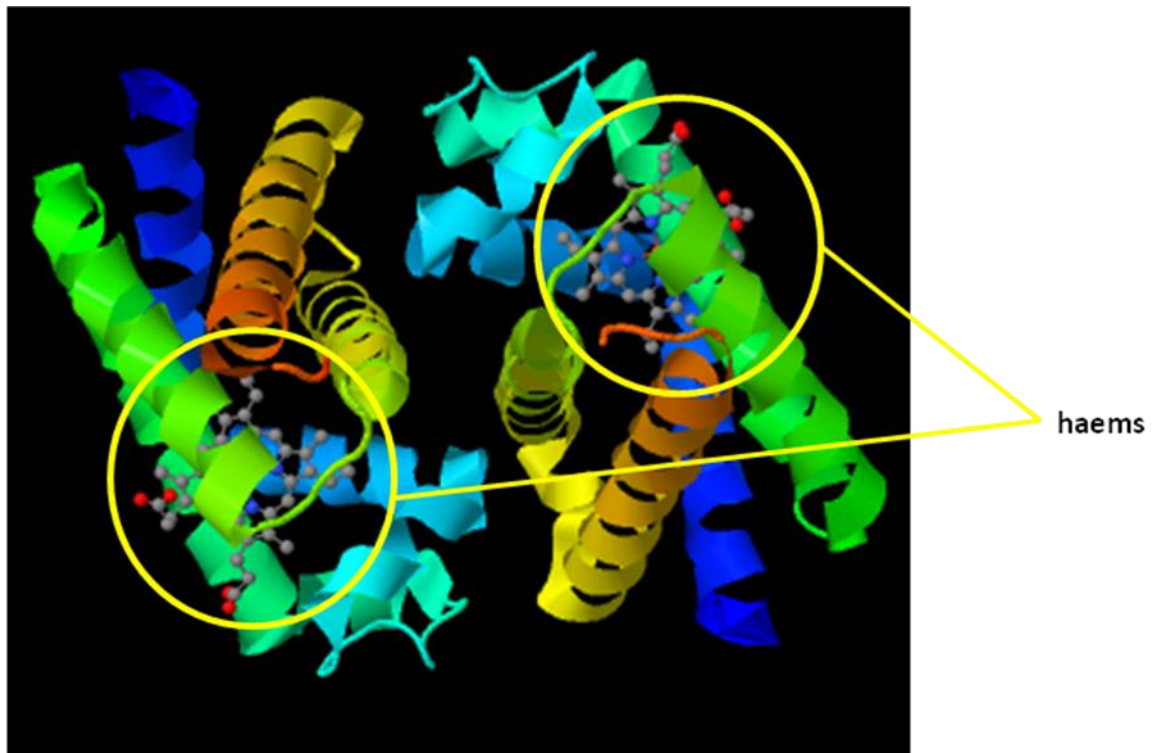


Figure 1.3: The crystal protein structure of homodimer of CYGB modified from <http://www.rcsb.org/pdb> access number 1UMO (de Sanctis et al., 2004).*J.Mol.Biol.* **336**: 917-927).

There is some debate over the conformation of CYGB, chromatographic analysis of purified-recombinant CYGB has suggested it exists in a dimeric form (as is depicted in Figure 1.3), which is stable and not based on disulfide bonds; however, when the central globular fragment is eluted on its own, it appears to be monomeric. CYGB is monomeric in solution as measured by Multi-Angle Laser Light Scattering (MALLS) in the concentration range expected *in vivo* with possibility of an intramolecular disulfide bridge, which affects helices conformation, and therefore could affect function, as described above (Lechauve *et al.*, 2010). Cysteine residues might be involved in the formation of intramolecular disulfide bonds, but early evidence suggested that truncated CYGB is monomeric (Hamdane *et al.*, 2003). A CYGB dimer could be formed via one or two intermolecular disulphide bonds between two monomers, but only a small fraction of CYGB formed dimers observed in mass spectrometry (Lechauve *et al.*, 2010, Cabrita *et al.*, 2011) . CYGB could possibly have haem-haem interactions, having Hill coefficients for co-operative binding of 0.63-1.63, which could be evidence for dimer formation (Fago *et al.*, 2004). Most recently, Tsujino *et al.*(2014) have shown that CYGB exist in three different forms – monomeric, dimeric and tetrameric – and these three forms have different binding affinities for cyanide, and also CO in the when in the ferrous form.

Reeder *et al.* (2011) observed that the optical spectrum for CYGB showed the haem iron in a low spin state - HisF8-Fe³⁺ –HisE7 coordination, and when the lipid oleate bound to ferric CYGB. The optical spectrum changed to a high spin state, and conformation of the haem changed from hexacoordinate to one consistent with a pentacoordinate haem like MB or HB - with water in the 6th coordinate, the same

phenomenon was observed with the lipid cardiolipin, but not with ferrous CYGB. Removing the intermolecular disulfide bridge appears to weaken the hexacoordination of CYGB, therefore, if CYGB exists in dimeric form, binding to one subunit of a CYGB dimer may influence the dissociation of the distal histidine from the iron of the other subunit, and have an effect on ligand binding. This could be important in the function of CYGB. Also this conformational change on binding with a lipid molecule in CYGB does not occur with other hexacoordinate haemoglobins like NGB, and may be a unique property of CYGB related to its function, such as the observed peroxidase activity discussed in 1.1.6.4.

1.1.4 Genetics of *Cygb*

In mammals *CYGB* is a single copy gene (Burmester *et al.*, 2002) and its evolution appears to be complex with many subfunctionalisation events (Burmester *et al.*, 2004). In humans it is mapped at the 17q25.3 chromosomal segment, where as in mice and rats it is on conserved syntenic segments (in the same chromosomal location) on chromosome MMU11E2 in mice and RNO10q32.2 in rats (Wystub *et al.*, 2004). It has been suggested that *CYGB* and *MB* might have originated from an ancient chromosome duplication event, as the chromosome regions representing *CYGB* (17q25) and *MB* (22q12) have long paralogous stretches of genomic DNA (McLysaght *et al.*, 2002), though if *cygb* is present in sea lampreys, as has been suggested, it diverged from the clade before *mb* (Shivapurkar *et al.*, 2008), making it unlikely that *cygb* and *mb* arose from a duplication event. *CYGB* consists of three introns, two of

which are in conserved regions: B12-2 and G7-0, typical of all globin molecules. HxHbs like *CYGB* also possess a third intron, which is positioned at H36-2 (Burmester *et al.*, 2002, Trent and Hargrove, 2002, Burmester *et al.*, 2004).

Mouse and human *Cygb* have 92.8% nucleotide sequence identity and 95.3% amino acid sequence identity in the coding region, whereas only 49% amino acid identity is shared between mammalian and zebra fish *Cygbs* (Burmester *et al.*, 2002). *Cygbs* show a high degree of amino acid sequence similarity to Hbs of Agnatha; between 26% and 33%. The high degree of conservation indicates a vital structural function for *Cygb*, and an amino acid substitution rate of approximately 0.3×10^{-9} replacements per site per year for *Cygb*, based on the assumed divergence of mice and humans 80MYA (Kimura, 1987), supports this theory. This substitution rate is substantially lower than those calculated for haemoglobins ($0.9-1.2 \times 10^{-9}$) and myoglobins ($0.8-1.2 \times 10^{-9}$) but is similar to the estimated substitution rate of Ngbs (0.4×10^{-9}) (Burmester *et al.*, 2002, Trent and Hargrove, 2002).

1.1.4.1 Regulation of *CYGB* expression

It has been reported that *CYGB*'s promoter region contains several transcription start points, a CpG island 1.4 kb in length, multiple CG boxes and Sp1 (stimulatory protein 1) binding sites, which might be recognised by transcription factors including Sp1, NFκB (nuclear factor kappa-light-chain-enhancer of activated B cells), Kruppel-like zinc finger proteins, and motifs which are recognised by AP (activator protein) -1, AP-2, C/EBP

(CCAAT-enhancer-binding protein) and NF-1 (nuclear factor 1) – which are conserved in position and sequence in humans and mice, also two human, rat and mouse conserved hypoxia regulatory elements (HREs), two HIF1 (hypoxia inducible factor 1) binding sites and EPO (erythropoietin) box motifs, a c-Ets-1 (cellular erythroblastosis virus E26 oncogene homolog 1) binding site, a site recognised by NFAT (Nuclear factor of activated T-cells) and a conserved HIPBS (hypoxia inducible protein binding site) are present, notably, the *CYGB* gene doesn't have a TATA box (Wystub *et al.*, 2004, Guo *et al.*, 2006). This collection of regulatory elements gives a strong indication that transcription of the *CYGB* gene is upregulated in hypoxic conditions (Shaw *et al.*, 2009, Genin *et al.*, 2008, Hockel and Vaupel, 2001). Upregulation of *CYGB* has been shown *in vitro* in glioblastoma (Emara *et al.*, 2010) and in a neonatal rat model of hypoxia-ischemia injury in the brain (Tian *et al.*, 2013), the function of *CYGB* in hypoxic conditions is discussed in section 1.1.6.3. The presence of a CpG island, which encompasses regulatory factor binding sites present in the promoter, indicates that *CYGB* expression has the potential to be controlled epigenetically. Evidence for epigenetic control was observed by Shaw *et al.*(2007), who reported CpG promoter methylation for *CYGB* in the tumours of patients with oral squamous cell carcinoma. It has also been reported that c-Ets-1 is important in extracellular matrix (ECM) remodelling and its expression has been found to be critical to ECM composition in fibroblast cells (Hockel *et al.*, 1996). Some of the regulatory elements present in *CYGB*'s promoter region are important in HSC modulation, overlapping elements are discussed in section 1.2.1.4, and the presence of these elements is suggestive of a role for *CYGB* in HSC activation.

Efficient transcription of *CYGB* is dependent on the region -1113 – 10 kb upstream of the ATG start codon, and the c-Ets-1 and Sp1 binding sites are critical for promoter activity in normoxic conditions (Guo *et al.*, 2006) while the HIF1 and EPO binding motifs are crucial for *CYGB* regulation under hypoxic conditions (Guo *et al.*, 2007). Further analysis has indicated that AP-1 and NFAT are more important in *CYGB* transcription than HIF1, as part of a calcineurin mediated response, under hypoxic conditions in mouse hearts (Singh *et al.*, 2009). Research by Nakatani *et al.* (2004) also indicates that *CYGB* transcription may be regulated by transforming growth factor β 1 (TGF β 1) and platelet derived growth factor-BB (PDGF-BB), which have been implicated in HSC activation (Reeves and Friedman, 2002).

1.1.5 Localisation of *CYGB*

CYGB is the most recent of the vertebrate globins to be identified, and with regards to its expression in human tissues, it was first reported as being ubiquitously expressed (Trent and Hargrove, 2002). It is present in many cell types myofibroblasts, osteoblasts, osteocytes, chondrocytes, fibroblasts, neurons of the peripheral and central nervous system and HSC (Kawada *et al.*, 2001, Asahina *et al.*, 2002, Nakatani *et al.*, 2004, Schmidt *et al.*, 2004), most recently *CYGB* has been identified in melanocytes and melanoma cells (Shaw *et al.*, 2013). It has been identified in a range of tissues such as heart, muscle, colon, kidney, liver, tendon, brain and skin in mouse, rat and human (Schmidt *et al.*, 2004). Research has indicated that *CYGB* expression is largely restricted to cells of a fibroblast lineage and some neurons in normal visceral organs. *Cygb*

positive cells have been observed in fibrotic tissue in fibroblast-like cells identified by morphological analysis (Nakatani *et al.*, 2004, Schmidt *et al.*, 2004). Schmidt *et al.*(2004) also reported that CYGB was not detected in hepatocytes or endothelial cells, sinusoidal and red blood cells, although its absence from hepatocytes is disputed, as others have reported observing CYGB in hepatocytes (Geuens *et al.*, 2003, Yang *et al.*, 2011), the most recent study analysing CYGB localisation has reported hepatocytes in the human liver to be negative for CYGB expression (Motoyama *et al.*, 2014).

There is debate over the subcellular localisation of CYGB, Schmidt *et al.*(2004) reported that within HSCs, CYGB was detected in the cytoplasm but not in the nucleus. CYGB labelling in fibroblasts, chondroblasts, osteoblasts and osteocytes was uniformly distributed within the cytoplasm and cytoplasmic extensions. There was no staining observed within the extracellular matrix or nuclei of cells, however CYGB was seen in neurons of myenteric plexus in the colon where staining occurred in both cytoplasm and nuclei. Geuens *et al.* (2003), reported nuclear expression of *Cygb* in a range of tissues including mouse brain, renal glomerular cells and distal and proximal tubuli and pancreatic cells. Shigematsu *et al.*(2008) also reported nuclear expression in hepatocytes, and Man *et al.* (2008) observed cytoplasmic and some nuclear staining in liver fibroblasts, and specifically cytoplasmic and nuclear staining of HSCs, but no staining in hepatocytes, as well as cytoplasmic staining in fibroblasts of lung, kidney and thigh muscle. Recently, Singh *et al.* (2014) reported nuclear and cytoplasmic *Cygb* expression in muscle progenitor cells and proliferating myoblasts and Fujita *et al.* (2014) also observed *Cygb* expression in the nuclei and cytoplasm of melanocytes, so this issue of subcellular localisation of *Cygb* remains unresolved. Itoh *et al.* (2013) have

observed that the nuclear receptors Neuronal PAS domain protein 2 and REV-ERB α , which are known to bind haem (Raghuram *et al.*, 2007, Ishida *et al.*, 2008), could facilitate Cygb translocation to the nucleus in HEK293T cells and HeLa cells. Li *et al.* (2014) recently reported that REV-ERB α is upregulated in activated primary rat HSC and in injured liver in *in vivo* rat models and human liver tissue. Guo *et al.* (2006) found that nuclear protein from BEAS-2B cells were able to bind to c-Ets-1 promoter fragment oligonucleotides containing the Sp1 binding motif from the *CYGB* promoter region. Therefore it is feasible that nuclear localisation of CYGB could be observed.

1.1.6 Putative functions of CYGB

Many functions for CYGB have been suggested; however, its specific role within a cell and its function in healthy and damaged tissues is still to be determined, and no definitive function for CYGB has been established. The following sections outline the current hypotheses about the possible functions of CYGB.

1.1.6.1 CYGB and O₂

It is generally assumed that intracellular globins, including CYGB, have an important role in oxygen homeostasis in mammalian cells. Therefore it was naturally assumed that CYGB might be involved in intracellular oxygen storage and transport, or have an oxygen sensing role. de Sanctis *et al.* (2004) proposed that, although CYGB differs in structure and tissue distribution from MB and HB, its function is likely to occupy a

similar niche as it belongs to the globin superfamily, and the two best studied human globins; HB and MB are involved in oxygen storage and transport (Ascenzi *et al.*, 2004). The equilibrium constants for O₂ and CO in Mb and CYGB are similar, which is suggestive of CYGB having a function as an O₂ reservoir, as Mb does in muscle tissue. However, localisation of CYGB is in cells that form connective and supportive tissue from a common ontogenetic origin, and these cells are not usually associated with high metabolic rates or high oxygen consumption. Also cellular expression levels cannot be reconciled with mitochondria and general metabolic activity, making it unlikely that CYGB is directly involved in respiratory chain O₂ supply, unlike MB, which shows relatively high expression in muscle tissues (Schmidt *et al.*, 2004). CYGB may have a role in supplying oxygen for cellular reactions unrelated to mitochondrial respiration (Fago *et al.*, 2004), but it has also been reported that dissociation rates of oxygen for h_xHbs are considered too slow for them to play a role in O₂ transport (Smagghe *et al.*, 2008).

Makino *et al.* (2011) proposed that if CYGB is a gas sensor, the conformational changes that occur to the structure might be a signal, encoding information regarding the O₂ tension and modulate downstream regulators. They also suggest that the crystal structure of the CO bound CYGB has a bend in the E helix on the distal side of the haem, this feature means the His side chain on the distal side of the haem is expelled from the sixth position and moves out of the haem pocket, which could have implications for ligand binding affinity. However, a gas sensing function for CYGB was dismissed by Schmidt *et al.* (2004) as CYGB expression is restricted to fibroblast type cells and a few neuronal cell types, and there is no apparent reason for this restriction in expression for an oxygen sensing molecule.

1.1.6.2 CYGB, reactive oxygen species and reactive nitrogen species

CYGB has been implicated in many possible roles in oxygen dependant metabolism such as decomposition of reactive oxygen species (ROS) or reactive nitrogen species (RNS), or as part of an O₂ mediated signalling pathway (Burmester *et al.*, 2007). It has been suggested that some functions involving O₂ metabolism, specific to fibroblast type cells, for example collagen synthesis or perhaps scavenging ROS (Li *et al.*, 2007, Ostojic *et al.*, 2008). *In vitro*, *Cygb* overexpressing kidney fibroblasts displayed increased ROS scavenging activity, and *in vivo* *Cygb* overexpressing transgenic rats showed decreased oxidative stress (Mimura *et al.*, 2010). Further evidence for a protective role was reported by Xu *et al.*(2006), where primary rat HSCs, transduced with rat *Cygb* were exposed to oxidative stress. *Cygb* expression reduced production of malondialdehyde (MDA) and 4-hydroxy-2-nonenal (4-HNE) lipid peroxidation products and total oxyradical scavenging capacity was increased. HSC differentiation into myofibroblast type cells induced by oxidative stress was also prevented by overexpression of *Cygb*. Hepatic necrosis induced by CCl₄ or bile duct ligation (BDL) induced liver fibrosis were inhibited by *Cygb* overexpression. The fibrogenic phenotype development was prevented by *Cygb* overexpression in CCl₄ treated rats, reducing the expression of procollagen 1, TGF-β1 and α-SMA. *Cygb* over expression in BDL rats prevented the formation of ascites and inhibited breakdown of liver architecture. These data suggest that *in vivo* up regulation of *Cygb* doesn't contribute to HSC-induced fibrosis but is a homeostatic mechanism for preventing free radical activation of HSC and subsequent fibrosis. Reeder *et al.* (2010) observed pro-oxidant activity of

CYGB, which contradicts the reports of CYGB protection against oxidative stress and ROS; however, they suggest that at physiological concentrations, and because the haem degrades when Fe undergoes redox reactions in the presence of oxygen producing ROS (Nagababu and Rifkind, 2004), it would be unlikely that extensive cellular damage would be caused, and therefore CYGB might form part of a cell signalling cascade inducing an antioxidant response. Fujita *et al.* (2014) observed increased intracellular ROS levels in a melanocyte cell line when CYGB is knocked down, as did Singh *et al.*(2014) in a myoblast cell line, and depletion of CYGB also resulted in an increase in cell death in myoblasts. A cytoprotective role for CYGB has been proposed; Hodges *et al.* (2008) reported that cytoprotection from oxidative DNA damage was afforded by CYGB against oxidative DNA damage by a singlet oxygen generator in a neuron-derived human medulloblastoma cell line, and McDonald *et al.* (2012) found that overexpression of CYGB in the oesophageal cancer cell line TE-8 was protective against oxidative stress induced by buthionine sulfoxamine, It is possible that CYGB is also involved in NO detoxification, neuronal cells that are positive for CYGB also express neuronal NO synthase which produces NO, therefore it is conceivable that CYGB is involved in either the production (Hankeln *et al.*, 2005) or detoxification of NO (Halligan *et al.*, 2009) or potentially both (Burmester and Hankeln, 2014). There is evidence that hxBs bind reversibly to NO (Herold *et al.*, 2004) and in the ferric form they react with NO and the oxyferric hxBs can oxidise NO to nitrate and that as a hxB it could act as an NO dioxygenase Smagghe (2008). Further evidence for NO dioxygenase activity was obtained by Gardner *et al.* (2010) who observed reductant activity for ascorbate and cytochrome b(5) and defined an NO

dioxygenase function for CYGB in hepatocytes. Halligan *et al.* (2009) observed *Cygb* expression in adventitial fibroblasts and vascular smooth muscle cells and that silencing of *Cygb* by short hairpin RNA in murine fibroblasts resulted in decreased NO consumption and intracellular nitrate production. However it has also been argued that due to the low concentrations of hxBs (including CYGB) *in vivo*, function as an NO scavenger is unlikely (Kakar *et al.*, 2010). Smagghe *et al.* (2008) report that human CYGB shows no ability to catalyse NO destruction and NO binding to ferric human CYGB is slower than MB, probably due to intramolecular His binding to the ligand binding site, and that it was less efficient as an NO dioxygenase than MB, further suggesting that a role in NO detoxification is unlikely.

1.1.6.3 CYGB in hypoxia

CYGB is upregulated *in vitro* and *in vivo* under hypoxia (Fordel *et al.*, 2004, Schmidt *et al.*, 2004) and CYGB upregulation was found to increase as a function of time under hypoxic conditions. Induction of CYGB has been observed in a range of tissues including tissues of heart and liver in the fibroblasts and also in the HN33 cell line (Fordel *et al.*, 2004). Induction was found to reach maximal levels at 48hr of hypoxia in the liver (Fordel *et al.*, 2007). Schmidt *et al.* (2004) also reported upregulation of *Cygb* mRNA in the heart and liver under hypoxic conditions, with a fold increase of 2.2 ± 0.8 and 2.3 ± 0.5 after 22hr and 44hr respectively in the liver. The hypoxia-inducibility and hypoxia response of *Cygb* demonstrates that it probably has a link with oxygen dependant metabolism in fibroblasts and fibroblast type cells. Emara *et al.* (2010),

found that *in vivo* exposure of mice to hypoxic conditions caused significant upregulation of CYGB mRNA in human tumours.

Hamdane *et al.* (2003) and Lechauve *et al.* (2010) report that the positions of the cysteine residues of CYGB might influence the position of the E helix which could affect the affinity of the distal histidine for the haem iron, as is discussed in section 1.1.2. The authors suggest that oxidative stress might cause a change in the local redox state in response to physiological stimuli and cause formation or breaking of an intramolecular B2-E9 disulphide bond, leading to a conformational change which affects oxygen affinity. They propose that, as hypoxia results in the accumulation of reducing agents in the cell, which have the ability to reduce the disulphide bond, CYGB may play a role in countering hypoxia by releasing oxygen via the conformational change induced under the reducing conditions caused by hypoxia. When oxygen concentration increases, the cysteines will be oxidised into the intramolecular disulphide bonds and oxygen affinity increased leading to oxygen storage, and this could be a signalling response, rather than O₂ storage *per se*. However this response does not explain why CYGB expression seems to be restricted to cells of a fibroblast lineage, but it could be involved in a signalling pathway specific to this cell type.

1.1.6.4 Enzymatic activity of CYGB

It has been postulated that Cygb might have an enzymatic function as a peroxidase. Kawada *et al.* (2001) found, on analysis of purified 'STAP', that it exhibited peroxidase activity and suggested a role for Cygb in facilitating oxygen diffusion to the respiratory chain of the mitochondria, along with Burmester *et al.* (2002). Peroxidase activity was also observed by Reeder *et al.* (2011), who suggested that disruption of hexacoordination along with the ability of CYGB to induce lipid oxidation *in vitro* may be an explanation for this activity, and could be important in the physiological role of CYGB. Schmidt *et al.* (2004) argue that a function as a terminal oxidase in anaerobic conditions is unlikely, and the strong pseudo-peroxidase exhibited by Cygb activity could be explained by its interaction with lipids, its ability to induce lipid oxidation reactions in *in vitro* experiments and the reported lipid-binding properties of Cygb. Authors have argued that this activity could have an important role in the physiological function of the Cygb protein (Schmidt *et al.*, 2004, Reeder *et al.*, 2011, Ascenzi *et al.*, 2013).

1.1.7 CYGB and collagen I synthesis

Schmidt *et al.* (2004) proposed that Cygb may supply oxygen to prolyl-4-hydroxylase for the hydroxylation of proline residues in the procollagen molecule (Pihlajaniemi *et al.*, 1991, Myllyharju and Kivirikko, 1999), as the degree of collagen hydroxylation depends on available oxygen (Yen *et al.*, 1979). This hypothesis is consistent with the

observation that Cygb is upregulated in fibrotic livers, where collagen synthesis is also increased (Kawada *et al.*, 2001). Collagen mRNA is also upregulated in hypoxic conditions *in vitro* and *in vivo* (Takahashi *et al.*, 2000, Genin *et al.*, 2008). Schmidt *et al.* (2004) found that Cygb is upregulated in hypoxic conditions, and hypothesise that Cygb compensates for low oxygen conditions and increased oxygen demand for collagen synthesis. Man *et al.* (2008) also indicate a link between Cygb upregulation and collagen synthesis. After *in vivo* treatment of mice with CCl₄, collagen staining was only observed after 48hrs. Cygb staining was stronger at 6hr increasing to 24hr and then decreased again at 48hr. Collagen mRNA expression was down regulated up to 24hr and then significantly upregulated at 48hr, suggesting Cygb could be involved in collagen synthesis. Also over 8 weeks of induced liver fibrosis the number of cells positive for Cygb in the fibrotic septa increased. However, *in vitro* primary cultured fibroblasts from transgenic rats showed Cygb overexpression at mRNA and protein levels but reduced collagen production. Also, mutant Cygb with an altered haem group to impair ligand binding showed no effect of reduced collagen production (Mimura *et al.*, 2010), evidence against a role for Cygb as an O₂ donor in collagen synthesis. These results, however, are only correlative, and no firm mechanistic link between Cygb and collagen synthesis has been established.

1.1.8 CYGB in disease

CYGB has been implicated in many disease states, it was first discovered on analysis of protein changes in a model of liver fibrosis as discussed in section 1.1 (Kawada *et al.*, 2001), it is also upregulated in kidney fibrosis (Mimura *et al.*, 2010) and some neurodegenerative disorders (Hedley-Whyte *et al.*, 2009). In the liver, loss of Cygb leads to increased chemically-induced tumorigenesis (Thuy le *et al.*, 2011) and it appears to have a role in cancer, with many cancers showing CpG site methylation of the *CYGB* promoter region (Xinarianos *et al.*, 2006, Shivapurkar *et al.*, 2008, Wojnarowicz *et al.*, 2012, Shaw *et al.*, 2013, Fujita *et al.*, 2014), leading to reports of it acting as a tumour suppressor (Shivapurkar *et al.*, 2008). However, upregulation has also been reported in some cancers, such as head and neck and alveolar soft-part sarcoma (Genin *et al.*, 2008, Shaw *et al.*, 2009). *Cygb* is upregulated in hypoxic conditions (Fordel *et al.*, 2004, Schmidt *et al.*, 2004) and solid tumours often have hypoxic regions and tumour hypoxia is associated with tumour progression (Hockel *et al.*, 1996, Hockel and Vaupel, 2001). These observations have led to the suggestion that *CYGB* can also act as an oncogene (Oleksiewicz *et al.*, 2013).

1.1.8.1 CYGB in cancer

CYGB was first associated genetically with cancer by McDonald *et al.* (2006) in tylosis with oesophageal cancer (TOC), which is an autosomal dominant hereditary disorder associated with higher risk of oesophageal cancer and oral lesions (Risk *et al.*, 1999).

The CpG site of *CYGB* can be methylated, and gene silencing of *CYGB* by methylation has been reported in many cancers including: non-small cell lung cancer (Xinarianos *et al.*, 2006), lung, colon, bladder and breast cancer and leukaemia, (Shivapurkar *et al.*, 2008), head and neck cancer (Shaw *et al.*, 2009), the recurrence of hepatocellular carcinoma (Yang *et al.*, 2011), ovarian cancer (Wojnarowicz *et al.*, 2012) oral squamous cell carcinoma (Shaw *et al.*, 2013) and melanoma cells (Fujita *et al.*, 2014). *CYGB* promoter methylation has proved to be useful in distinguishing cancerous from normal tissue (Shivapurkar *et al.*, 2008), suggesting that it might be useful as epigenetic biomarker for cancer detection (Shaw *et al.*, 2007). It is known that promoter hypermethylation that is related to cancer frequently affects expression of tumour suppressor genes the expression of tumour suppressor genes (Esteller, 2007), and it has been postulated that *CYGB* acts as a tumour suppressor (Shivapurkar *et al.*, 2008, Oleksiewicz *et al.*, 2013). It has been shown that increased expression of *CYGB* reduced colony formation in lung and breast cancer cell lines (Shivapurkar *et al.*, 2008), cell migration, invasion and anchorage in lung cancer cell lines (Oleksiewicz *et al.*, 2013) and proliferation in ovarian cancer cell lines (Chen *et al.*, 2014), conversely, *CYGB* silencing via siRNA in melanoma cells increased cell proliferation (Fujita *et al.*, 2014). Thuyet *al.* (2011) demonstrated increased tumorigenesis in the livers of *Cygb* deficient mice treated with DEN (N,N-diethylnitrosamine)

However, it also appears that *CYGB* can have tumour promoter properties as well, it is upregulated in head and neck cancer, lung carcinoma and alveolar soft-part sarcoma (Xinarianos *et al.*, 2006, Genin *et al.*, 2008, Shaw *et al.*, 2009, Oleksiewicz *et al.*, 2013). Hypoxia response seems to be a component of upregulation in these cancers. In

hypoxic conditions *Cygb* is upregulated (Fordel *et al.*, 2004, Schmidt *et al.*, 2004) and tumour hypoxia is associated with tumour progression and resistance to radiotherapy and chemotherapy (Hockel *et al.*, 1996, Hockel and Vaupel, 2001). It is thought that CYGB might offer cytoprotection under stress conditions such as hypoxia (see section 1.1.6.3), which might be the mechanism for CYGB's tumour promoter properties. Oleksiewicz *et al.* (2013) recently demonstrated CYGB conferred protection on lung cancer cell lines, in a cell specific manner, under hypoxic conditions.

1.1.8.2 CYGB in fibrosis

Fibrosis is a common complication of the chemotherapy and radiation treatments that are used for the treatment of cancer (Mancini and Sonis, 2014), as well as being apparent in other types of disease such as kidney and liver disease. It has also been argued that the formation of a fibrotic extracellular matrix stimulates cells to proliferate, creating conditions for cancer development (Cernaro *et al.*, 2012). A role for CYGB in the process of fibrosis has been suggested because several studies shown it be upregulated during fibrogenesis along with collagen expression (Kristensen *et al.*, 2000, Nakatani *et al.*, 2004, Schmidt *et al.*, 2004, Mimura *et al.*, 2010, He *et al.*, 2011). *Cygb* has been reported to be induced in *in vivo* in a fibrotic liver, and *in vitro* in activated HSCs implying it has an active role in the process of fibrosis as HSC are the major ECM producing cells in an injured liver, there contribute greatly to fibrogenesis in this organ (Kristensen *et al.*, 2000) (section 1.2.1.2). Schmidt *et al.* (2004) observed strong *Cygb* expression in HSCs, and also in the fibroblasts forming connective tissue of

blood vessels, and fibroblasts in many other tissues, but not in hepatocytes. Hydrogen peroxide, which induces a fibrotic response in cells, induced CYGB upregulation in N2a neuroblastoma cells (Li *et al.*, 2007) and upregulation of CYGB has not been observed with other forms of stress such as heat stress, high osmolarity and UV radiation (Reeder *et al.*, 2011). Mimura *et al.* (2010) found that *Cygb* is upregulated in an *in vivo* model of the fibrotic kidney in a time dependant manner in both mRNA and protein expression, along with collagen and HIF expression. Initial data indicated that *Cygb* could be profibrotic; however more recent research has suggested an antifibrotic effect of increased *Cygb* expression. He *et al.* (2011) demonstrated that treatment with *Cygb* reduced collagen deposition and fibrotic marker expression in thioacetamide induced fibrosis in rats *in vivo*, and reduced cell viability, in a concentration dependent manner, in HSC cell lines *in vitro*. Cui *et al.* (2012) observed that arundic acid inhibited HSC activation via an increase in CYGB expression in a human HSC cell line and primary rat HSCs. *Cygb* deficient mice develop more fibrosis after ischemia-reperfusion (IR) injury in the heart (Singh *et al.*, 2013) and inhibition of pancreatic stellate cell activation by halofuginone reduces pancreas fibrosis and was accompanied by an increase in *Cygb* in these cells (Zion *et al.*, 2009).

There are as yet no definitive answers to the question of the role of CYGB within healthy or diseased tissue, or in cells. However, many aspects of CYGB indicate a role within the processes of disease and fibrosis.

1.2 Hepatic Stellate Cells

Cygb was first identified in an *in vivo* proteomic study of liver fibrosis in rats treated with CCl₄. It was reported as an unidentified protein upregulated in HSC upon their activation, and named STAP (Kristensen *et al.*, 2000), as described in section 1.1. HSC are key players in the process of liver fibrosis and are the major source of the ECM which forms the hepatic scar in a fibrotic liver (outlined in more detail in section 1.2.1.2). CYGB has been implicated in fibrosis (see section 1.1.8.2) and therefore its regulation in hepatic cells might be important in the activation state of these cells and their role in liver fibrosis.

HSCs were first described as 'sternzellen' (German for 'star cells') by Kupffer in 1876, who visualised them using gold chloride to detect Vitamin A containing droplets (Wake, 1971). An important functional role for stellate cells in the injury response of the liver was described by Kent *et al.* (1976) Okanoue *et al.*(1983) and Yokoi *et al.*(1984), who observed that HSCs were found in close proximity to collagen fibres in a fibrotic liver. This work also suggested that HSCs might be the antecedent of the fibroblasts frequently described in liver injury. There was also evidence for regular association between HSC and ECM (Martinez-Hernandez, 1984).

It became evident that the multitude of names used to describe HSCs, such as Ito cells, lipocytes, parasinusoidal or perisinusoidal cells and fat storing cells, was causing confusion in the scientific field (Friedman, 2008b), so in 1996 the international community of researchers in the field of nonparenchymal liver cell biology and liver

fibrosis made the recommendation that they should be referred to as 'hepatic stellate cells' in all publications from January 1997 onwards.

1.2.1 HSC function

It is widely accepted that HSCs are the principle effectors of hepatic fibrogenesis and have become recognised as versatile mesenchymal cells, which are vital for hepatocellular function, and the liver's response to injury (Friedman, 2008b). On liver injury HSC transform from quiescent vitamin A storing cells to activated myofibroblast type cells. However, they are not the sole effectors as other mesenchymal cells, such as hepatocytes, cholangiocytes, and portal fibroblasts also secrete ECM, and so contribute to the formation of the hepatic scar (Friedman, 2008a). HSC activation, however, is the dominant profibrotic pathway (Friedman, 2008c) in liver fibrosis and it has been suggested that HSCs are only one source of myofibroblast like cell, which deposit ECM during liver fibrosis (Kinnman *et al.*, 2003, Beaussier *et al.*, 2007). In a fate tracing experiment, Mederacke *et al.* (2013) found that HSCs became 82-96% of myofibroblasts in *in vivo* mice models of toxic, cholestatic and fatty liver disease, it is therefore obvious that HSCs are important in the fibrotic process in the liver.

1.2.1.1 HSCs in a normal liver

HSCs are located between the basolateral surface of hepatocytes and the anti-luminal side of the sinusoidal endothelial cells in the subendothelial space (Space of Disse)

(Figure 1.4). They account for approximately one third of the nonparenchymal cells of the liver and 15% of the total liver cell population of a normal liver (Giampieri *et al.*, 1981, Jezequel *et al.*, 1984). In an uninjured liver HSC are quiescent, and a major characteristic of quiescent HSCs is the presence of intracellular retinoids in the form of cytoplasmic lipid droplets, this constitutes 70-80% of total liver - and therefore whole body - retinol content. These retinoids are released on HSC activation, and there is a marked depletion in retinoic acid (RA) content of activated HSC (Senoo, 2004, She *et al.*, 2005, Krizhanovsky *et al.*, 2008, Kisseleva *et al.*, 2012).

1.2.1.2 Function on liver injury

Activation of HSCs upon liver injury, by any means, occurs in two major phases: initiation and perpetuation. Initiation is mainly induced by paracrine stimulation whilst the perpetuation phase involves autocrine as well as paracrine loops. During activation HSC become highly proliferative and excrete ECM rich in collagen type I (Reeves and Friedman, 2002).

Initiation is characterised by early stage changes in gene expression and phenotype, making cells responsive to cytokines and other stimuli (Reeves and Friedman, 2002), initiation is also known as the 'preinflammatory stage'. These first stages of changes to HSCs are primarily caused by paracrine stimulation by all adjacent cell types including hepatocytes, sinusoidal epithelial cells, Kupffer cells and platelets, which together result in the production of fibronectin, transforming growth factor beta(TGF- β)',

platelet derived growth factor (PDGF) and epidermal growth factor (EGF). Damaged hepatocytes are also an important source of lipid peroxides and apoptosis of hepatocytes has been shown to be profibrogenic to HSC in culture (Canbay *et al.*, 2002, Friedman, 2008a). Also implicated in the initiation phase of HSC activation is cytochrome P450 2E1 (CYP2E1), which was shown to have an important role in the production of ROS such as H₂O₂ when the rat HSC-T6 cell line was co-cultured with the hepatocyte cell line Hep-G2, which in turn stimulate HSCs (Nieto *et al.*, 2002). As discussed in section 1.1.6.2 CYGB has been implicated in ROS regulation, potentially having a protective role, or it might be involved in ROS mediated signalling to initiate processes specific to fibroblast type cells such as collagen synthesis (Li *et al.*, 2007, Ostojic *et al.*, 2008). HSCs are stimulated by ROS and also deposit collagen upon activation, therefore the presence of CYGB in these cells suggests a role in redox regulation or signalling in HSCs. Recent research has indicated that CYGB has an antifibrotic role as discussed in section 1.1.8.2.

Perpetuation refers to the effect of these paracrine stimuli on HSCs, where the activated phenotype is maintained, sustaining the fibrogenic process. Perpetuation is dependent on a number of functional changes such as stellate cell proliferation and chemotaxis, matrix degradation, fibrogenesis, increased cell contractility, inflammatory cell infiltration and loss of retinoids (Reeves and Friedman, 2002, Friedman, 2008b). In total, six separate changes in cell behaviour are required for perpetuation of HSC activation (Friedman, 2008b). Firstly proliferation is provoked, PDGF has been implicated as the main protagonist in the process of proliferation (Pinzani, 2002, Borkham-Kamphorst *et al.*, 2008). PDGF is also involved in the chemotaxis of stellate

cells towards cytokine chemoattractants (Ikeda *et al.*, 1999, Kinnman *et al.*, 2000). Fibrosis is due to increased HSC numbers and increased matrix production, predominantly collagen 1 α 1 (Friedman, 2008a). The most potent stimulus for fibrosis is the cytokine TGF- β , from both paracrine and autocrine sources (Gressner *et al.*, 2002, Breitkopf *et al.*, 2006, Inagaki and Okazaki, 2007). Increased amounts of α -smooth muscle actin (α SMA) are expressed in activated cells, and this is used as a marker of HSC activation (Reynaert *et al.*, 2002).

1.2.1.3 Senescence of HSCs

It is known that removal of the injury inducing insult to the liver, be it infection or drug toxicity, results in apoptosis and senescence of HSC and their clearance by natural killer cells (Weiner *et al.*, 1992, Ohata *et al.*, 1997, Iredale *et al.*, 1998, Krizhanovsky *et al.*, 2008), and a corresponding decrease in fibrosis is observed, discussed in section 1.2.4. Recent research has reported that HSCs can also return to an inactive phenotype, rather than just apoptosing and being cleared. Hazra *et al.*, (2004), demonstrated that forced expression of peroxisome proliferator-activated receptor γ (PPAR- γ) confers a quiescent phenotype on culture activated primary rat HSCs, as observed by cell morphology, proliferation and DNA synthesis, activation marker gene expression, such as α 1 procollagen, TGF- β 1, α SMA and collagen I and also retinyl ester accumulation. Kisseleva *et al.*, (2012) reported that not all HSCs are cleared from a regressed liver, some return to an inactivated state, which is similar to, but distinct from quiescent HSCs in terms of gene expression and a more ready response to

fibrogenic stimuli, they termed these inactivated HSCs (iHSCs). Figure 1.5 is a schematic of the activation of HSC through initiation, perpetuation and resolution.

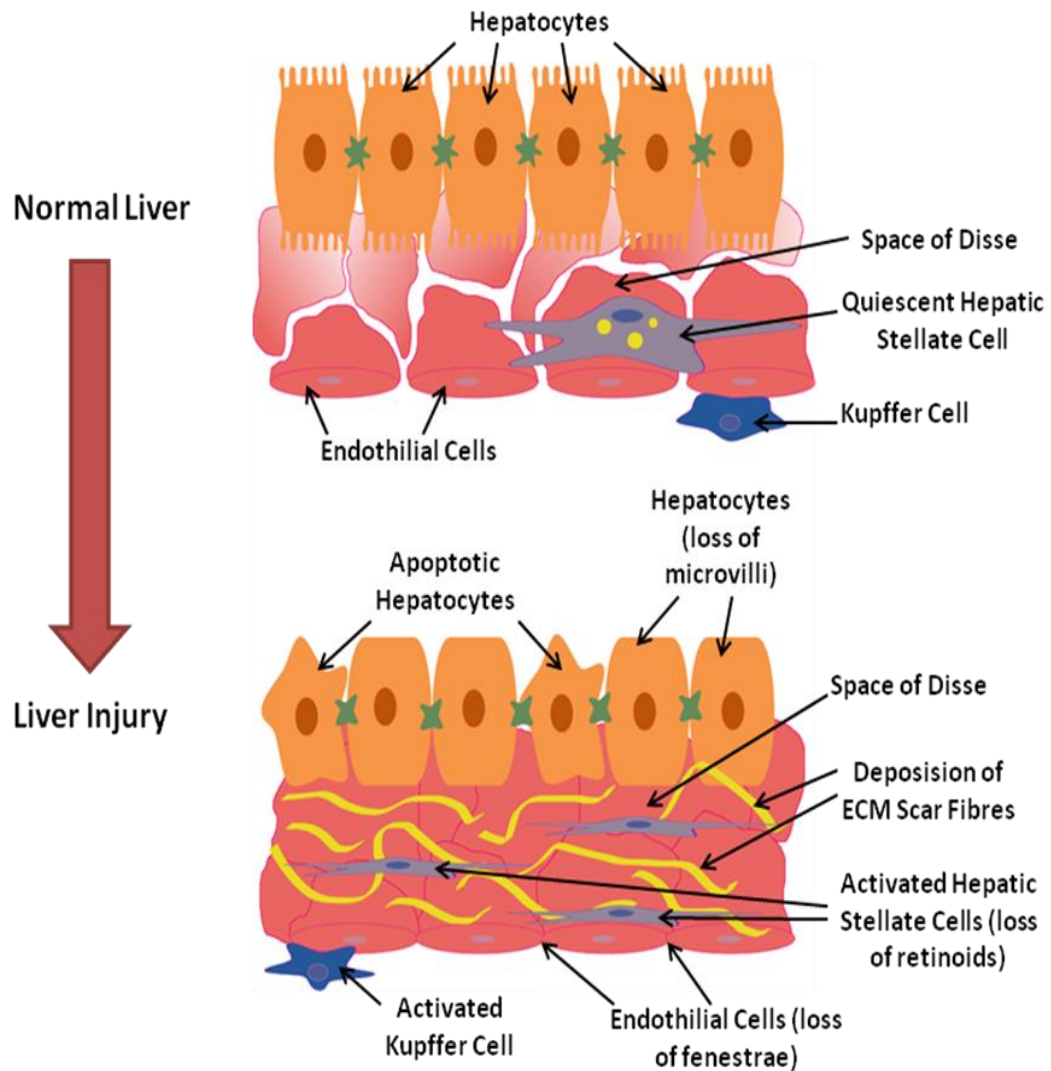


Figure 1.4: Changes in the sinusoid and Space of Disse on liver injury and development of fibrosis. Apoptosis of hepatocytes and activation of Kupffer cells contributes to activation of Hepatic Stellate Cells, leading to loss of hepatocyte microvilli and deposition of ECM scar proteins.

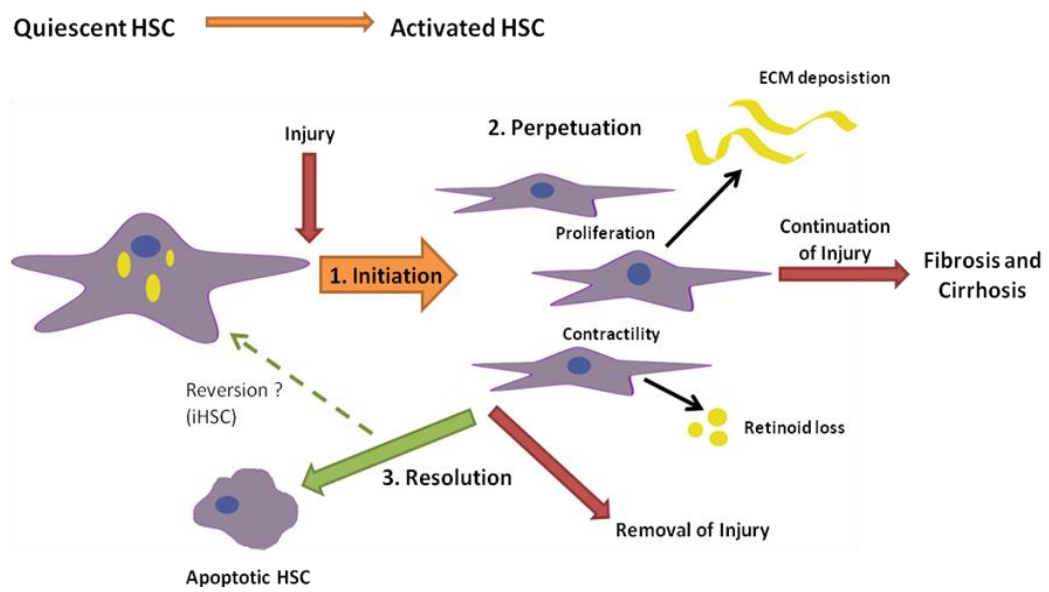


Figure 1.5: The process of HSC activation through initiation, perpetuation and possible resolution.

1.2.1.4 Transcription factors involved in the regulation of HSC activation and quiescence in the context of *CYGB* regulatory elements

The transformation of quiescent HSC to activated HSC and vice versa requires many changes in gene expression, and regulation of gene transcription is, therefore, important in the conversion and maintenance of an activated HSC phenotype in an injured liver (Mann and Mann, 2009). *Cygb* is reported to be upregulated in activated HSC compared with quiescent HSC (Kristensen *et al.*, 2000), indicating transcriptional regulation of *CYGB* in the transformation of HSC from a quiescent to an activated. Regulation of *CYGB* expression is discussed in section 1.1.4.1, and there is overlap between transcription factor binding sites present in the *CYGB* promoter region and transcription factors that are important in HSC modulation, Figure 1.6 depicts this overlap. HSCs express α , β and δ C/EBPs (Huang *et al.*, 2004), and *CYGB* contains a C/EBP binding site within its promoter. Huang *et al.* (2009), discovered that C/EBP α (which controls differentiation in adipocytes) is downregulated in activated HSCs and forced overexpression inhibited proliferation, ECM producing gene expression and induced lipid droplet storage in HSC suggesting a more quiescent phenotype, indicating a role for C/EBP α in HSC differentiation. Kruppel-like zinc finger proteins are also expressed in HSC, most significant with regards to *CYGB* is SP1, which is induced on HSC activation, and its DNA binding activity increased. SP1 has been shown to induce *collagen 1 α* gene transcription in activated HSCs; however interactions with NF κ B reduced SP1's transcriptional activity (Mann and Mann, 2009). Increased expression of SP1 in activated HSC may impact *CYGB* gene transcription in these cells. AP-1 factors such as c-Jun, JunB, Jun D, and c-Fos, Fra1 (Fos-related antigen 1), Fra2, and Fos-B (FBJ

murine osteosarcoma viral oncogene homolog B) are regulators of tissue inhibitors of metalloproteinase (TIMP) -1 expression, which is involved in inhibiting ECM degradation – an important event in fibrosis. In quiescent HSCs, DNA binding of AP-1 is not detectable, but is induced during the early stages of HSC activation (Knittel *et al.*, 1999, Friedman, 2008b, Mann and Mann, 2009), where it could influence *CYGB* gene transcription. Another transcription factor involved in HSC regulation which might have a role in *CYGB* transcription is AP-2, which also regulates collagen 1 promoter activity in HSCs (Chen *et al.*, 1996). Binding of the transcription factor NF-1 can also regulate *collagen* gene transcription in activated HSCs (Anania *et al.*, 1995). Quiescent and activated HSCs both express Ets1 (E26 transformation-specific transcription factor), but it is more highly expressed in quiescent HSCs, as HSCs activate, the transcription, protein and binding activity of Ets1 are greatly reduced (Knittel *et al.*, 1999). The *CYGB* promoter contains a c-Ets-1 binding motif, so the expression pattern of Ets1 in HSCs could influence *CYGB* expression in this cell type. NFκB is also expressed in both quiescent and activated HSC, and transcriptionally active NFκB is increased in activated HSC, this activation seems to be a permanent reprogramming, and an increase in basal activity levels to perpetuate pro-inflammatory and pro-fibrogenic gene expression and prevent apoptosis of HSC (Elsharkawy *et al.*, 2005, Tergaonkar, 2006). Antioxidants have been shown to have an inhibitory effect on NFκB (Chen *et al.*, 1996), and *CYGB* has been shown to have antioxidant activity (see section 1.1.6.2), so feedback could be occurring through NFκB binding to the *CYGB* promoter.

To date no studies have specifically looked at the binding of transcription factors that are involved in HSC differentiation to the *CYGB* promoter region in these cells, so it is not yet known if the overlap between transcription factors expressed by HSC and *CYGB* regulatory elements is of significance in these cells. Transcriptional regulation of HSC is complex, and many transcription factors interact, making understanding these processes difficult. However it is clear that HSC differentiation and *CYGB* expression correlate. Motoyama *et al.* (2014) have since reported that *Cygb* expression is specific HSCs, whether they are quiescent or activated, in normal and fibrotic livers and is present in primary mouse HSC throughout 7 days of culture. Thus *Cygb* could be used to distinguish myofibroblasts originating from HSCs from those derived from other cell types. It is also possible that *CYGB* could be a target for manipulating HSC transformation, the crossover between many transcription factors involved in HSC activation and *CYGB* genetic regulation are indicative of a role in this process for *CYGB*. Mann and Mann (2009), expressed the view that unravelling the signalling processes involved in HSC regulation could lead to therapeutic targets for prevention and reversion of liver fibrosis.

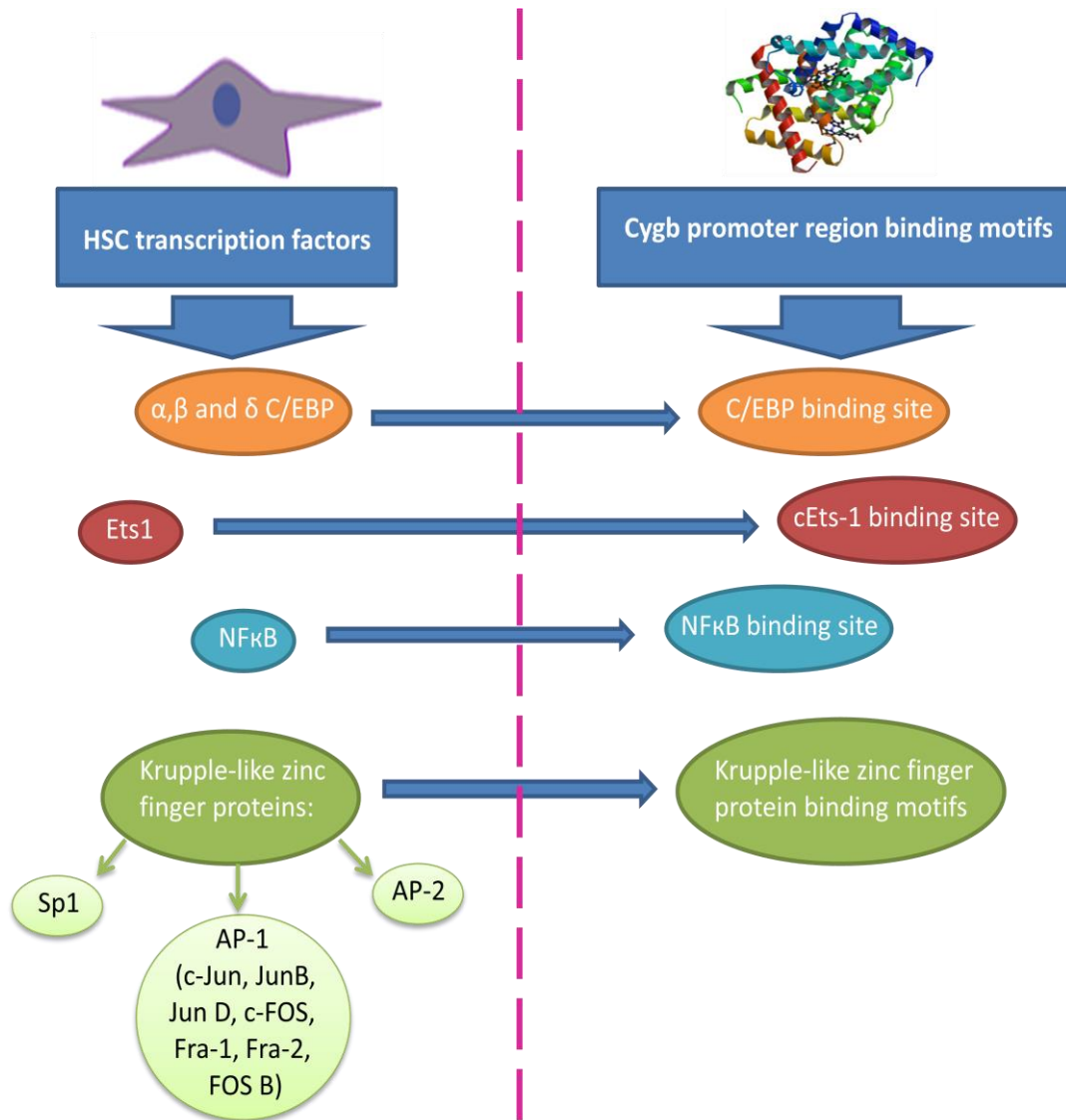


Figure 1.6: Transcription factors important in hepatic stellate cell (HSC) activation that are also important in the context of regulatory elements present in the promoter region of cytoglobin (*CYGB*). Abbreviations: C/EBP = CCAAT-enhancer-binding protein, Ets1 = E26 transformation-specific transcription factor, cEts-1 = cellular erythroblastosis virus E26 oncogene homolog 1, NFκB = nuclear factor kappa-light-chain-enhancer of activated B cells, AP = activator protein, SP = stimulatory protein. Crystal protein structure of homodimer of Cygb modified from <http://www.rcsb.org/pdb> access number 1UMO (de Sanctis et al., 2004)

1.2.2 Liver fibrosis

Liver fibrosis is caused by chronic damage to the liver and is characterised by the accumulation of ECM (Friedman, 2003). Acute liver injury causes regeneration and replacement of necrotic and apoptotic cells by parenchymal cells in association with an inflammatory response with limited ECM deposition. However if the injury is chronic then the regenerative response fails and scar tissue containing fibrillar collagen forms in the place of hepatocytes. If liver injury is continuous, or the liver is repeatedly assaulted, then the wound healing response in the liver results in fibrosis, the increased ECM consists mainly of collagen and creates a hepatic scar (Reeves and Friedman, 2002). Advancing of liver disease causes bridging fibrosis, and then cirrhosis occurs. The onset of liver fibrosis normally goes clinically undetected as morbidity and mortality only occur after cirrhosis develops (Poynard *et al.*, 2003). The progression of fibrosis to cirrhosis can take 15—20 years, and can include complications such as renal failure, hepatic encephalopathy and hepatocellular carcinoma. In compensated cirrhosis, patients can survive complication free for several years; however decompensated cirrhosis is associated with short survival. It is possible that in some circumstances fibrosis can proceed rapidly to cirrhosis, including acute alcoholic hepatitis (Bataller and Brenner, 2005).

Fibrosis occurs due to a series of events; inflammation usually precedes fibrosis and involves the recruitment of inflammatory cells to the site of injury, which is a normal part of wound healing. Then chronic injury occurs, which involves immediate damage to the barrier between the epithelial and endothelial cells and release of TGF- β 1. This

in turn induces ROS production, and myofibroblast type cells, which deposit collagen, are activated, these include HSCs, which lose their retinoids and activate in the manner described in section 1.2.1.2. If the injury is removed then fibrosis is reversed, however if it is continuous then fibrosis can develop into cirrhosis (Wallace *et al.*, 2008). Fibrosis is defined as detectable deposits of ECM. In a non-fibrotic liver, ECM constitutes approximately 3% of the relative area of a liver section, where as in a cirrhotic liver, approximately 22% the area of liver section is covered (Lin *et al.*, 1998). As the major contributors to ECM deposition on liver injury, activated HSCs are very important in the progression of fibrosis in the liver. Figure 1.4 illustrates the changes which occur to the liver on injury.

There is increasing evidence that a regression of fibrosis in the liver is possible, despite the impression clinically that it is not, discussed in section 1.2.4 (Davis *et al.*, 1990, Troen *et al.*, 1994, Sato *et al.*, 1995, Benyon and Iredale, 2000, Ramachandran and Iredale, 2012).

1.2.3 Changes in ECM

The amount and composition of ECM is altered during fibrosis (Benyon and Iredale, 2000). In advanced liver fibrosis there can be six times more ECM than found in a non-fibrotic liver. The composition changes from one dominated by collagen IV and laminin (Martinez-Hernandez and Amenta, 1995), to one of fibrillar collagen, predominantly collagen I and III with a corresponding increase in fibronectin and elastin amongst

other components (Friedman, 2008c). ECM accumulation is caused by an increase in synthesis and a decrease in degradation (Arthur, 2000). The imbalance between matrix production and degradation is critical in liver fibrosis, and early degradation of normal matrix causes replacement with scar matrix (Friedman, 2008c). The ECM provides several functions within the liver, it is a mechanical scaffold for cellular adhesion, migration and interactions, and it acts as a reservoir for paracrine soluble factors such as PDGF and TGF- β , as well as other stimuli involved in activation and matrix modulation (Reeves and Friedman, 2002). Changes in ECM composition also drive changes in membrane receptors, particularly integrins, indicating the ECMs' role not only as a scaffold but as part of the cell-cell communication network via cell-surface receptors (Benyon and Iredale, 2000, Bedossa and Paradis, 2003, Friedman, 2008c).

The primary source of ECM in the liver are activated HSCs (Gabele *et al.*, 2003), outlined in section 1.2.2. Activated HSCs deposit collagens type I and III into the ECM (Friedman, 2008b) and the initiation of HSC activation takes place alongside the progressive changes in the surrounding ECM.

1.2.4 The reversibility of liver fibrosis

Liver fibrosis has traditionally been thought of as an irreversible process; however this view is changing, Pellicono *et al.* (2012) described the belief that fibrosis is unidirectional as obsolete. It has been shown that abstinence from alcohol can improve lesions in the liver in patients with alcoholic liver disease (Pares *et al.*, 1986) and pegylated interferon and ribavirin combination therapy for hepatitis C reversed

cirrhosis in 49% of patients (Poynard *et al.*, 2002). Experimental models have shown feasibility of reversing liver fibrosis *in vivo*, Iredale *et al.* (1998) showed that spontaneous recovery from CCl₄ induced liver fibrosis occurred over a 28wk period in rats. A similar result was observed by Issa *et al.* (2004), in CCl₄ induced liver cirrhosis in a rat model. Tissue inhibitor of metalloproteinase-1 (TIMP-1) seems to have an important role in preventing fibrosis resolution in the liver, it has an antiapoptotic effect on HSCs and activated HSCs are a source of TIMP-1, when a liver spontaneously recovers from fibrosis there is a corresponding decrease in TIMP-1 expression (Murphy *et al.*, 2002). It has been observed that during spontaneous resolution of liver fibrosis apoptosis of HSC occurs and they are cleared by natural killer cells (Weiner *et al.*, 1992, Ohata *et al.*, 1997, Iredale *et al.*, 1998, Krizhanovsky *et al.*, 2008). Recent research has also shown that HSCs can senesce as discussed in section 1.2.1.3, stopping their profibrogenic activity and returning to a quiescent state, which could also be an important factor in the reversal of liver fibrosis.

1.3 Liver disease

Activated HSCs are the major contributors to the hepatic scar, which, if it progresses, leads to cirrhosis. All chronic liver diseases can lead to fibrosis and eventually cirrhosis. The incidence of liver disease is increasing, and it is therefore important to understand the process of HSC activation and discover possible treatment targets like CYGB.

1.3.1 Overview of liver disease

Approximately 29 million people in Europe suffer from a chronic liver condition; liver cirrhosis is the cause of around 170,000 deaths, and liver cancer 47,000 deaths, per annum in Europe. Mortality from liver disease is comparable with other diseases that have a high degree of public and media attention, such as breast cancer (Blachier *et al.*, 2013). Effiong *et al.*, (2012) reported that deaths from liver disease in England are increasing. Between 2001 and 2009 there was a rise of 25% in deaths from liver disease, and liver disease now accounts for approximately 2% of deaths in England, this statistic contrasts with many other causes death due to disease which are in decline. Liver fibrosis is apparent in all chronic liver diseases, and fibrogenesis is the physiological response of the liver to insult or injury (Reeves and Friedman, 2002, Bedossa and Paradis, 2003), which can result in organ failure if not treated (Rojkind *et al.*, 2002).

1.3.2 Types of liver disease

The major causes of liver fibrosis in industrialised countries are HCV infection, excessive alcohol consumption and non-alcoholic steatohepatitis (NASH), liver diseases such as haemochromatosis and toxins, immune system disorders and parasitic infections are also prevalent (Reeves and Friedman, 2002). The development of liver fibrosis is determined by genetic as well as environmental factors (Bataller and Brenner, 2005). But, despite the different forms injury induction may take, the

response of the liver in terms of cellular behaviour and paracrine soluble factor release is similar (Reeves and Friedman, 2002). Table 1.1 outlines some of the major aetiologies and diseases associated with the development of liver fibrosis.

As well as the diseases outlined in Table 1.1, liver cancer is a major disease of the liver, responsible for around 47,000 deaths in the European Union per year and the mortality rate is close to the incidence rate as survival is low (Blachier *et al.*, 2013).

Primary research into HSC activation has the potential to identify targets for the treatment of liver disease. Factors important in the transition of HSCs from quiescent to activated could be targeted and manipulated to ameliorate ECM deposition and lessen fibrogenesis, or return activated HSCs to a quiescent state, preventing further deposition of ECM and assisting the process of fibrosis reversal. It is conceivable that CYGB could be one of these targets.

Table 1.1: Diseases of the liver

Disease	Pathogenesis	Epidemiology	References
Alcoholic Liver Disease (ALD)	Not completely understood, however involves metabolism of alcohol through cytochrome P450 2E1 producing reactive oxygen species (ROS) leading to lipid peroxidation, and also to acetaldehyde then acetate, which in turn leads to the production of nicotinamide adenine dinucleotide (NADH) inhibiting fatty acid oxidation.	Alcohol is the main cause of liver disease in England and Europe as a whole. Alcohol consumption increased and stabilised between 2004 and 2006 but there is great variation between countries.	(Forrest and Reed, 2011, Effiong <i>et al.</i> , 2012, Blachier <i>et al.</i> , 2013)
Alcoholic Steatohepatitis (ASH)	A subtype of ALD, ASH is the consequence of alcohol metabolism inhibition of fatty acid oxidation and lipid accumulation in the liver.	As with ALD	(Stickel and Seitz, 2010)
Non-Alcoholic Fatty Liver Disease (NAFLD)	Accumulation of fat in livers from dietary free fatty acids (FFAs) and FFA influx, and <i>de novo</i> lipogenesis due to insulin resistance (IR). Defined as the presence of steatosis in histological samples.	Considered the manifestation of IR in the liver 20% to 30% of those presenting NAFLD develop non-alcoholic steatohepatitis. 80-90% of NAFLD patients are obese adults. It is endemic in Europe and causes 0.1% of all deaths in England.	(Petta <i>et al.</i> , 2009, Bellentani <i>et al.</i> , 2010, Effiong <i>et al.</i> , 2012, Blachier <i>et al.</i> , 2013)

<p>Non-Alcoholic Steatohepatitis (NASH)</p>	<p>Pathogenesis of NASH is poorly defined. Fatty liver consequently leads to NASH, and a 'two-hit' model has been proposed. The first hit involving obesity, IR and adipokines and cytokines, and the second hit involving oxidative stress, apoptosis and endotoxins. NASH is defined as the presence of fatty degeneration of a liver biopsy sample with inflammation and with or without fibrosis.</p>	<p>Diagnosis requires a liver biopsy so prevalence in the general population is unknown, and the majority of patients are asymptomatic. But it is a progression from NAFLD.</p>	<p>(Powell <i>et al.</i>, 1990, Petta <i>et al.</i>, 2009, Khedmat and Taheri, 2011)</p>
<p>Viral Hepatitis</p>	<p>Inflammation of the liver due to one of five hepatitis viruses; hepatitis A (HAV) has mainly faecal-oral transmission through contaminated food and water, hepatitis B (HBV) transmitted through percutaneous and mucosal exposure to infected body fluids, hepatitis C (HCV) is transmitted through exposure to infected blood, hepatitis D (HDV) requires the presence of HBV to be</p>	<p>HAV: Global occurrence, but regions vary in severity, rarely fatal but has a substantial economic burden.</p> <p>HBV: One of the world's most widespread infections. 500,000-700,000 deaths are associated with HBV.</p> <p>HCV: Estimated 150 million people have a chronic HCV infection and 350,000 deaths a year are associated with HCV.</p> <p>HDV: Dual infection with</p>	<p>(Forrest and Reed, 2011, Chuang <i>et al.</i>, 2009)</p>

	<p>infective, hepatitis E (HEV) is also faecally transmitted as with HAV.</p> <p>All cause liver disease but vary in their epidemiology, prevention and diagnosis.</p>	<p>HBV produces worse patient outcomes.</p> <p>HEV: There are an estimated 3.4 million symptomatic cases, 70,000 deaths and 3000 still births associated with HEV per year.</p>	
Primary Biliary Cirrhosis (PBC)	<p>An auto-immune disease, and there is also evidence that genetic predisposition is a factor in development. Precise mechanisms are unknown, but there is a progressive destruction of biliary epithelial cells and therefore intra-hepatic bile ducts leading to liver cirrhosis and liver failure.</p>	<p>There is a predominance of PBC in women, but it is a rare disease in general. Progression is variable.</p>	(Blachier <i>et al.</i> , 2013)
Primary Sclerosing Cholangitis (PSC)	<p>Regarded as immune mediated, rather than auto-immune, PSC has an unknown aetiology, but it has an association with inflammatory bowel disease (IBD), toxic bile composition and genetic susceptibility. It is asymptomatic and differs in its manifestation.</p>	<p>PSC is rare, but has a greater prevalence in Northern and Nordic countries. It is predominant in young men, aged between 30 to 40yrs.</p>	(Stickel and Seitz, 2010, Blachier <i>et al.</i> , 2013)

Haemochromatosis	Haemochromatosis is associated with missense mutations in the 'High Iron' or HFE (Fe for iron) gene (chromosome 6p21.3) which facilitates and regulates iron transport in hepatocytes, and also hepcidin (a ferroportin degradation hormone) deficiency, leading to increased iron absorption and iron overload.	Haemochromatosis is rare and diagnosis often delayed. Gene homozygosity is most prevalent in north western European countries.	(Khedmat and Taheri, 2011)
------------------	--	--	----------------------------

1.4 Hypothesis, Aims and Objectives

Whilst no specific function for CYGB has yet been discovered, it appears to be linked to the fibrotic process within the liver due the reported changes in its expression in HSC on their activation, and could be an important target in the treatment of liver disease. It is feasible that ECM protein signalling may play a role in activation of HSCs and CYGB regulation via cell surface receptors. This study investigates the effect of cell culture on different common ECM proteins, on the activation state and Cygb expression in a model HSC lines HSC-T6 and LX-2.

1.4.1 Hypothesis

ECM environment affects HSC phenotype, activation state and Cygb expression within HSCs via cell surface receptor signalling.

1.4.2 Aims and Objectives

- To investigate the effect of culture on different ECM proteins on HSC phenotype, activation state and Cygb expression.
- To investigate the signalling method by which any effect is occurring.
- To investigate Cygb expression in *in vivo* liver injury

Chapter 2

Materials and Methods

2.1 Chemicals and consumables

Unless otherwise stated, all chemicals and consumables were purchased from Sigma-Aldrich-UK.

2.2 Cell lines

2.2.1 HSC-T6 cell line

The HSC-T6 cell line was developed in the Friedman Laboratories due to the need for an immortalised HSC cell line and was first reported by Friedman *et al.* (1997). HSC-T6s were created from isolated primary stellate cells from male Sprague Dawley rats, maintained as a primary culture for 15 days on plastic dishes. After 15 days approximately 2×10^6 were transiently transfected with lipofectamine containing cDNA, then after 5-7 days emerging clones were harvested and plated, and single cell clones were isolated and amplified without the use of antibiotic selection. Of more than 20 clones the one labelled HSC-T6 was expanded for further characterisation based on preliminary cytoskeleton analysis, revealing the clone phenotype was closest to isolated primary stellate cells. These cells were maintained in culture with 10% foetal bovine serum (FBS), penicillin-streptomycin (100 μ l/ml and 100mg/ml, respectively). The phenotype has been reported as stable over forty passages (Vogel *et al.*, 2000). HSC-T6 exhibit an activated phenotype, supported by their fibroblast-like shape and rapid proliferation in culture. They also express cytoskeleton proteins typical of stellate cells in the active state, such as desmin α SMA, glial acidic fibrillary protein and

vimentin. HSC-T6 also show retinoid-related parameters similar to those of freshly isolated quiescent rat HSC including expression of all six nuclear retinoid receptors (Vogel *et al.*, 2000). HSC-T6 cells were kindly provided by Francis Chang at the Institute of Cancer Research, Royal Cancer Hospital.

2.2.2 LX-2 cell line

LX-2 cells are immortalised human hepatic stellate cells, developed due to the paucity of human tissue for research purposes, coupled with low yields of HSC when isolated from a liver. HSC were isolated from liver tissue wedges as described by Friedman *et al.* (1992). Cells were passaged three times, plated at 40% confluency for 24hrs, then transfected with pRSVTag encoding for SV40 large T antigen with RSV promoter and cultured for 24hrs. The cells were maintained for seven passages until morphologically distinct and more proliferative than normal passaged cells. The LX-1 cell line was then established from a single clone and the LX-2s by selecting a subculture of LX-1s with the ability to grow in reduced serum culture, then growing on a single clone from that culture. LX-2s express α SMA and are stimulated by PDGF and TGF- β 1, they also express discoidin domain receptor 2 (DDR2), pro-matrix metalloproteinase 2 (MMP-2) and relatively small amounts of tissue inhibitors of metalloproteinase 2 (TIMP-2) protein and α 1(1) procollagen mRNA. LX-2s also have the ability to metabolise retinoids (Golubovskaya *et al.*, 2008). LX-2 cells were kindly provided by Christopher Weston, IBR, University of Birmingham.

2.2.3 Primary rat HSCs

Primary rat HSC cells were a kind gift from Rebecca Aucott from the School of Clinical Sciences at the University of Edinburgh. HSCs were isolated from one female Sprague Dawley rat. The liver was harvested, cut into ~2-3mm pieces and digested at 37°C with collagenase, pronase and DNase for ~20mins. Then the tissue was filtered through a Nybolt mesh, and a density gradient set up using optiprep. After centrifugation the top cell fragment was plated onto T₇₅ flasks, cultured for ~14days (Iredale et al., 1998).

2.3 Continual Cell Culture

Cell culture was undertaken in a class II tissue culture hood (Aura B4, Bio Air, Italy) under sterile conditions. Chemicals and consumables were purchased sterile or autoclaved before use in cell culture.

Cells were cultured in Dulbecco's Modified Eagle's Medium (DMEM) - high glucose supplemented with 10%(v/v) foetal bovine serum FBS for HSC-T6s, 2%(v/v) FBS for LX-2s and 20% FBS (v/v) for primary HSCs , 1% v/v penicillin/streptomycin (10,000 units penicillin, 10mg streptomycin per ml in 0.9% NaCl) (PAA, Somerset, UK), 1% v/v L-glutamine 200mM (100x) (PAA, Somerset, UK) and 1% v/v MEM non-essential amino acids (100x), in BD Falcon tissue culture treated T₂₅ Flasks with vented caps. Cells were maintained at 37°C in 5% CO₂ (MCO-15AC, Sanyo, Japan) and passaged at confluence.

2.3.1 Cell Cryopreservation

Cells were trypsinised (trypsin-EDTA 1x solution), resuspended in 1ml complete media and centrifuged for 3 min at 900 rcf (Rotofix 32, Hettich Zentrifugen, Germany) at room temperature. Media was removed and replaced with 3 ml freezing mix (FBS containing 1% v/v sterile dimethyl sulfoxide [DMSO]). Cells were resuspended and transferred to 1ml cryovials (Nalgene, USA) and placed in a Mr Frosty (Nalgene, USA) and stored at -80°C for 24hrs before transferring them to vapour phase liquid nitrogen for long term storage.

2.4 Culture on different ECM proteins

HSC-T6 cells were cultured as described above in section 2.3.3 until enough cells were accumulated for experimental purposes. Cells were then trypsinised for 5 min at 37°C, pooled in serum containing media and spun down at 900 rcf for 3min. Cells were resuspended in 1ml of media and a cell count was taken using a haemocytometer to determine cell density. Cells were diluted to 100,000 cells/ml for HSC-T6s and primary rat HSCs and 300,000 cells/ml for LX-2s and 5 ml of cell suspension was added to each T₂₅, 2 ml per well of a 6-well plate, 1 ml per well of a 12-well plate. Four different ECM protein surfaces were tested: collagen I, collagen IV, laminin and fibronectin (BD BioCoat), alongside normal non-coated T₂₅ flasks. Gelatin was also tested as a coating in an addition to the ECM proteins as it is denatured collagen and there is increasing research around fibrosis resolution and matrix degradation (section 1.2.4) (Friedman,

2008c, Ramachandran and Iredale, 2012). Non-coated flasks were coated with sterile 0.1% gelatin solution and incubated at 37°C for 30 min, any remaining liquid was aspirated off and the flask was washed with phosphate buffered saline (PBS). Cells were grown for 48hrs on each surface and then passaged back onto the same surface over three passages. After 48hrs of culture, cells were trypsinised and a cell count undertaken to determine final cell density per flask. In some experiments collagen I solution from rat tail was either diluted into culture media at 10, 20, 40 or 60 µg/ml, or used to coat plates at 0.4, 0.8, 1.8, 2.4, 6 and 10 µg/cm². The collagen coating procedure is described in section 2.4.1. Some experiments also required coating of the culture surface with laminin (UltraPure, BD Bioscience), this procedure is detailed in section 2.4.2 Cells were then cultured for 48 hours and RNA was extracted for real-time polymerase chain reaction (RT-PCR) or whole cell protein was extracted for analysis by western blot (see section 2.12). To investigate the possible interaction between collagen I and laminin, six well plates were coated with different amounts of collagen I and laminin as follows – 10:0, 10:5, 10:10, 5:10 and 0:10 µg/cm² collagen I: laminin, in these cases, the collagen I coating procedure was followed.

2.4.1 Collagen coating procedure

Stock collagen I solution from rat tail was diluted to the required concentration in sterile tissue grade water and was then added 6 well plates for the correct concentration per cm², and incubated for 8hrs at room temperature. The excess fluid was removed and the plates dried overnight. The plates were then washed with PBS

before cells were seeded on to them.

2.4.2 Laminin coating procedure

Laminin was diluted to the required concentration in serum free culture medium and the appropriate volume added to the 6-well plate for the correct concentration per cm^2 . The plates were then incubated for 1 hr at room temperature. The remaining fluid was aspirated off and the plates washed with PBS. Cells were then seeded in to the plates.

2.4.3 Mixed matrix effects on HSC-T6 cells

Six well plates were coated as described in section 2.4, HSC-T6 cells were seeded at 100,000cell/ml, 2 ml per well and cultured for 48hrs then images were taken.

2.5 Cell imaging using Light Microscopy

Cells were imaged on a Nikon Eclipse TS100 light microscope and pictures taken using a Canon EOS 7D digital camera 24hrs post seeding at 40x and 400x magnification. Images were enhanced using the one step Photo Fix function on Jasc Paint Shop Pro V 9.00.

2.6 Retinoic Acid uptake on different culture surfaces

Glass coverslips were coated with 10 $\mu\text{g}/\text{cm}^2$ of either collagen I or 5 $\mu\text{g}/\text{cm}^2$ laminin (described in section 2.4) or sterilised and put into a well of a six well plate. Cells were seeded at 100,000 cells/ml, 2ml per well for HSC-T6s, or 300,000 cells/ml, 2ml per well for LX-2s, all *trans* retinoic acid (ATRA) was diluted to 1 μM into the culture media and cells were cultured for 48hrs. Cells were fixed in 4% paraformaldehyde and the coverslips mounted onto microscope slides using hydromount. Cells were imaged using a Leica TSC SP2 confocal microscope (Leica Microsystems) using a 63x oil immersion objective NA 1.32, retinoids were excited with an argon laser at 351 nm and emission detected at 515 nm. All images were processed in an identical manner using AdobePhotoshop PS3E.

2.7 Ribonucleic acid isolation

Total ribonucleic acid (RNA) was isolated using Qiagen RNeasy Miniprep Kit including a QiaShredder step and a DNase I step (Qiagen). Briefly, cells were washed with PBS then trypsinised at 37 °C for 5 min. Cells were then collected into a 1.5 ml microcentrifuge tube in 1 ml of serum containing media and centrifuged at 4000 rcf for 4 min. The supernatant was removed and cells were disrupted in 350 μl of Buffer RLT containing 2-mercaptoethanol (10 $\mu\text{l}/\text{ml}$). The lysate was then pipetted into a QiaShredder and centrifuged for 2 min at 13,200 rpm. After the addition of 70% ethanol in a 1:1 ratio the sample was then added to an RNeasy spin column and centrifuged at 9,200 rpm for

30 sec. The sample was washed with 350 μ l RW1 buffer and centrifuged as before. The DNase I step was then executed, 10 μ l of reconstituted DNase was diluted in 70 μ l RDD buffer, and this was then added to the spin column and incubated at room temperature for 15 min. The sample was then washed with RW1 buffer as previously described. The sample was then washed twice with 500 μ l RPE buffer, once as previously described with RW1 buffer, then centrifuged for 2 min at 9,200 rpm. The column was then dried by centrifugation at 13,200 rpm for 1 min and RNA eluted into 30 μ l RNase-free water by centrifugation for 1 min at 9,200 rpm. RNA was quantified spectrophotometrically on a Nanodrop ND1000 and stored at -80 °C.

2.8 Complementary DNA synthesis

Complementary DNA (cDNA) was synthesised using Agilent Affinity Script Multitemp cDNA synthesis kit utilising oligo (dT) primers (Agilent, UK). Briefly, 0.5 μ g of isolated RNA was added to 1.0 μ l of oligo (dT) primer (0.5 μ g/ μ l) and the reaction volume made up to 15.7 μ l with RNase-free water. The primers were annealed to the RNA by incubating the sample at 65° C for 5 min and cooled at room temperature for 10 min. The following components were then added to each sample, in order: 2.0 μ l of 10 \times AffinityScript RT buffer, 0.8 μ l of dNTP (deoxynucleotide triphosphates) mix (25 mM each dNTP), 0.5 μ l of RNase Block Ribonuclease Inhibitor (40 U/ μ l) and 1 μ l of AffinityScript Multiple Temperature RT for a final reaction volume of 20 μ l. The samples were then incubated for 1 hr at 45 °C then the reaction was terminated by incubation at 70 °C for 15 min. The samples were then cooled and stored at -80 °C until

required.

2.9 Quantitative RT-PCR

RT-PCR was conducted using 500 ng cDNA, 1 μ l primer-probe (Applied Biosystems or Primer Design) and 10 μ l qPCR Brilliant III Ultra-Fast QPCR MasterMix (Agilent), made up to 20 μ l with RNase-free water (Qiagen). The RT-PCR run then consisted of one cycle at 95 °C for 3 min, then 50 cycles of 95 °C for 20 sec then 60 °C for 20 sec, during which the data was gathered. Table 2.1 shows the TaqMan-style primer sequences. All primer-probes were FAM labelled except for *hexokinase 1 (HK1)* which was VIC labelled. *HK1* was chosen as the housekeeping gene for RT-PCR experiments based on the findings of Wang and Xu (2010), who investigated the expression stability of six common house-keeping genes in eight types of hepatic cells, including HSCs, isolated at different time points from a liver regenerating after partial hepatectomy. *HK1* was found to be the most stable gene, along with *β -Actin*, in HSCs. Amplification of the housekeeping gene, *HK1* was conducted simultaneously with target gene amplification, reactions were undertaken in triplicate and Cts averaged across a sample.

2.10 Proliferation Assay

2.10.1 HSC-T6 manual count time-course

Cells were seeded at a density of 100,000 cells/ml for HSC-T6s and 300,000 cells/ml for LX-2s and 5 ml put into a collagen I coated (BD BioCoat) or non-coated (BD

Biosciences) T₂₅. Cell counts were taken using a haemocytometer at 8, 24, 32 and 48 hr post seeding by trypsinising the cells and centrifuging them as described in section 2.3. Cells were then resuspended in 1 ml of media, 100 µl was added to a solution containing 100 µl Trypan Blue and 800 µl PBS. This cell suspension was mixed well then 20 µl was added to both chambers of the haemocytometer. Five counts from each chamber were taken and averaged and total cell density per flask determined.

2.10.2 Cell IQ analysis for HSC-T6 cells and LX-2 cells

HSC-T6 cells were seeded 100,000 cells, and LX-2 cells at 300,000 cells, per well on collagen I coated, laminin coated or non-coated wells of a 24-well plate, coating with matrix protein was conducted as described in section 2.4.1 and 2.4.2. Cells were allowed to settle for 10 min at room temperature and then placed in the CellIQ (C M Technologies, UK) at 37 °C, 5 % CO₂ for 72 hrs, images of the cells were taken every 15 sec. CellIQ Analyser software was used to create videos and estimate cell number across the culture period.

Table 2.1: Details Of TaqMan Style Primer-Probes used in this Study

Gene	Species	Company	Forward (Sense)	Reverse (Anti-sense)
<i>Cytoglobin (Cygb)</i>	Rat	Applied Biosystems	n/a Unique Assay ID: Rn00590627_m1	
		Primer Design Ltd	CCCCGTGTGTACCCCTTG	AAAGACAGGCAGTTACAGGAAG
<i>α Smooth Muscle Actin (αSMA)</i>	Rat	Applied Biosystems	n/a Unique Assay ID: Rn01759928_g1	
<i>Discoidin Domain Receptor 1 (DDR1)</i>	Rat	Primer Design Ltd	TGATTACAGACTACATGGAGAACG	GGAAGCCCCTGAGTGAAC
<i>Discoidin Domain Receptor 2 (DDR2)</i>	Rat	Primer Design Ltd	TCATCCTGCTGGCTGTCAT	GCTAACTGTCATTTTCATCATCCA
<i>Integrin Beta 1 (β1)</i>	Rat	Primer Design Ltd	TCTGATGAATGAAATGAAATGAGGAGGAT	TTGCTGGTGTTGTACTAATGTATG
<i>Integrin alpha 11 (α11)</i>	Rat	Primer Design Ltd	CCTCTGCTTCGGACCTATCTT	CCGTGGCATATACCGTCTCT
<i>Integrin alpha 2 (α2)</i>	Rat	Primer Design Ltd	CAGCACCAGTTTCTTG AAGGA	GCGAACCAACAATCACATCATT
<i>Integrin Beta 4 (β4)</i>	Rat	Primer Design Ltd	CAGGGTGGAGAAGAC TACGA	ACCAGGTGCTCAGTGT CAT
<i>Integrin alpha 6 (α6)</i>	Rat	Primer Design Ltd	CCGCCGCTCAGAATAT CAAG	CCACCACGCTATCCCTGAA
<i>Integrin alpha 5 (α5)</i>	Rat	Applied Biosystems	n/a Unique Assay ID: 01761831_m1	
<i>Focal Adhesion Kinase (Ptk2)</i>	Rat	Primer Design Ltd	AGTGAAGACAAAGAC AGGAAAGG	GATCAGGTCCAGCCATGTTCTC
<i>Integrin Beta 3(β3)</i>	Rat	Applied Biosystems	n/a Unique Assay ID: 00596601_m1	
<i>Hexokinase 1 (HK1)</i>	Rat	Applied Biosystems	n/a Unique Assay ID: Rn00562436_m1	
		Primer Design Ltd	CCCTGCCGAATCCAAG A	CATCATAGTCCCCTCGCTTCT

2.11 Whole Cell Protein Isolation

2.11.1 Buffers

6x laemmli buffer: 418 mM SDS (sodium dodecyl sulfate), 867 μ M bromophenol blue, 47 % v/v glycerol, 60 mM Tris-HCl pH 6.8, 1.6M 2-mercaptoethanol, made up to volume with ddH₂O and stored at -20 °C.

RIPA buffer: Tris-HCl pH 7.5 (25 mM) NP-40 (1 % v/v) NaCl (150 mM), sodium dodecyl sulfate (0.1 % v/v), sodium deoxycholate (1% w/v) and mammalian protease cocktail inhibitor (10 μ l/ml).

2.11.2 Procedure

HSC-T6 cells were seeded at 100,000 cells/ml, 2 ml per well, and cultured on noncoated or collagen I coated (BD BioCoat) six well plates for 48 hrs. For analysis of Cygb protein cells were lysed directly in RIPA buffer, incubated on ice with agitation of 15 min, centrifuged for 10 min at 4°C and the supernatant removed and stored at -80°C until required. For analysis of phosphorylated focal adhesion kinase (pFAK) protein was extracted directly into 500 μ L 6x Laemmli Buffer warmed to 60 °C, by means of a cell scraper. Samples were sonicated 4 times and heated to 95 °C for 3 min and stored at -80 °C until required.

2.11.3 Bradford assay for protein quantification

Estimates of protein concentration from whole cell extracts into RIPA buffer were undertaken using the Bradford method (Bradford, 1976), using BSA (1-10 µg) as a standard.

2.12 Western blot for Cygb and phosphorylated FAK

2.12.1 Buffers

1X TBS: Tris base (20 mM) and NaCl (0.15 M), adjusted to pH 7.5

1X TBS-0.05% Tween 20: Tris base (20 mM), NaCl (0.15 M) and Tween 20 (0.05 %), adjusted to pH 7.5.

SDS-PAGE running buffer: Tris base (25 mM), glycine (192 mM), and SDS (0.1 %).

Transfer buffer: Tris base (20 mM), glycine (150 mM) and methanol (20% v/v).

Blocking buffer: Low-fat powdered milk (Marvel, U.K.), or bovine serum albumin (BSA), (5% w/v) in 1X TBS-0.05 % Tween 20

2.12.2 Gels

12.5 % Resolving gel: Acrylamide:bisacrylamide 30 % solution (12.5 %) (Geneflow, UK) Tris-HCl pH 8.8 (375 mM), (Fischer Scientific, UK) SDS (0.1 %). Immediately prior to casting N,N,N,N-tetramethylethylenediamine (TEMED) (15 µl per 10 ml) and 10% w/v

ammonium persulfate (APS) (150 μ l per 10 ml) were added.

2.12.3 Assay procedure

For protein analysis by western blot, either 30 μ l of protein extract for pFAK investigation, or 20 μ g total protein in RIPA buffer, incubated for 5 min at 95 °C with laemmli buffer diluted to 1x concentration, for Cygb investigation, was resolved on a 12.5 % SDS-PAGE electrophoresis gel at 120 V for 90 mins and transferred to a PVDF (polyvinylidene difluoride) membrane (Millipore) by means of a mini trans-blot electrophoretic transfer cell (Bio-Rad), at 100 V for 120 min at 4°C. Blocking was achieved by incubating the PVDF membrane with blocking buffer, for 16 hrs at 4°C for pFAK or 1hr at room temperature for Cygb, on a rocking platform (Stuart Scientific STR9, U.K.). The membrane was then incubated with polyclonal antibody (Ab) against Focal Adhesion Kinase (FAK) pY397 raised in mouse (BD Bioscience) 1:500 diluted in blocking buffer or polyclonal Ab against Cygb raised in rabbit (Santa-Cruz) 1:200 or polyclonal Ab against β Actin raised in mouse (Sigma) 1:10000 diluted in blocking buffer, for 1 hour at room temperature for pFAK and β -actin, or overnight at 4 °C for Cygb, on a rocking platform at room temperature. The membrane was washed three times in 1X TBS-0.05% Tween 20 solution for 10 min each time, then incubated with a horseradish peroxidase (HRP)-conjugated anti-mouse secondary antibody (1:500 dilution, DAKO, U.K.) for pFAK and β -actin or conjugated anti-rabbit antibody (1:1000 dilution, DAKO, UK) in blocking buffer at room temperature for 1hr. 1X TBS-0.05% Tween 20 solution was used to wash again (2 \times 10mins), followed by a final wash in 1X

TBS for 10min. The membrane was then incubated with SuperSignal West Pico Enhanced Chemiluminescence (ECL) Substrate (Thermo Scientific) for pFAK and β -actin, or Westar Supernova Femto ECL Substrate (Geneflow, UK) for *Cygb* prepared as per manufacturer's instructions. Protein bands were visualised via exposure to ECL hyperfilm (Amersham Biosciences) and development in an X-ograph machine (AGFA Curix60).

2.13 Exploration of the effects of collagen I

Several assays were conducted to explore the effects of collagen I on *Cygb* expression in HSC-T6 cells, a time course was conducted over 48 hrs, with cell counts and RNA extracted as previously described in 2.7, at 8, 24, 32 and 48 hr. Cells were seeded at a density of 100,000 cells per ml, 5ml per flask onto non-coated (BD Biosciences) or collagen I coated T₂₅ flasks (BD BioCoat). RT-PCR was conducted as described in sections 2.8 – 2.9.

Two concentration response assays were conducted to investigate whether attachment to collagen was necessary for the effects on *Cygb* to occur. Collagen I solution from rat tail was either diluted into culture media at 10, 20, 40 or 60 $\mu\text{g/ml}$, or coated on to 6 well plates (BD) at 0.4, 1.8, 2.4, 6 or 10 $\mu\text{g/cm}^2$, as described in section 2.4.1. Cells were cultured for 48 hrs and RNA was extracted as in 2.7 and RT-PCR conducted as in 2.8 and 2.9, RNA from cells grown on a pre-coated collagen I (BD BioCoat) positive control was also extracted.

2.14 pFAK expression and pFAK Inhibition Assays

MTT cell viability studies were conducted using FAK Inhibitor 14 (FAKI) (Tocris) prior to flow cytometry and confocal microscopy investigation.

2.14.1 4 3-(4,5-Dimethyl-2-thiazolyl)-2,5-diphenyl-2H-tetrazolium bromide (MTT) reduction assay

MTT is a water soluble dye, which is yellow in colour and able to cross cell membranes. In the cell it is reduced by mitochondrial succinate dehydrogenase producing an insoluble crystalline formazan product. When dissolved in DMSO the formazan crystals form a purple solution allowing quantification of cell viability via a colorimetric assay, by measuring the absorbance of the solution between 500 and 570 nm. The greater the absorbance reading, the greater the number of viable cells.

2.14.2 Assay procedure

Cells were seeded at 100,000 cell/ml, 100 μ l per well of both a non-coated (BD) and a collagen I coated (BD BioCoat) 96 well plates. Cells were incubated with either 0, 1, 10, 50 or 100 μ M, or 0, 0.05, 0.1, 0.5 or 1 μ M FAK Inhibitor 14 (FAKI) for 46hrs. Cells were washed with PBS (200 μ l) and 100 μ l fresh medium was added along with 10 % 3-(4,5-Dimethyl-2-thiazolyl)-2,5-diphenyl-2H-tetrazolium bromide (MTT) (0.5 mg/ml final concentration). Following incubation at 37 °C for hrs in a humidified chamber the medium was removed and DMSO was added (200 μ l) to dissolve the blue formazan

product. The absorbance was determined immediately at 570 nm using a Bio-Tek FL600 plate reader (Bio-Tek Instruments Inc. U.S.A.) against a DMSO blank. Concentrations 0.1, 0.5 and 1 μ M were then taken forward to confocal microscopy and flow cytometry analysis, with cell cultured on non-coated (BD) or collagen I coated (BD BioCoat) 6-well plates.

2.14.3 Flow cytometry for pFAK and FAKI

HSC-T6 cells were cultured as described in section 2.4 on non-coated and collagen I coated plates. FAKI diluted to the desired concentration was added to the media for the final 24 hrs of culture. At 48hrs cells were trypsinised, centrifuged as before and resuspended in 4 % paraformaldehyde for 1 min on ice. Cells were then spun down and the fixative removed and replaced with 90 % methanol at -20 °C for 10 min, and stored at 20 °C until required.

For analysis by flow cytometry, 2 ml of blocking buffer (3 % FBS in PBS) was added to the cell suspension and cells were rinsed by centrifugation (3 min at 900 rcf) twice. Cells were blocked by incubation in 100 μ l blocking buffer for 10 min with agitation. pFAK Y397 Ab (BD Bioscience) was added to a final concentration of 1 μ g/ml and sample were incubated at room temperature for 1 hr. Samples were then rinsed by centrifugation as before, then 100 μ l of FITC (fluorescein isothiocyanate) conjugated anti-mouse 2° Ab (Dako, UK) diluted 1:20 in incubation buffer was added and samples were incubated in the dark for 30 min at room temperature with agitation. Cells were

then rinsed as before and resuspended in 500 μ l PBS for analysis by flow cytometry. FITC fluorescence of 10,000 live cells was analysed using a BD FACScalibur™ (BD Bioscience) and Weasel software (Walter and Elisa Hall Institute of Medical Research, Australia) was used for data analysis.

2.14.4 Confocal microscopy for pFAK and FAKI

Cells were set up as described in 2.14 and were grown for 48 hrs or treated with FAK I as outlined in section 2.14.2. Cells were then fixed as described in section 2.14 and permeabilised with 4 °C 90 % methanol and washed with twice with PBS. Samples were then blocked in blocking buffer for 30 min at room temperature on a rocker. Blocking buffer was removed and cells were incubated with pFAK Y397 (BD Bioscience, UK) 1°Ab diluted to 5 μ g/ml for 1 hr at room temperature. Samples were then rinsed twice in incubation buffer and incubated in the dark in FITC conjugated anti-mouse 2°Ab (Dako, UK) diluted 1:200 in blocking buffer for 1 hr at room temperature. Cells were then rinsed three times in PBS and the nuclei were counter-stained by adding 200 μ l of 2 μ g/ml Hoechst 33342 in 1 \times PBS 15min before imaging. Slides were mounted using 50 μ l of hydromount and stored in the dark at 4 °C until required. Cells were then imaged on the Leica confocal microscope (Leica Microsystems) using a 63x oil immersion objective NA 1.32, the excitation wavelength was 405 nm for Hoechst 33342 and 488 nm for FITC. All images were processed in an identical manner using Adobe Photoshop PS3E.

2.15 Intracellular ROS assay with 2',7'-dichlorodihydrofluorescein diacetate (H₂DCF-DA)

Cells were seeded 100,000 cells/well on collagen I coated, laminin coated or non-coated wells of a 24-well plate, coating with matrix protein was conducted as described in section 2.4.1 and 2.4.2, and grown for 45 hrs. Positive control wells were then treated with 10 μ M H₂O₂ for 1hr. At 46hrs H₂DCF-DA was added to the wells to a final concentration of 10 μ M and cells were incubated for 2 hrs at 37°C. Cells were then trypsinised for 10 min at 37°C to obtain a single cell suspension, then the cells were pelleted by centrifugation for 3 min at 900 rcf. The cell pellet was resuspended in 1 ml of PBS and the samples analysed for fluorescence as described in section 2.14.3.

2.16 RNA inhibition (RNAi) of FAK

2.16.1 Optimisation of RNAi

HSC-T6 cells were seeded at 50,000, 100,000 or 200,000 cells/ml, 2 mls per well in antibiotic-free culture media, in a non-coated 6-well plate and cultured for 24hrs before transfection with short interfering RNA (siRNA) - either targeting *FAK* (*Ptk2*), non-targeting negative control (NT2 and NT4) (Thermo Scientific, UK) or untreated. Resuspension of siRNA was conducted according to instructions; tubes were briefly centrifuged resuspended in 1x siRNA buffer (5x siRNA buffer [Thermo Scientific, UK] diluted 1:5 with RNAase-free sterile water [QIAGEN, UK]) to a final stock concentration of 20 μ M. The solution was pipetted up and down 3–5 times, and placed a shaker for 90min at room temperature. Tubes were centrifuged and aliquoted for storage at -

20°C until required. siRNA was prepared as recommended in Opti-MEM 1 media (Life Technologies, UK) and DharmaFECT solution 1 (Thermo Scientific, UK). For optimisation, four different volumes of DharmaFECT were tried—1, 2, 4 and 6 µl. Stock siRNA was diluted to 5 µM in Opti-MEM and then further diluted 1:20, 200 µl of this solution was used per well. In a separate tube, the appropriate volume of DharmaFECT was prepared in Opti-MEM, for a final volume of this solution of 200 µl per well. The tubes were mixed by pipetting then incubated at room temperature for 5min, then the two tubes were combined for a final volume of 400 µl per well. This solution was mixed by pipetting and incubated a room temperature for 20 min, and then 1600 µl of antibiotic-free culture media was added for a final siRNA concentration of 25 nM. Culture media was replaced with transfection media and cells were cultured for 24 hrs, transfection media was then replaced with culture media and culture continued for a further 24 hrs. RNA was then extracted as described in section 2.7 and RT-PCR conducted as outlined in section 2.8 and 2.9 to determine optimal RNAi conditions.

2.16.2 Optimised RNAi

Results of the RNAi optimisation experiment revealed that 4µl of DharmaFECT and 200,000 cells/ml provided optimal conditions of interference of Ptk2 RNA with the fewest off-target effects. Therefore, these conditions were used in all future experiments, where cells were set up as described in section 2.16.1, but cultured on a collagen I coated surface (see section 2.4.1) as well as non-coated plastic. The experiment was continued as described in 2.16.1 and then RNA extracted as described

in section 2.7 and RT-PCR conducted as outlined in section 2.8 and 2.9, samples were then analysed for FAK and *Cygb* expression.

2.17 *In vivo* mouse models of liver disease

RNA samples from mouse models of liver disease were a kind gift from Dr Christopher Weston from the University of Birmingham. Details of the disease models and sample preparation are given below. Animal studies were performed in accordance with the UK Animals (Scientific Procedures) Act of 1986 with approval granted by the UK Home Office (project license PPL 40/3201, Shrewsbury office) (Weston et al., 2014).

2.17.1 CCl₄-induced liver fibrosis in murine models

Mice were maintained under conventional conditions at the Biomedical Services Unit, University of Birmingham, and in accordance with the UK Animals (Scientific Procedures) Act of 1986 and were injected twice weekly for 8 weeks with either CCl₄ (1.0 ml/kg CCl₄ diluted 1:4 in mineral oil) or mineral oil alone as a control. Animals were sacrificed 96hr after the final dose of CCl₄ by cervical dislocation after withdrawing blood samples by cardiac puncture during isoflurane anaesthesia. Livers were dissected and tissue was stored in RNeasy (Qiagen, UK) until RNA extraction was conducted.

2.17.2 Murine models of steatohepatitis

Mice were maintained as described in section 2.17.1, there were five mice housed per cage at 23°C under an alternating light-dark cycle of 12hrs duration. For methionine choline deficient diet (MCD) induced liver disease mice were fed the MCD diet (MP Biomedicals, UK) *ad libitum* for 4-6 weeks. For the western lifestyle model of liver disease (WLM) mice were fed a diet consisted of 45 % calories coming from fat, and 30% of the fat was in the form of partially hydrogenated vegetable oil (Harlan Laboratories, US. Custom Research Diet TD.06303), these mice also received fructose supplemented drinking water (55 % fructose, 45 % glucose by weight at a concentration of 42 g/L) *ad libitum* for either 6, 9 or 12 months. Control animals received normal chow (NC) and non-supplemented drinking water. Mice were sacrificed and livers processed as stated in section 2.17.1.

2.18 Protein and RNA extraction from human liver tissue

Protein was extracted from human liver tissue blocks weighing 70-90 mg. Samples were cut, placed into separate M-tubes (MiltenyiBiotec) and cells lysed in 20 µl of CelLyticMT buffer per mg tissue containing 1x protease inhibitors (Complete ULTRA, Roche, 2x stock made from 1 tablet in 5 ml CelLytic MT), 1x PhosSTOP phosphatase inhibitor (Roche, 10x stock made from 1 tablet in 1 mL CelLytic) and 5 U/ml DNase-I (Roche on program Protein-01 in GentleMACS (MiltenyiBiotec). Extracts were then centrifuged at 1000 x g for 2 min, to collect the protein sample. The whole supernatant

was then transferred to a labelled microcentrifuge tube and placed on a Vibraplatform at 4 °C to shake the samples for 1 hr. The suspension was centrifuged in a microcentrifuge at 13,000 rpm for 10 mins, and the supernatant was then transferred to a clean microcentrifuge tube and kept on ice, the volume was made up to 500 µl with CelLyticMT. Protein concentration was determined using the BCA/Biuret assay and samples stored in aliquots at -80 °C.

For RNA extraction ~20 mg of tissue was cut and transferred to a gentleMACS M-tube. A Qiagen RNEasy kit was used to extract RNA, 600 µl of RLT buffer (containing 2-mercaptoethanol) and the tissue was disrupted using the GentleMACS. Samples were centrifuged at 800 x g for 2 mins and transferred to a microcentrifuge tube then centrifuged again at top speed for 3 mins. The supernatant was transferred to a new microcentrifuge tube and 1 volume of 70 % ethanol was added and mixed immediately by pipetting. 700 µl of sample, including precipitate, was transferred to a mini column in a 2ml collection tube. Samples were spun at >8000 x g for 15 secs, and flow through discarded, 350 µl buffer RW1 was added and samples were centrifuge for 15 secs at >8000 x g. 10 µl DNaseI was added to 70 µl buffer RDD and mixed by inverting, the DNase I mix was applied to the RNeasy spin membrane and incubated at room temperature for 15 mins. 350 µl buffer RW1 was added to the samples and they were centrifuged for 15secs at >8000 x g. Flow through was discarded and 500 µl buffer RPE was added to the sample and it was centrifuged for 15 secs at >8000 x g. Flow through was discarded, 500 µl buffer RPE added and samples were centrifuged for 2 mins at >8000 x g. The spin column was transferred to a new 2 ml tube and centrifuged at full

speed for 1min to dry the column. The column was then transferred to 1 ml collection tube. 40 µl of RNase-free water was added directly onto the silica-gel membrane and samples were spun for 1min at >8000 x g, this process was repeated, the concentration of RNA was determined and samples were stored at -80 °C until needed.

2.19 Human tissue section staining

After local ethics committee approval, human tissue and blood samples were collected from consenting patients attending the University Hospitals Birmingham and Newcastle upon Tyne Hospitals NHS Foundation Trusts. Tissue samples were obtained from patients, in accordance with local ethics committee approval (REC reference, 06/Q2702/61) with informed consent. Liver tissue that was surplus to surgical requirements from explanted livers for a normal organ donor, or from uninvolved liver removed at hepatic resection for secondary liver tumours; Patients undergoing liver transplantation for chronic liver disease provided diseased tissue.

Acetone fixed, fresh frozen sections (10 µm thickness) from normal and diseased livers were defrosted and warmed to room temperature. They were immediately refixed in acetone for 5 mins and transferred into TBS-Tween buffer (TBS pH 7.6 + 0.05 % Tween20) for 5 mins. The Endogenous peroxidases were blocked by incubation with 0.3% hydrogen peroxide in methanol and slides were washed in TBS-Tween buffer for 5mins. Samples were then incubated for 20 mins in normal blocking serum (10 % FCS in TBS Tween), then 1°Ab in TBS Tween buffer plus 2% FCS in a humidified chamber, overnight at 4°C (Cygb – Santa Cruz 0.2 mg/ml stock 1:200 dilution, IgG - rabbit control

0.2 mg/ml stock 1:200 dilution). Slides were then washed twice for 5mins in TBS-Tween buffer and incubated for 30mins with ImmPRESS rabbit/universal reagent (Vector Labs) then washed as before. NovaRed (Vector Labs) reagent was prepared according to manufacturer's instructions; 3 drops of reagent 1 was added to 5ml of distilled H₂O and mixed well then 2 drops of reagent 2 were added and mixed, 2 drops of reagent 3 were added and mixed and finally 2 drops of H₂O₂ were mixed in. Sections were incubated in NovaRed until desired intensity developed (between 10 and 30 mins) and sections washed in TBS Tween as before. Slides were counter-stained with Mayers haematoxylin for 30secs and rinsed in tap water. Finally sections were dehydrated through alcohol and clearene, mounted with DPX (Distrene 80, Plasticizer and Xylene) mountant and left to dry. Stained sections were visualised using a Zeiss Axioskop 40. Images were captured with an AxioCam MRc5 and subsequently processed with AxioVision software (Carl Zeiss MicroImaging Inc.).

2.20 Statistical Analysis

Quantitative real-time RT-PCR was analysed using the Pfaffl method (Pfaffl, 2001). Primer efficiencies were estimated using either a standard curve or linReg PCR software. Data was assessed for normality (Anderson-Darling) and then analysed using one-way ANOVA, students *t* test, Kruskal-Wallis or Mann-Whitney U tests using Minitab 16 software. Error bars are given as +/- standard error of the mean (SEM).

Chapter 3

CYGB expression in liver disease

3.1 Introduction

The first indication that *Cygb* could have a role within the fibrotic process in the liver *in vivo* was reported by Kawada *et al.* (2001), who observed upregulation of *Cygb* in activated HSC in thioacetamide induced liver fibrosis in rats, it was then characterised in the human liver by Asahina *et al.* (2002). There is much debate around the cellular and sub-cellular location of CYGB within the liver which is discussed in section 1.1.5, however there is a general agreement that it is upregulated during fibrosis, whether in the liver or in other organs (section 1.1.8). In this chapter, observations of *Cygb* expression in mouse models of liver disease and also diseased human liver are presented.

3.2 Results

3.2.1 *Cygb* RNA expression in murine models of liver disease

Cygb RNA expression was analysed in three mouse models of liver disease; CCl₄-induced liver fibrosis, methionine choline deficient diet (MCD), a model of NASH, and western lifestyle model of liver disease (WLM). All models of liver disease showed significant upregulation of *Cygb* RNA, shown in Figure 3.1 A-C. In CCl₄ induced liver fibrosis, *Cygb* is significantly upregulated compared with mineral oil treatment, with expression five times that of the control ($p=0.016$ two-tailed t-test) (Figure 3.1 A). In the MCD diet, *Cygb* expression in the liver was also five-fold greater than in mice fed a normal diet ($p=0.040$ two-tailed t-test) (Figure 3.1 B). Interestingly, the treatment that

had the most marked effect on *Cygb* expression in the liver was in WLD, where an eight-fold increase was observed ($p < 0.01$ two-tailed t-test) (Figure 3.1 C).

3.2.2 CYGB expression in different disease pathologies in human liver

Observations of CYGB expression in different human liver pathologies were made by RT-PCR, western blot and immunohistochemistry. Samples were matched so RT-PCR, western blot and immunohistochemistry were performed on samples from the same liver, for each disease, only one liver was analysed, therefore no statistical analysis was possible. The diseases investigated were: alcoholic liver disease (ALD), autoimmune hepatitis (AIH), primary sclerosing cholangitis (PSC), primary biliary cirrhosis (PBC) and non-alcoholic fatty liver disease (NASH), Figure 3.2 A shows the results of the RT-PCR analysis of the whole liver RNA extracts from a sample of these diseases, *CYGB* expression is depicted relative to expression in a donor liver and all diseases analysed showed upregulation of *CYGB*. ALD and PSC exhibited a doubling in *CYGB* expression, where as both PBC and NASH showed an approximately two fold increase, AIH had the most marked increase in *CYGB* expression with an approximately six fold increase. Western blot analysis of protein expression (Figure 3.2 B) doesn't give any indication of relative differences in *CYGB* expression between diseases; however there are three protein bands at different weights, ~25 kDa, ~70 kDa and ~80 kDa and these proteins of different weights are differentially expressed between donor and diseased whole liver lysates and also the liver diseases themselves. Most obviously the donor liver sample has a single dark protein band at around 70 kDa, where as all the diseased liver

samples have a band at around 80 kDa, which is not present in the donor liver. Other notable observations are that the ALD liver only contains a single protein band at approximately 80 kDa, and no other bands are visible in this sample, the NASH liver sample also exhibits a dark band at around 21 kDa, the other liver disease samples, except for ALD, contain a faint band at this weight, but the protein at this weight in NASH is notably upregulated.

Immunohistochemistry analysis of these samples (Figure 3.3) again revealed interesting results (see appendix 1 for immuno-matched controls, which show no staining). CYGB is expressed in the donor liver in hepatocytes, and mainly in the cytoplasm of these cells, although some nuclear staining is visible. CYGB expression investigated by immunohistochemistry in the diseased livers appears to be upregulated compared with the donor liver, and is mostly associated with fibrotic regions, where HSCs are found, in the cytoplasm of cells. Infiltrating cells are negative for staining, suggesting these cell types do not express CYGB. There is also some staining evident in non-fibrotic regions of tissue in hepatocytes, this is especially evident in PSC, where staining overall is much darker than in the other disease sections or in the donor liver. In the NASH liver sample there is also staining visible around bile duct. Different disease pathways, although mechanistically different converge on the same stress response pathway, which involves HSC activation; here evidence is presented showing that upregulation of CYGB is also part of this stress response in several disease pathways.

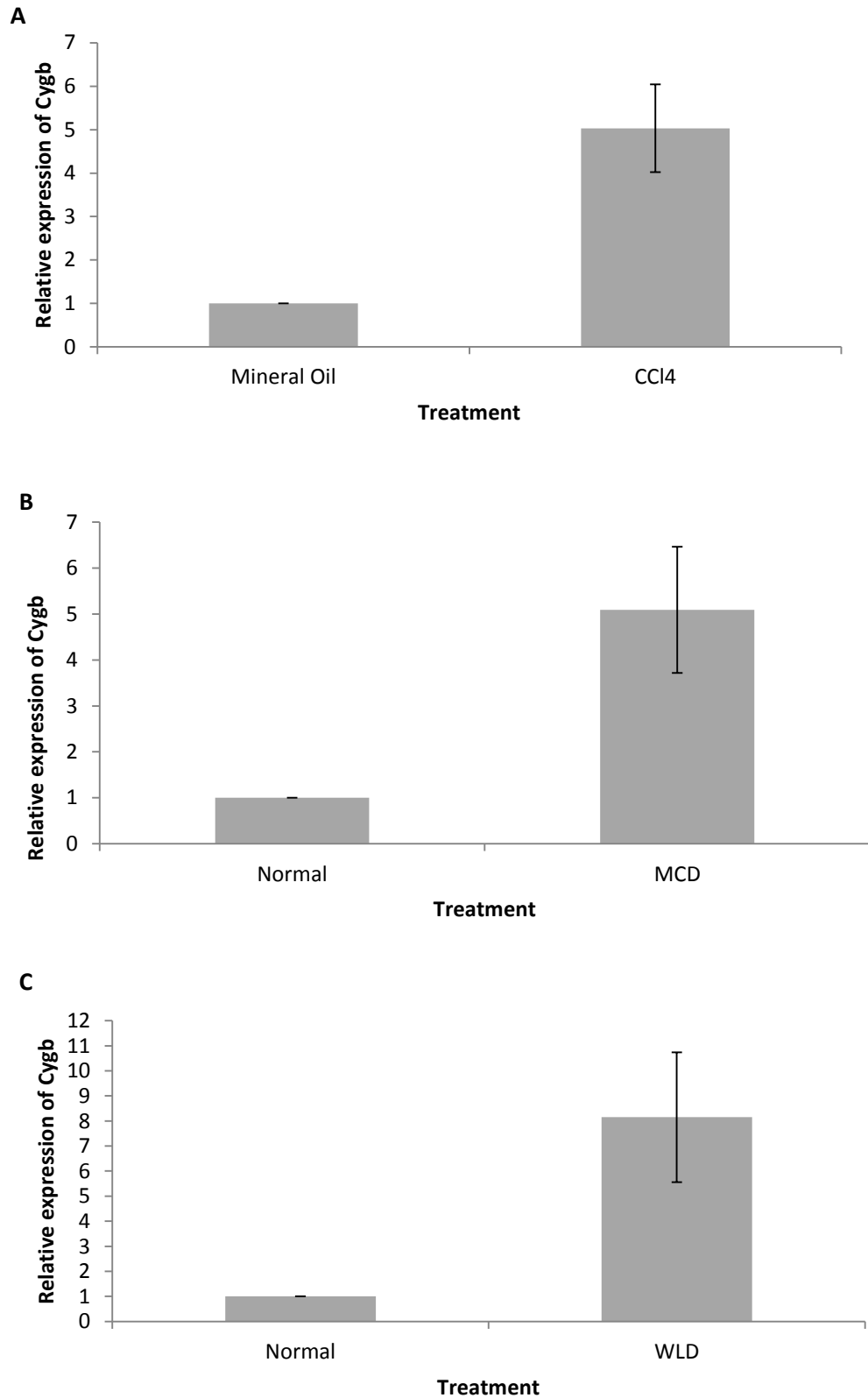


Figure 3.1: Fold change in *Cygb* gene expression by RT-PCR analysis of RNA extractions from whole mouse liver from models of liver disease A) CCl₄ treatment B) MCD treatment C) WLD treatment. N of at least 3 per treatment, +/-

SEM

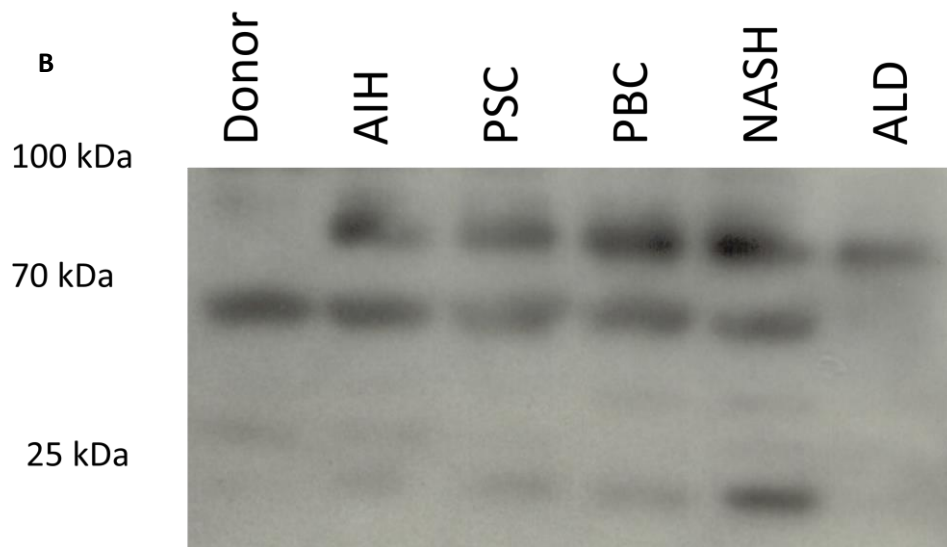
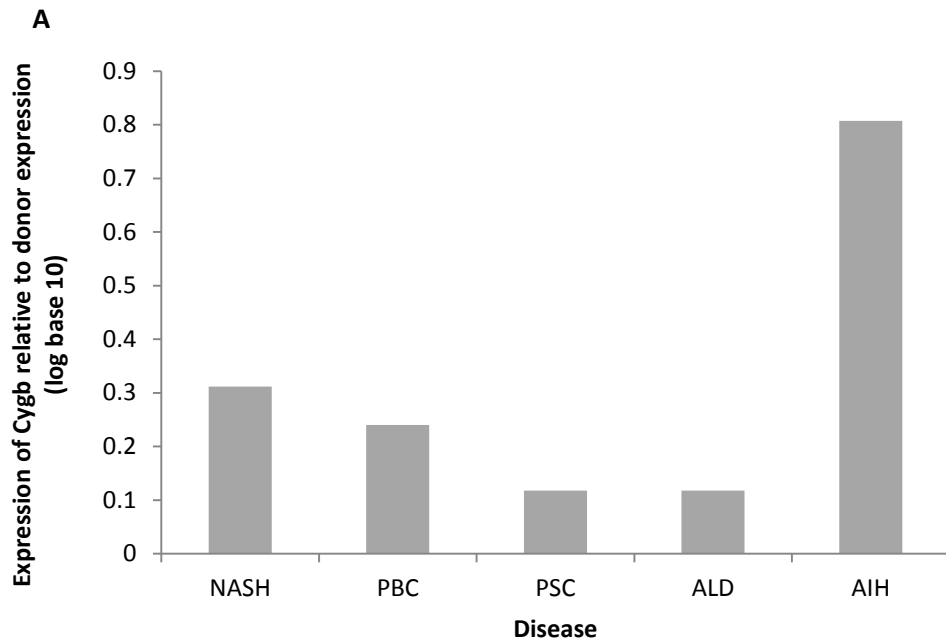


Figure 3.2: Investigation of *CYGB* expression in human liver diseases by A) RT-PCR analysis of whole liver RNA extractions, B) Western blot analysis by 12.5% SDS electrophoresis of whole liver protein lysates and Abbreviations: *CYGB* = cytoglobin,, NASH = non-alcoholic fatty liver disease, PBC = primary biliary cirrhosis, PSC = pulmonary sclerosing cholangitis, ALD = alcoholic liver disease, AIH = autoimmune hepatitis. N=1

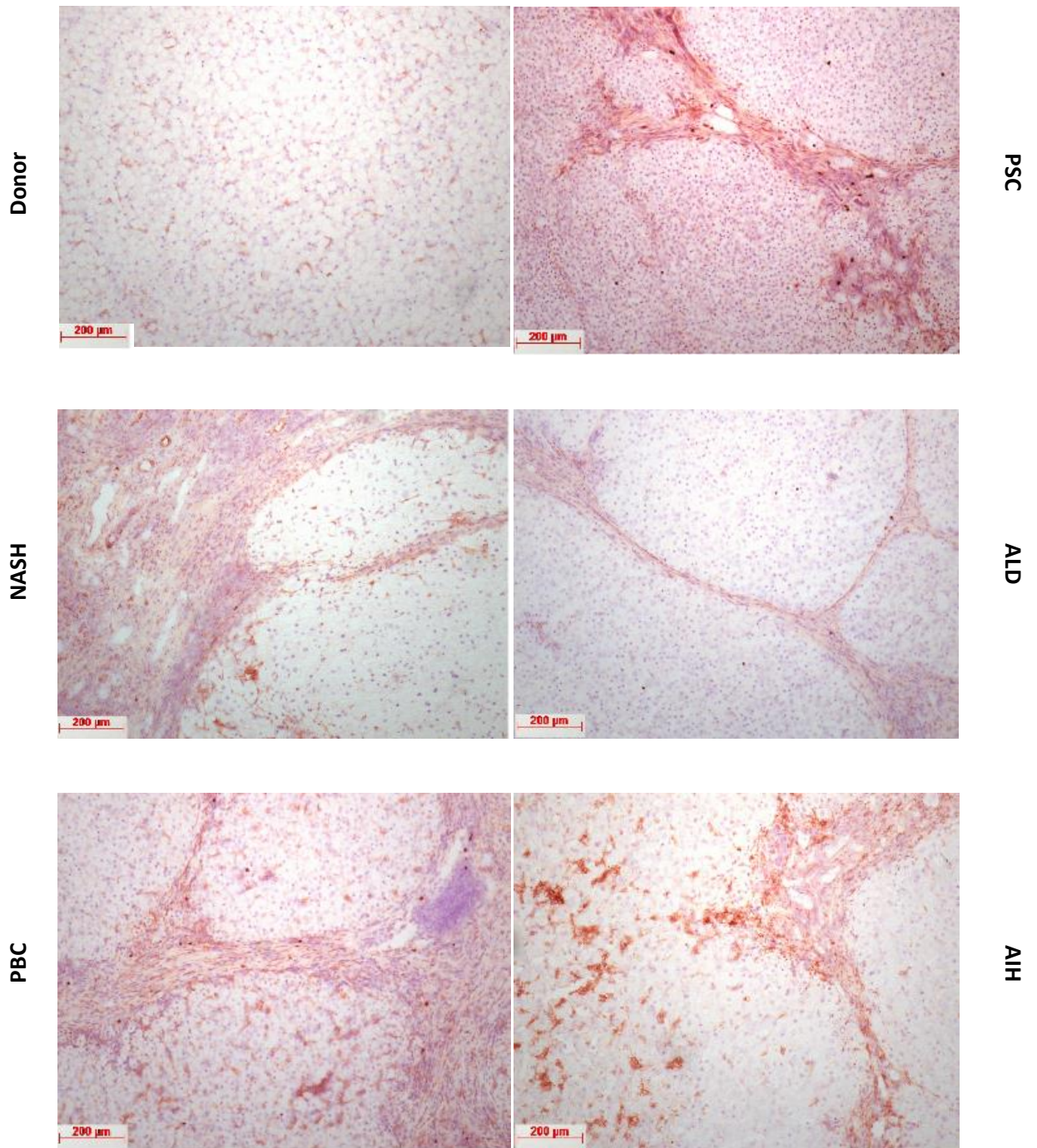


Figure 3.3: Immunohistochemistry analysis of frozen liver sections with CYGB antibody 1:200. Abbreviations: CYGB = cytoglobin, NASH = non-alcoholic fatty liver disease, PBC = primary biliary cirrhosis, PSC = pulmonary sclerosing cholangitis, ALD = alcoholic liver disease, AIH = autoimmune hepatitis. N=1

3.3 Discussion

In vivo observations of *Cygb* expression in murine models of liver disease and in diseased human liver tissue indicate that it is upregulated at both the RNA and protein level in the liver as a whole. However, in the current study, levels of RNA and protein do not seem to correlate across human liver diseases, however only one sample of each disease was analysed, and the donor liver sample came from a different person, and therefore the levels of variability between samples or within diseases cannot be quantified. The other factor to take into account is that these samples, both mouse and human, are from whole livers, and are not from specific cell types within the liver. *Cygb* has been reported to be HSC specific (Kawada *et al.*, 2001, Asahina *et al.*, 2002, Schmidt *et al.*, 2004, Motoyama *et al.*, 2014), here staining is observed in hepatocytes and more greatly fibrotic regions, with which HSCs are associated (Narmada *et al.*, 2013). If this HSC specificity was indeed the case, then the increase in *Cygb* observed in liver fibrosis could just be an artefact of the increased numbers of HSC present in a fibrotic liver. However initial studies on *Cygb* reported it to be upregulated in activated HSC compared with quiescent HSC (Kawada *et al.*, 2001, Asahina *et al.*, 2002), so as well as there being more HSCs, *Cygb* might also be upregulated within activated HSCs, increasing its expression further in a fibrotic liver. However, there is debate over which cell types in the liver express CYGB, with several authors reporting observing expression in hepatocytes (Geuens *et al.*, 2003, Shigematsu *et al.*, 2008, Yang *et al.*, 2011), which is also true of this study, therefore, the issue remains unresolved. Indeed Burmester and Hankeln (2014) have commented that caution must be taken when

attempting to identify cellular localisation of CYGB by antibody validation, owing to the quality of available antibodies. If indeed CYGB is expressed in hepatocytes as well as HSCs then the observed upregulation in fibrotic livers suggests a function for CYGB within the fibrotic process. Observations from immunohistochemistry analysis in this report (Figure 3.3) indicate that, although CYGB is not specific to the fibrotic regions, it is more highly associated with these areas of the liver tissue than the tissue containing no fibrosis. This is further evidence for a role for CYGB in fibrosis, as discussed in section 1.1.8.2. Given the clear involvement of CYGB in the fibrotic process, reported, though disputed, HSC specificity, the involvement of HSCs in the progression of fibrosis and the remodelling of ECM to form the hepatic scar, the effect of ECM on HSC and on Cygb expression in HSC was explored in Chapters 4 and 5.

Chapter 4

Effect of ECM on HSC

phenotype

4.1 Introduction

Far from only being the scaffold it was once thought to be, the ECM has an active role in the behaviour of the cells of the liver (Reeves and Friedman, 2002) . It is now recognised that the ECM plays an important role in the activation of HSC, as well as providing structure for adhesion and acting as a reservoir for cytokines, there is evidence for ECM itself signalling to HSC (Reeves and Friedman, 2002). Friedman *et al.* (1989) reported that primary rat HSC cultured on a basement membrane type matrix; Engelbreth-Holm-Swarm (EHS), which is laminin rich, maintained a quiescent phenotype compared with those cultured on plastic. Priya and Sudhakaran (2008) reported that retinol uptake ability and synthesis of collagen and proteoglycan in primary rat HSC varied depending on culture substrate, with cells grown on collagen I showing a more activated phenotype and lower rate of apoptosis compared with those on collagen IV and laminin. Carloni *et al.* (1996) also reported that primary human HSC show lower adhesion to laminin I than collagen I and collagen IV. Collagen I is the predominant ECM protein in a fibrotic liver (Friedman, 2008a) where as ECM in a normal liver is dominated by collagen IV and laminin (Martinez-Hernandez and Amenta, 1995).

With this in mind, the aim of this study was to further investigate the phenotypic effects of different ECM substrates on HSC cell lines and primary HSCs and relate any observed changes on expression and regulation of *Cygb* (Chapters 4 and 5).

4.2 Results

4.2.1 Different ECM proteins affect the morphology and proliferation of HSC-T6 cells

HSC-T6 cells were cultured on different ECM protein coated surfaces; collagen I, collagen IV, fibronectin, laminin and gelatin as well as non-coated plastic. Images taken 24hrs post seeding at 100,000 cells/ml show that culture on laminin has a marked effect on HSC-T6 cells attachment, morphology and proliferation (Figure 4.1F), with cells not exhibiting the elongate shape observed on the other substrates (Figure 4.1 A-E). Cells cultured on laminin are rounded, and have not flattened like those grown on other substrates; cells on laminin also appear to be lower density, single, and not clustered, suggesting they divide more slowly.

4.2.1.1 Culture on mixed collagen I and laminin matrices alters the observed morphology in HSC-T6 cells

Figure 4.2 shows the effects of mixed collagen I and laminin matrix on the morphology of HSC-T6 cells in the presence of both proteins as a growth matrix. Increasing amounts of laminin appear to effect cell size and the shape of a minority of cells in the presence of both laminin and collagen I (Figure 4.2B to D) where their morphology appears similar to those cultured on laminin alone (Figure 4.2E). However the presence of collagen, even at lower concentrations, where the concentration of laminin is greater (Figure 4.2-D), appears to dominate over laminin.

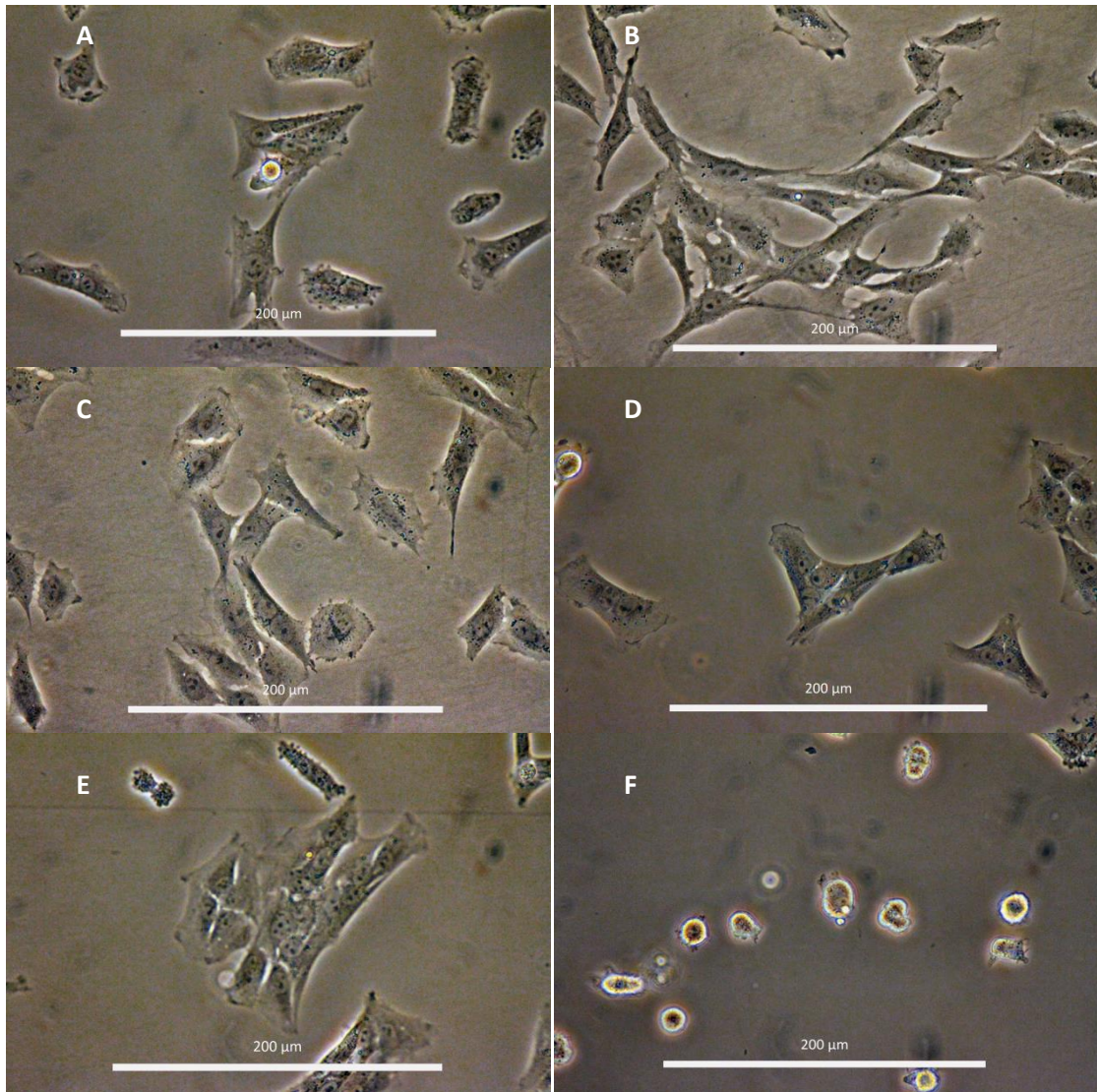


Figure 4.1: HSC-T6 cell morphology on different ECM proteins. Cells were imaged 24hrs post seeding at 400x magnification. Enhanced using the one step Photo Fix function on Jasc Paint Shop Pro V 9.00. A) Non-coated. B) Gelatin. C) Collagen I. D) Collagen IV. E) Fibronectin. F) Laminin.

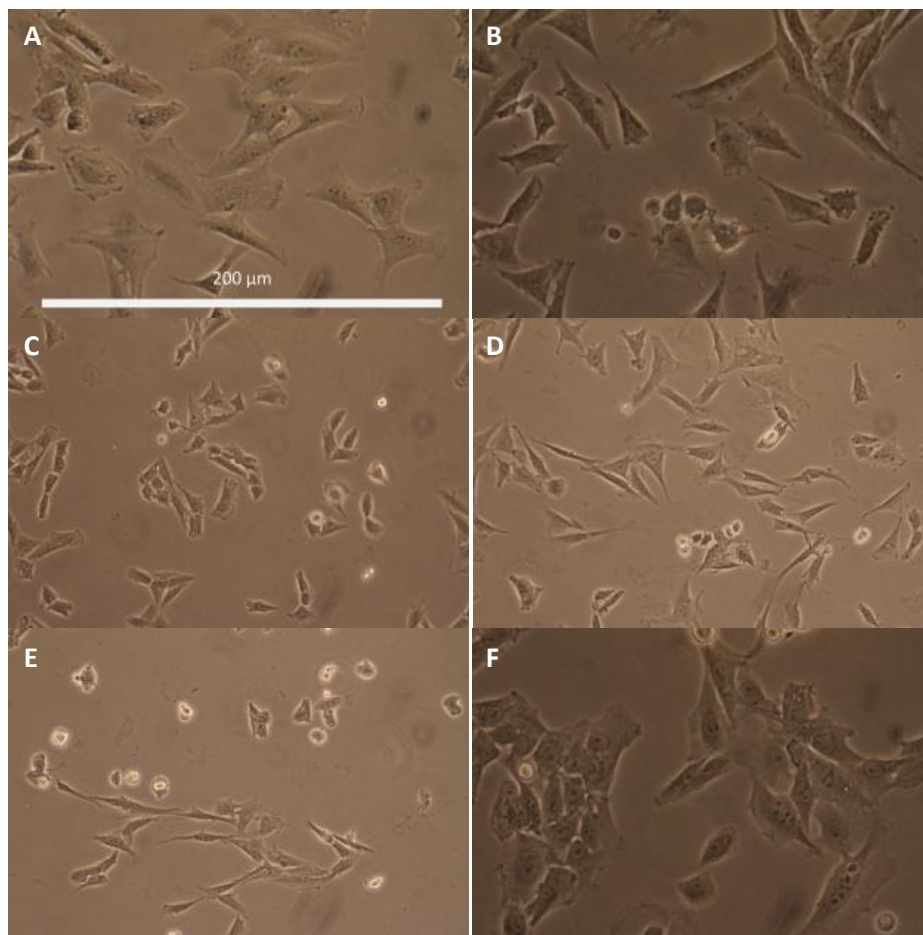


Figure 4.2: Images of HSC-T6 cells cultured on mixed matrix surfaces of collagen I and laminin in differing concentrations 48hrs post seeding at 400x magnification. A) 10:0 $\mu\text{g}/\text{cm}^2$ B) 10:5 $\mu\text{g}/\text{cm}^2$ C) 10:10 $\mu\text{g}/\text{cm}^2$ D) 5:10 $\mu\text{g}/\text{cm}^2$ E) 0:10 $\mu\text{g}/\text{cm}^2$ collagen I: laminin and F) non-coated control.

4.2.2 Proliferation of HSC-T6 cells is affected by ECM

Observation of HSC-T6 in culture on different ECM substrates indicated that proliferation was affected by culture on these proteins. To this end, end point cell counts and Cell-IQ analysis were performed to investigate these affects.

4.2.2.1 Endpoint cell counts of HSC-T6 after 48 hrs of culture

To investigate possible differences in the rate of proliferation on different ECM surfaces, cell number was quantified 48hrs post seeding. Number of cells on laminin was significantly reduced when compared with the non-coated control, whilst cell number on gelatin was significantly increased compared with the non-coated control ($p < 0.05$, one-way ANOVA with Tukey's post-hoc t -test, Figure 4.3). There was a slight increase in the number of cells present after 48hrs of culture on collagen I compared with those on non-coated plastic; however this is was not statistically significant. Other ECM proteins have no statistically significant effects on HSC-T6 cell number compared with culture on non-coated plastic; collagen I accumulates in the liver during fibrosis and becomes the predominant protein in ECM composition (Bedossa and Paradis, 2003, Friedman, 2008a). On activation, HSCs produce and deposit collagen I into the ECM and are the primary source of ECM deposition in liver fibrosis (Gabele *et al.*, 2003, Friedman, 2008b). For this reason, collagen I and laminin were chosen for further investigation into their effects on HSCs.

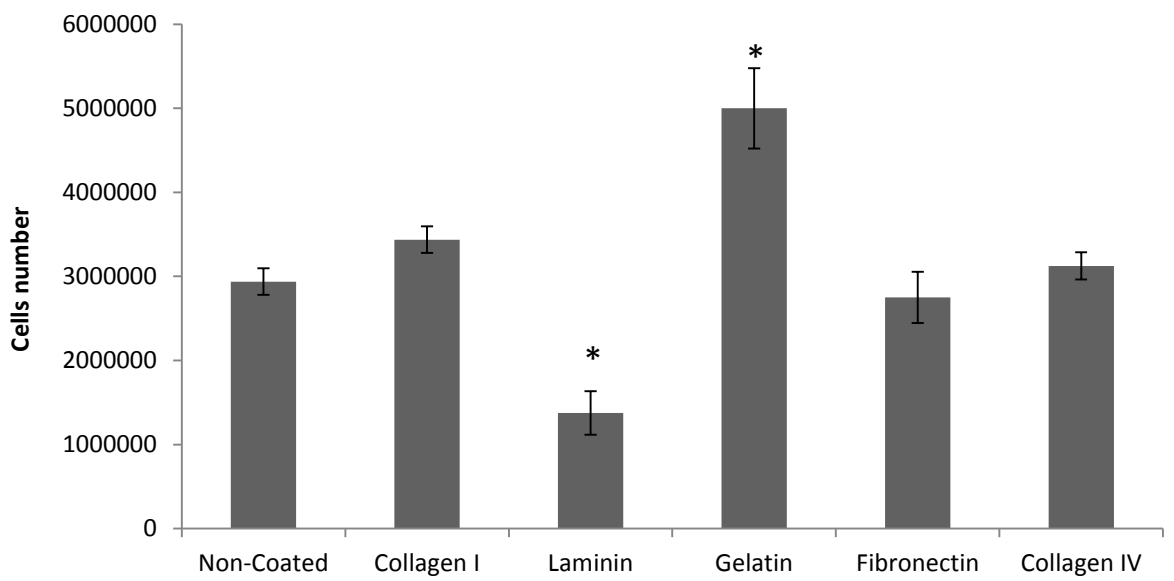


Figure 4.3: Mean (+/- SEM) number of HSC-T6 cells on different ECM proteins. * denotes significantly different from non-coated control at $p < 0.05$ according to one-way ANOVA with Tukey's post-hoc *t*-test. Cells were seeded at 100,000 cells/ml and counted on a haemocytometer 48 hrs post seeding; three independent repeats were conducted and cell number averaged across the repeats. Cell density is expressed as cells per T_{25} flask.

A time course of cell number was conducted over 48hrs (Figure 4.4). At no time point was cell number significantly different on collagen I compared with non-coated plastic. However cell number on collagen I is consistently higher across all time points measured up to passage at 48hrs. This may be due to cells attaching faster on collagen I than on non-coated plastic and therefore entering the cell cycle earlier (faster attachment observed but not quantified).

4.2.2.2 Cell-IQ analysis of HSC-T6 proliferation

To investigate in more detail the effect of collagen I and laminin on proliferation of HSC-T6 cells, proliferation was quantified in real-time by Cell-IQ analysis. Cells were cultured in the Cell-IQ over 72 hrs, a video of the time course can be viewed on the attached CD (see appendix 2). A curve of estimated cell number per well was generated using the mean cell counts estimated by the Cell-IQ analysis software at 5 hr intervals up to 70 hrs of culture. As can be seen from Figure 4.5, both collagen I and laminin have a marked effect on proliferation in HSC-T6 cells compared with proliferation on non-coated plastic. Collagen I promotes proliferation, whereas laminin inhibits it. Statistical analysis showed that there was no significant difference in initial cell density at 0 hrs ($p > 0.1$ One-Way ANOVA). After 5 hrs in culture, the number of cells on laminin is already significantly reduced compared with collagen I and non-coated plastic ($p < 0.01$ One-Way ANOVA). By 15 hrs in culture, cells cultured cell count on collagen I is significantly greater than cell number on non-coated plastic, which is also significantly greater than the numbers on cells on laminin ($p < 0.01$ One-

Way ANOVA). This trend of altered growth is maintained and at 25 hrs cell number on collagen I remains significantly higher ($p < 0.01$ One-Way ANOVA) than cell numbers laminin and non-coated plastic, though cell counts on laminin and non-coated plastic no longer differ statistically. Cell numbers on collagen I remain significantly different according to One-Way ANOVA ($p < 0.01$) from cell number on non-coated plastic and laminin up to hour 45 of culture, and reach plateau at 40 hrs. Cell numbers on laminin are significantly fewer at 45 hrs of culture than those on non-coated plastic or collagen I ($p < 0.01$), but cell counts on collagen I and non-coated plastic do not significantly differ. By 55 hrs of culture cell growth has plateaued on all surfaces and there is no statistically significant difference between cell numbers on any surface.

4.2.3 The morphology of human LX-2 cells and rat primary HSC is not affected ECM

To further study the role of ECM on stellate cell behaviour the effects of ECM on another stellate cell line, LX-2, which are derived from human HSC were cultured on collagen I and laminin, as these proteins were the substrate that had the most marked effect on HSC-T6 cells. Images taken 48 hrs post seeding show no visible effect of collagen I or laminin on LX-2 cells attachment or morphology, LX-2 proliferation on laminin was slightly reduced, though this effect is not as marked as in HSC-T6 cells (Figure 4.6).

Rat primary HSC cells were also cultured on collagen I and laminin, to investigate any effects of these proteins on primary HSCs. Images taken 24 hrs post seeding show no

effect of collagen I or laminin effect on primary rat HSCs cells attachment or morphology (Figure 4.7, similar to the observations of culture on laminin and collagen I on LX-2s (Figure 4.6).

4.2.4 Different ECM proteins do not significantly affect the proliferation of LX-2 cells at passage end point, but proliferation is affected by laminin over a passage

Observation of LX-2s in culture on different ECM substrates indicated that proliferation might be affected by culture on laminin (Figure 4.6), therefore, end point cell counts and Cell-IQ analysis were performed to investigate this affect.

4.2.4.1 End point cell counts of LX-2s after 48 hrs of culture

Cell counts per flask were conducted at 48 hrs post seeding, as previously described for HSC-T6 cells, to investigate cell growth on these substrates. No significant difference was observed in the proliferation of LX-2s on non-coated plastic, collagen I and laminin (Figure 4.8), but cell number on laminin does appear reduced compared with collagen I and non-coated plastic, in line with observations made in culture (Figure 4.7).

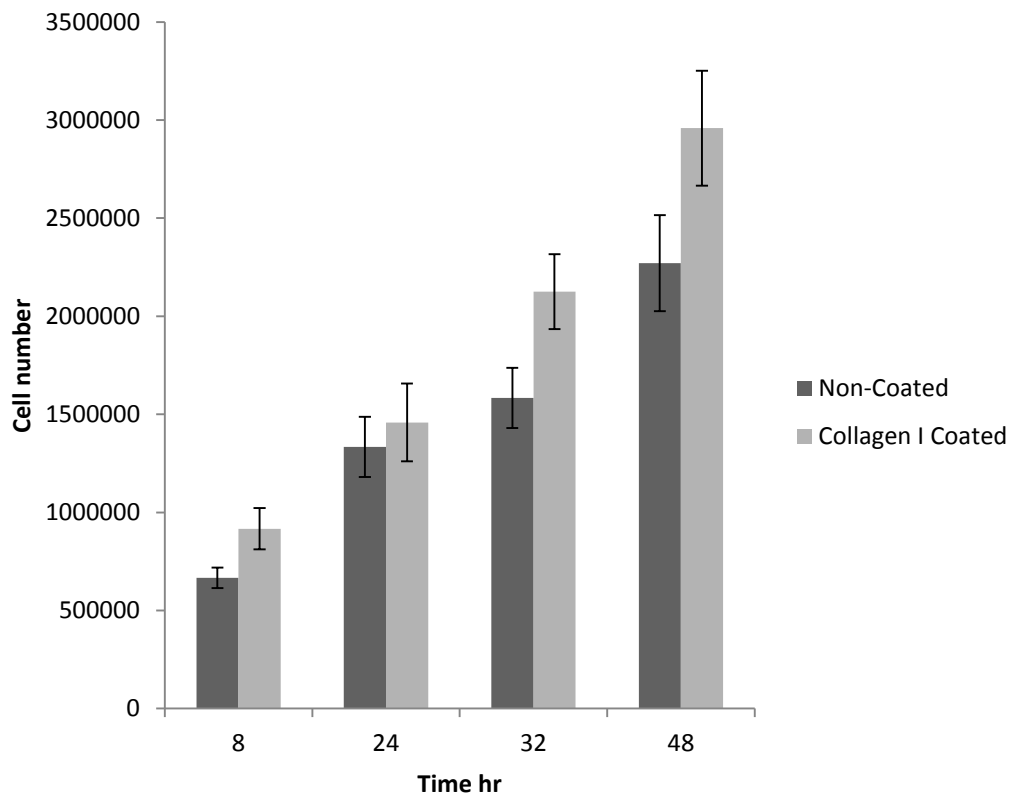


Figure 4.4: Affect of ECM on HSC-T6 cell number per T25 across a passage (48 hr). Cells from the same population were seeded at 100,000 cells/ml , 5ml per flask and grown on non-coated and collagen I coated flasks. Cells were counted on a haemocytometer at four different time points, three independent repeats were conducted and cell number averaged across the repeats (+/- SEM). N=3. Not significant (one – way ANOVA $p = 0.34$). N=3

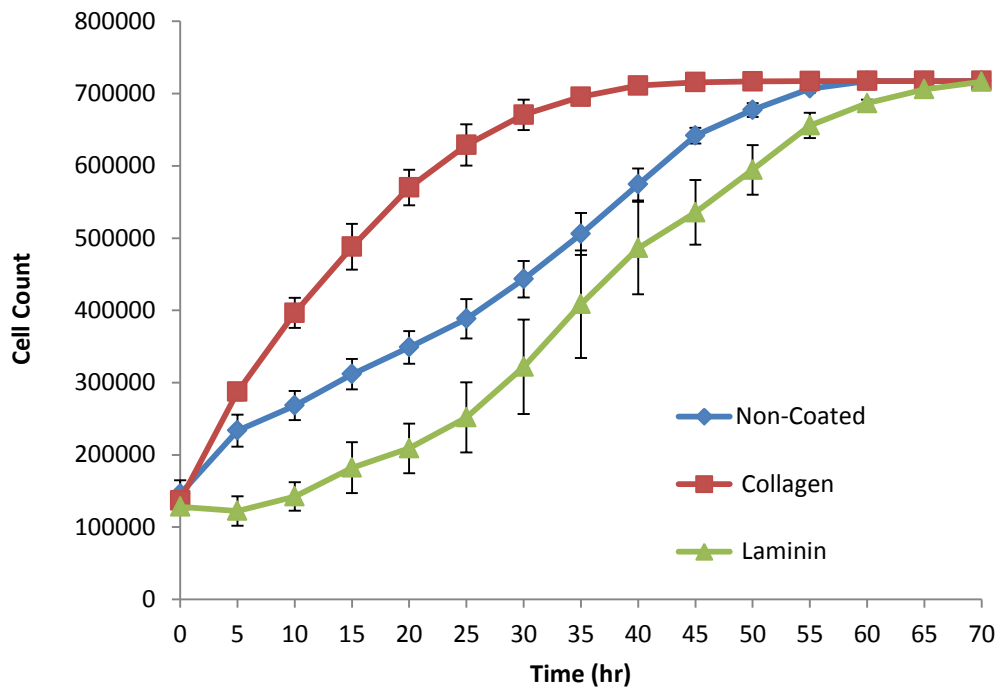


Figure 4.5: Estimated cell number per well across 70 hrs for HSC-T6s cultured on non-coated plastic, collagen I and laminin. Cells from the same population were seeded at 100,000 cells/ml, 1 ml per well and grown on non-coated plastic, laminin on collagen I. Cell number was estimated by the Cell-IQ analysis software. Cell number on laminin is significantly different ($p < 0.01$ one-way ANOVA) from cell number on non-coated plastic or on collagen I between 5-45 hrs hours of culture, with the exception of hour 25. Number of cells on collagen I are significantly different from cell number on non-coated plastic between 15 hrs and 40 hrs. Mean \pm SEM, N=3.

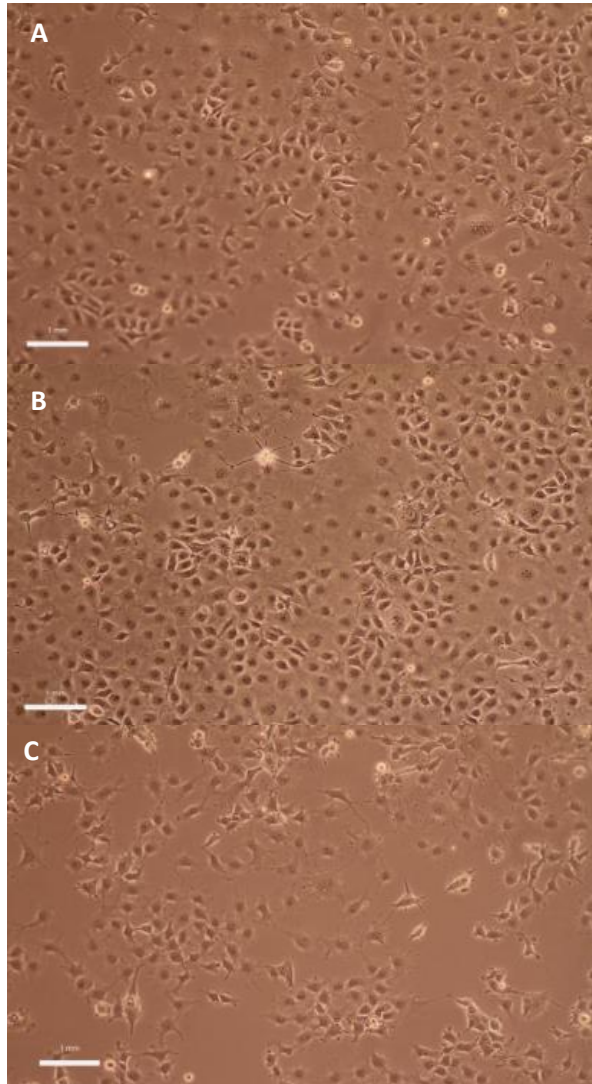


Figure 4.6: LX-2 cell morphology on different ECM proteins. Cells were seeded at 300,000 cells/ml imaged 48 hrs post seeding at 100x magnification. A) Non-coated. B) Collagen I. C) Laminin.

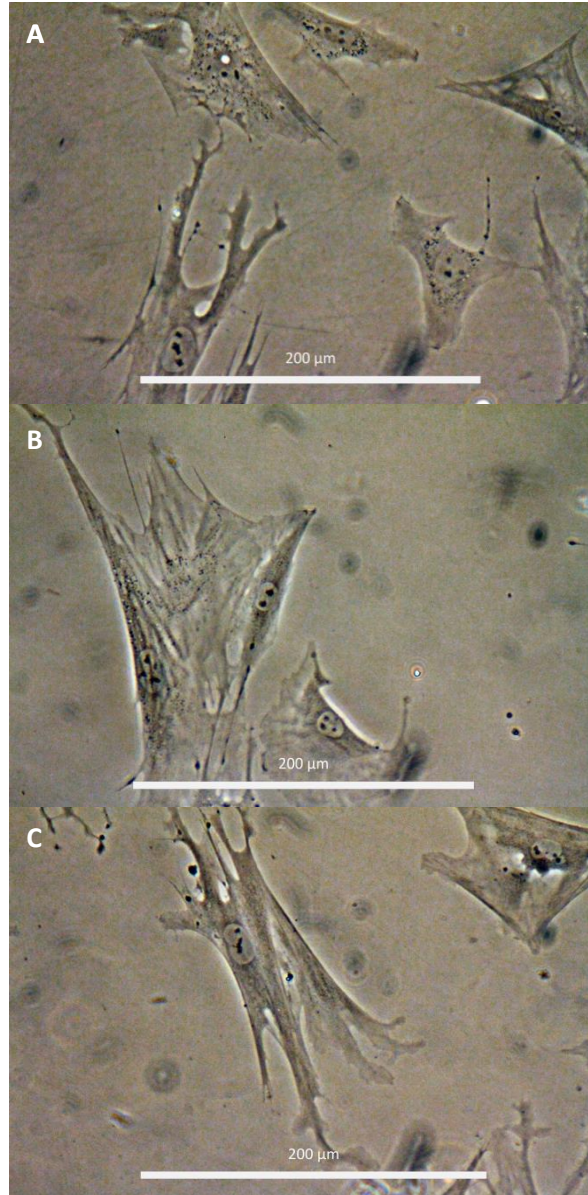


Figure 4.7: Primary rat HSC cell morphology on different ECM proteins. Cells were seeded at 100,000 cells/ml and imaged 48 hrs post seeding at 400x magnification. A) Non-coated. B) Collagen I. C) Laminin.

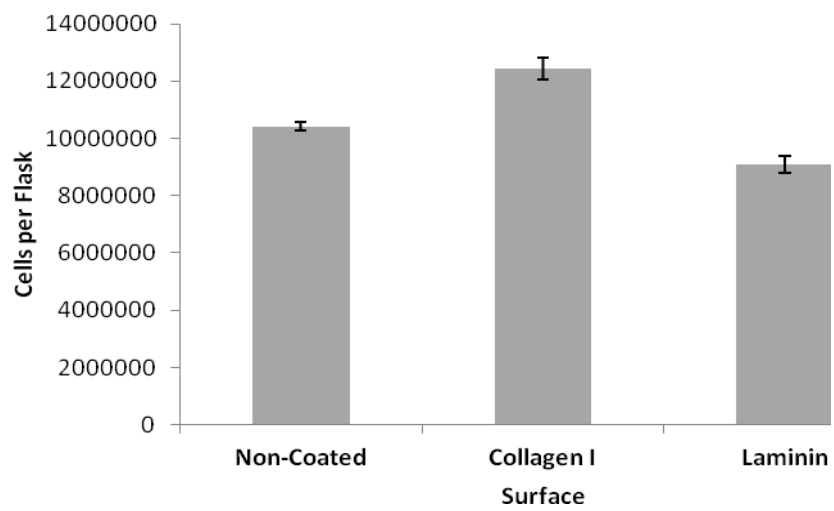


Figure 4.8 Mean number (+/- SEM) of LX-2 cells seeded at 300,000 cells/ml on different ECM proteins counted on a haemocytometer taken at 48hrs post seeding, N=3. Cell density is expressed as cells per T₂₅ flask

4.2.4.2 Cell-IQ analysis of LX-2 proliferation.

To investigate the effects of collagen I and laminin on LX-2 proliferation in more detail, Cell-IQ analysis was undertaken. Cells were cultured in the Cell-IQ over 72 hrs but cell number reached plateau at 40 hrs. A video of the time course can be viewed on the attached CD (appendix 3). As can be seen from Figure 4.9, laminin has a marked effect on proliferation in LX-2 cells compared with proliferation on non-coated plastic and collagen I. There was no significant difference in seeded cell density ($p > 0.05$ one-way ANOVA), by 5 hrs of culture cell number on laminin is significantly lower than cell number on collagen ($p < 0.05$ One-Way ANOVA); however there is no difference between cell number on non-coated plastic and cell number on either laminin or collagen I. At 10 hrs after seeding, cell number on laminin is significantly reduced compared with both cell counts on non-coated plastic and collagen I ($p < 0.01$ One-Way ANOVA), but there is no difference between the number of cells on non-coated plastic and collagen I. This trend in reduced cell number is maintained over 20hrs in culture, but there is no significant difference in cell number by 35hrs after seeding ($p > 0.05$ one-way ANOVA).

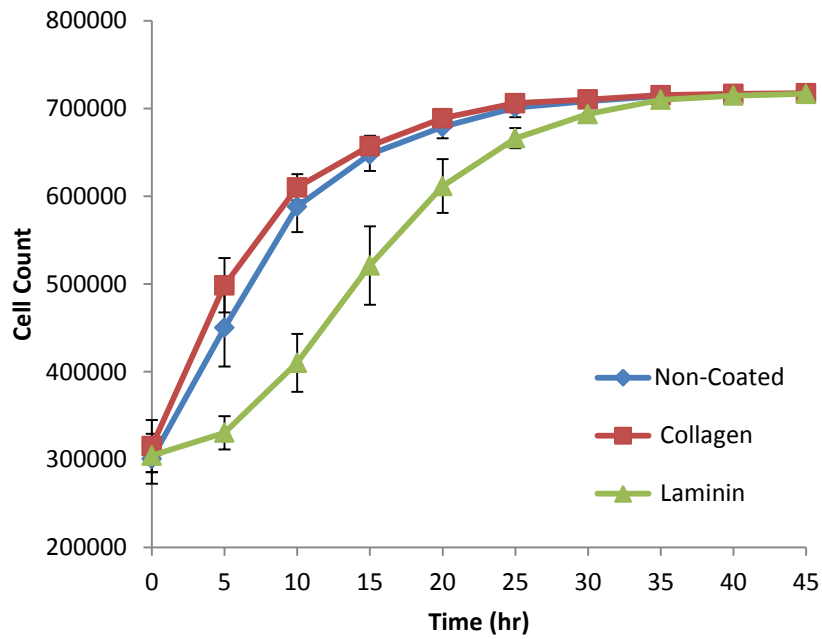


Figure 4.9: Estimated cell number per well across 45 hrs for LX-2s cultured on non-coated plastic, collagen I and laminin. Cells from the same population were seeded at 300,000 cells/ml, 1 ml per well and grown on non-coated plastic, laminin on collagen I. Cell number was estimated by the Cell-IQ analysis software. Cell number on laminin is significantly different ($p < 0.01$ one-way ANOVA) from cell number collagen I between 5-35 hrs hours of culture and non-coated plastic between 10-35 hrs, with the exception of hour 20.

4.2.5 Culture on laminin increases ATRA uptake in HSC-T6 cells and LX-2 cells

HSC-T6 cells grown on laminin do not have the typical elongated shape of activated HSCs. In contrast they appear rounded and lack projections. Their morphology on laminin might be indicative of a quiescent phenotype. A feature of quiescent HSC is their capacity to store vitamin A as lipid droplets in the cytoplasm, this is an ability they lose on activation (Burmester *et al.*, 2002, Fordel *et al.*, 2004) (discussed section 1.2.1.2). To investigate whether HSCs cultured on laminin or collagen I have the vitamin A storing capacity of quiescent HSCs, HSC-T6 and LX-2 cells were treated with ATRA, a metabolite of vitamin A, and uptake was assessed by confocal microscopy. The effect of culturing HSC-T6 and LX-2 cells in the presence of 1 μ M ATRA when grown on collagen I, laminin and glass is shown in Figure 4.11 and 4.12, respectively. Figure 4.11- E and F and 4.12 – D and E show increased auto-fluorescence of both HSC cell lines cultured on laminin in the presence of ATRA when compared with those cultured on glass or collagen I in the presence in ATRA (Figure 4.10- A toK). This observation indicates that HCS-T6s and LX-2s take up ATRA more readily from the extracellular environment when they are cultured on laminin, which is supportive of the hypothesis that both these cells have a more quiescent phenotype, compared with those cells cultured on collagen I and glass.

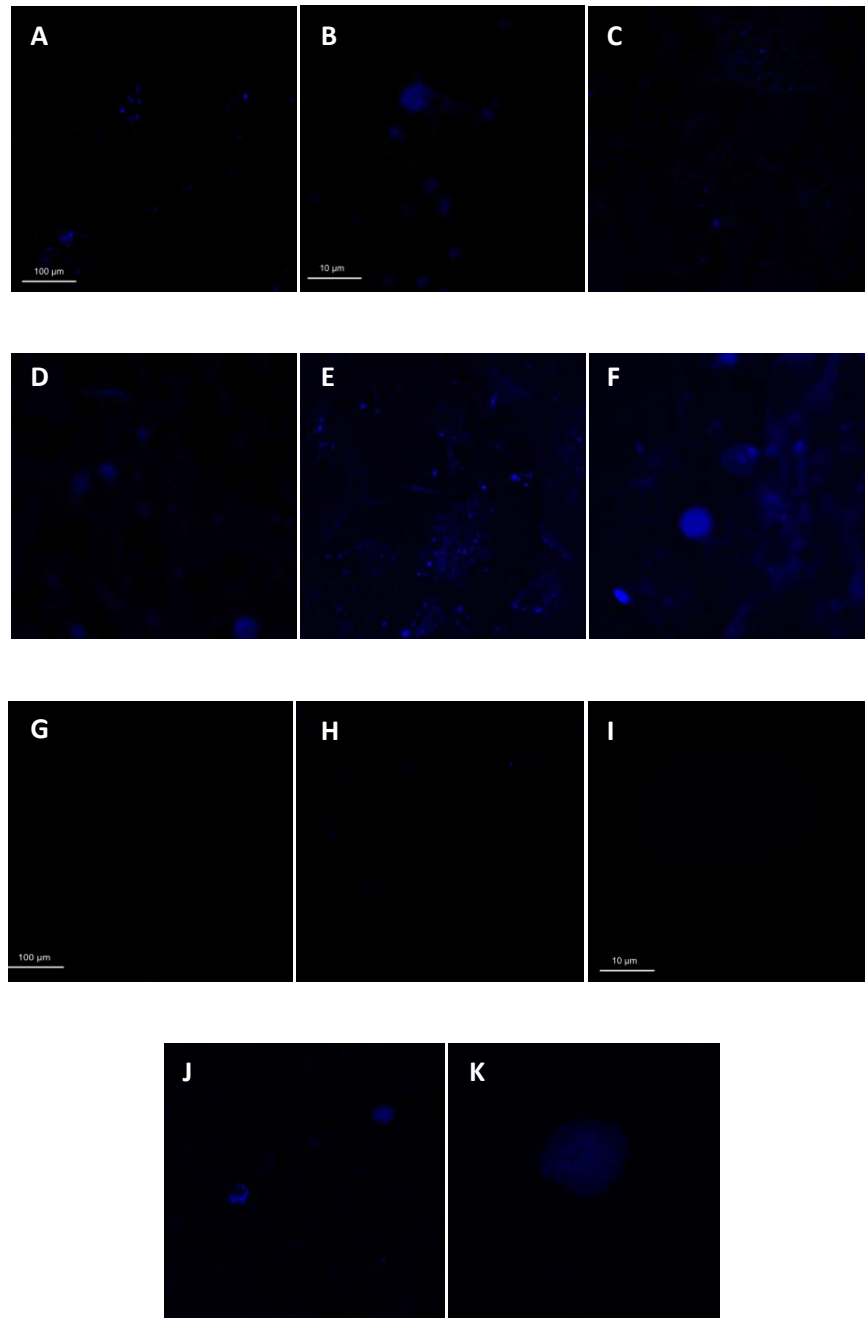


Figure 4.10: A-F) Confocal images of HSC-T6 cells seeded at 100,000 cells/ml on Glass, collagen I and laminin coverslips 48hrs post seeding, looking at retinoid auto-fluorescence activated at 351nm and detected at 515nm. A) glass, B) glass zoom, C) collagen I, D) collagen I zoom, E) laminin, F) laminin zoom. G-K) Confocal Images of LX-2 cells treated with ATRA cultured on glass, collagen I and laminin 48hrs post seeding at 300,000 cells/ml, looking at retinoid auto-fluorescence activated at 351nm and detected at 515nm. A) glass, B) collagen I, C) collagen I zoom, D) laminin, E) laminin zoom.

4.3 Discussion

The observations of this study show that different ECM matrices can influence the phenotype and behaviour of HSC-T6 and LX-2 cells. Laminin has a most marked effect on the morphology of HSC-T6s, with cells not showing the typical elongate shape seen on other substrates; however no morphological differences were seen in LX-2s or primary rat HSCs on any ECM matrix. Cellular response to ECM is determined by membrane receptors in HSCs, therefore, this observation suggests that HSC-T6s might have different membrane receptor expression, or differences in their downstream signalling cascades, in response to ECM from both LX-2s, which are derived from human HSCs, and primary rat HSCs. As the HSC-T6 cell line is derived from rat primary HSCs (Vogel *et al.*, 2000), it is unlikely that the difference in morphology in response to culture on laminin is due to species differences between rat and human HSCs. Collagen I alone, although a major constituent of the hepatic scar, seems to have no effect on morphology in HSC-T6s, LX-2s or primary rat HSCs. The mixed collagen I – laminin matrices affect the morphology of HSC-T6 cells, with increasing concentrations of laminin, and decreasing concentrations of collagen I having an observable effect on cell shape. However, collagen I seems to exert a dominant effect, as even at its lower concentrations, more cells exhibit an elongate rather than rounded shape.

Cell proliferation of both HSC-T6 and LX-2 cell lines is affected by ECM; however the response of each cell line is different. Both collagen I and laminin affect cell proliferation in HSC-T6s compared with the proliferation observed on non-coated plastic, with increased proliferation and faster time to confluence observed on

collagen I compared with culture on non-coated plastic and laminin. Laminin, on the other hand, suppresses proliferation in HSC-T6 cells initially. Laminin also reduces proliferation in LX-2 cells, with these cells reaching confluence slower than LX-2s grown on non-coated plastic or collagen I. However, interestingly collagen I does not increase cell proliferation compared with non-coated plastic in LX-2s, in contrast to the observations of the effect of collagen I on cell proliferation in HSC-T6 cells. This difference could be due to differences in receptor expression between cell lines, or be attributable to the basal activation state of the immortalised cell lines – HSC-T6 cells can be described as being semi-activated as they express α SMA, glial acidic fibrillary protein and vimentin, which are markers of activation, but they also show retinoid-related parameters similar to those of freshly isolated quiescent rat HSC including expression of all six nuclear retinoid receptors (Vogel *et al.*, 2000). LX-2s have an activated phenotype, they express α SMA, β PDGF Receptor subunit, which is not expressed by quiescent HSCs and proliferate in response to stimulation with BB-PDGF (Xu *et al.*, 2005). The observation that laminin suppresses proliferation in both HSC cell lines is in contrast to the different response of these cell type in terms of their morphology on this substrate, but might indicate that different signalling mechanisms are involved in the morphological and proliferative responses. Further evidence of matrix effects on phenotype is seen in HSC-T6 and LX-2 cells ability to take – up ATRA. Cells cultured on laminin show increased ability to store ATRA in the form of retinoids compared with those grown on collagen I or glass. ATRA has been shown to modulate primary rat HSC phenotype, reducing the production of collagen I and III and also fibronectin and reduced proliferation (Goodman *et al.*, 1987). Interestingly, the effect

of laminin on ATRA up – take appears to be the same in both cell lines, in spite of the differences between HSC-T6s and LX-2s in terms of morphology and proliferation, on these substrates.

ECM effects on HSCs have been previously documented (Friedman, 2008b), Friedman *et al.* (1989) reported that basement membrane matrix maintained a differentiated phenotype in primary rat HSCs in culture. HSCs were cultured on EHS, comprising approximately 90% laminin, 6% collagen type IV and 4% heparin sulfate proteoglycan, and, therefore, approximated ECM in a normal liver. ESH was found to affect cell morphology and reduce collagen synthesis and proliferation. Gaça *et al.*(2003), found that Matrigel, a basement-membrane type coating containing collagen IV and laminin, reduced primary rat HSC proliferation, collagen synthesis and expression of markers of activation such as α SMA, but collagen IV and laminin alone did not produce a reduction in marker expression. These observations are in-line with the results presented in the current study, where cultures of HSC-T6s on laminin, a major constituent of the basement matrix in a normal liver, appear rounded, and proliferation of HSC-T6s and LX-2s is reduced when cultured on laminin. Collagen I has been reported to support and activated phenotype in HSC, Davis (1988) observed that primary HSC cultured on collagen I showed increased responsiveness to stimulation with TGF- β , with greater accumulation of collagen I and collagen III. Collagen I has also been shown to enhance migration in HSC-T6s and LX-2s (Yang *et al.*, 2008), however, unlike the results presented here, collagen I did not alter proliferation. This difference between the results reported here and the observations of Yang *et al.* (2008) might be due to this group only performing end point analysis of HSC proliferation, and not a

time course as is presented here. End point analysis shows no significant difference in cell number after 48hrs of culture in LX-2s or HSC-T6s for this study either, but time course analysis shows differences in proliferation across the culture period.

Davis *et al.* (1990) have shown that retinol and retinoic acid also have an impact on the behaviour of primary rat HSCs. Treatment with retinol and retinoic acid inhibited cell proliferation, with retinoic acid having a more potent effect. Retinoic acid also reduced interstitial collagen and TGF- β production in these cells, implying these cells were exhibiting a more quiescent phenotype. Demonstrated here is the effect that ECM culture substrate can have on the ability of HSC-T6s and LX-2s to take up ATRA and store retinoids, a feature of quiescent HSCs, where collagen does not increase ATRA uptake, but laminin has a marked effect.

The effect of culture on gelatin (denatured collagen) on HSC proliferation was a surprising result, and was marked, new research into fibrosis resolution and matrix degradation suggests that HSC may come into contact with a form of denatured collagen during the resolution process, which might be similar in structure to gelatin (Friedman, 2008c, Ramachandran and Iredale, 2012). The reasons for this increased proliferation are unknown and were not explored within this study. It might be that increased exposure of binding sites caused by denaturation is causing increased signalling and subsequent cell proliferation, but further work would be required to confirm whether an increase in signalling is the cause of the increase in proliferation.

The results of this study are consistent with those that have been previously reported, namely that HSC culture on different ECM substrates effects cell behaviour and

phenotype. Specifically culture on a substrate that resembles the basement membrane matrix of a normal liver confers a more quiescent phenotype on HSCs, and culture on a substrate resembling the collagen I rich hepatic scar that develops on liver injury gives a more activated phenotype. *Cygb* has been implicated in the activation of HSCs as is discussed in Chapter 1, sections 1.1.8.2 and 1.2.1.4; however the influence of ECM on *Cygb* expression has not been investigated. As it is clear that ECM can affect HSC phenotype, it is feasible that modulation of *Cygb* expression could also be influenced via the ECM signalling pathway. The effect of ECM culture substrate on *Cygb* expression is investigated in Chapter 5.

Chapter 5

Regulation of Cygb

by ECM

5.1 Introduction

Results presented in Chapter 4, demonstrate that ECM components can influence HSC morphology, and also phenotype in terms of the ability of HSC to take up ATRA, suggesting differences in HSC activation state. What is not yet known is if these effects extend to regulation of *Cygb* expression, which has been reported to be upregulated in HSCs in a fibrotic liver (Kristensen *et al.*, 2000, Kawada *et al.*, 2001). Changes in *Cygb* expression in these HSCs during fibrogenesis could be important to cell function (for example collagen synthesis and deposition). ECM signalling has been shown to influence behaviour and gene expression in HSCs (see section 4.3); therefore basement substrate might also influence *Cygb* expression. This study aims to characterise *Cygb* gene expression in HSCs cultured on different ECM substrates and to investigate possible signalling mechanisms linking ECM to *Cygb* expression.

5.2 Results

5.2.1 ECM proteins affect the expression of *Cygb* and α SMA

RT-PCR was undertaken on RNA extracted from HSC-T6 cells at the end of three passages. *Cygb* expression was investigated and α SMA was chosen as early stage marker of stellate cell activation (Friedman, 2008b). Figure 5.1 shows a significant increase in α SMA expression on collagen I, collagen IV, fibronectin and gelatin, whereas expression is significantly decreased on laminin (Fold changes in log base 2: 1.4, 0.7, 0.6, 1.1 and -0.6, respectively). Therefore, activation status of HSC-T6 cells according to α SMA mRNA (messenger RNA) expression was significantly affected by all

of the ECM proteins tested when compared with expression on non-coated tissue culture treated plastic ($p < 0.05$ one-way ANOVA with Tukey's Post-Hoc or t -test assuming equal variances).

RT-PCR analysis of *Cygb* mRNA expression showed that ECM proteins also changed expression of *Cygb* in the HSC-T6 line. Three of the ECM proteins tested showed significant differences in expression when compared with *Cygb* expression in HSC-T6 cells cultured on a non-coated surface. HSC-T6 cells cultured on laminin show a significant increase in *Cygb* expression ($p < 0.05$, one-way ANOVA with Tukey's post-hoc, fold change [log base 2] 1.0), in contrast to those grown on collagen I ($p < 0.05$ t -test, fold change [log base 2] -0.6) or gelatin ($p < 0.05$ one-way ANOVA with Tukey's post-hoc, fold change [log base 2] -0.9), which show a decrease in expression when compared with expression in cells cultured on a non-coated control. Interestingly, change in expression of *Cygb* on all three of these coatings was reciprocal to the expression of α SMA. The upregulation of *Cygb* in HSC-T6 cells on laminin compared with collagen I and non-coated plastic was also confirmed by western blot at the protein level (Figure 5.2).

To confirm that this effect was not specific to HSC-T6 cells the effect of collagen I and laminin on *CYGB* expression was also interrogated in LX-2 cells. Figure 5.3 shows that in LX-2 cells, culture on collagen significantly decreases ($p = 0.05$, Kruskal Wallace, fold change [log base 2] -1.9) *CYGB* mRNA levels compared with non-coated plastic, in line with the observations of the effect of collagen I on *CYGB* expression in HSC-T6 cells. However, unlike HSC-T6 cells, laminin has no effect on *CYGB* expression in LX-2 cells.

5.2.2 Time dependant expression of *Cygb* on collagen I

To explore *Cygb* expression on collagen I and non-coated plastic in more detail, RNA was extracted from HSC-T6 cells cultured on non-coated plastic and collagen I at four time points across a passage and compared with RNA extracted from cells grown to confluence on a non-coated tissue culture surface. Figure 5.4 shows that *Cygb* mRNA expression changes in a time dependent manner on both surfaces, with expression decreasing at lower cell densities. At 48 hrs *Cygb* mRNA expression remains repressed in cells cultured on collagen I, whereas on non-coated plastic *Cygb* mRNA levels return to levels comparable with the control RNA extractions from a confluent non-coated flask, there is only a significant difference between *Cygb* mRNA expression in cells cultured on collagen I compared with cells grown on non-coated plastic at 48hrs after seeding ($p < 0.05$ Mann-Whitney fold change [log base 2] non-coated – 0.4, collagen I coated – 1.1)

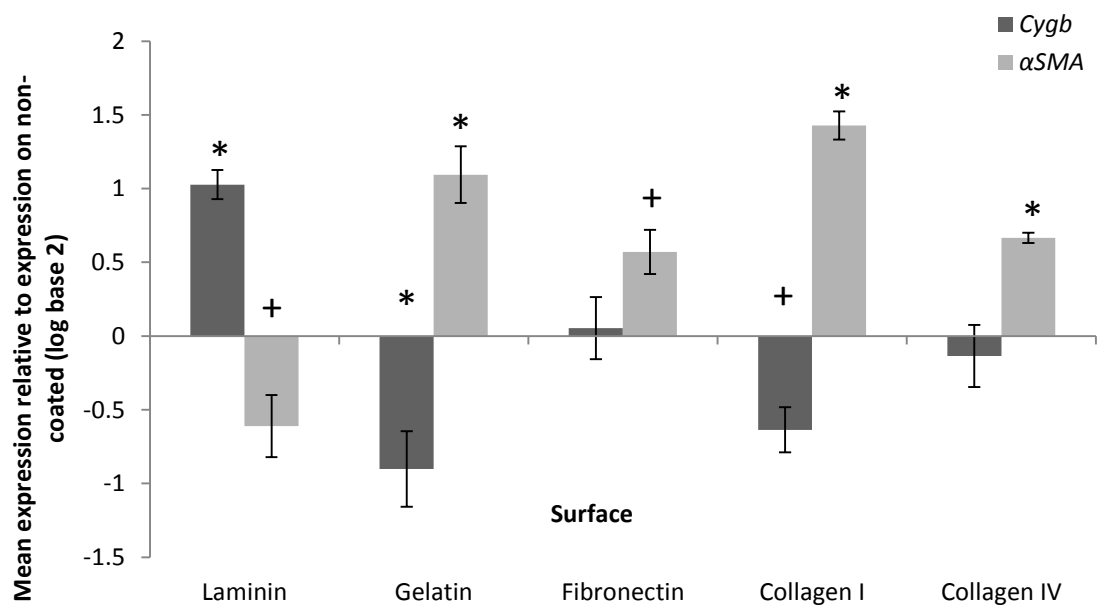


Figure 5.1: Mean (+/- SEM) expression of *Cygb* and α SMA in HSC-T6 cells cultured on different ECM proteins analysed by RT-qPCR calibrated to expression on non-coated flasks. * denotes significance at $p < 0.05$ according to one-way ANOVA with Tukey's post-hoc *t*-test, + denotes significance at $p < 0.05$ according to *t*-test assuming equal variances when compared with expression on the non-coated control. N=3

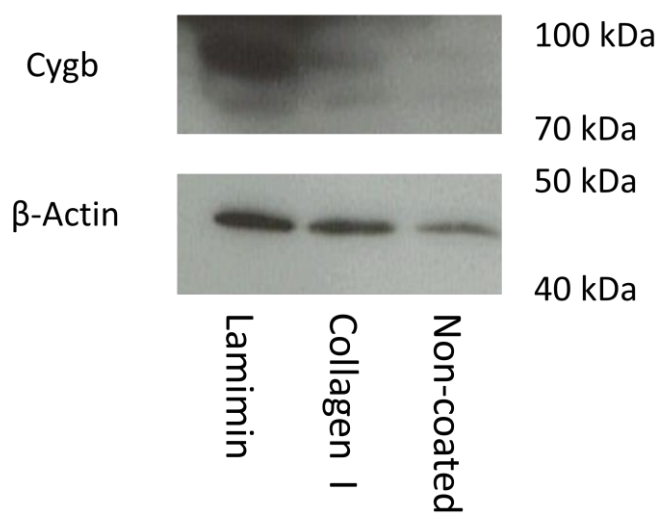


Figure 5.2: Expression of Cygb in HSC-T6 cells cultured on laminin, collagen I and non-coated plastic analysed by western blot.

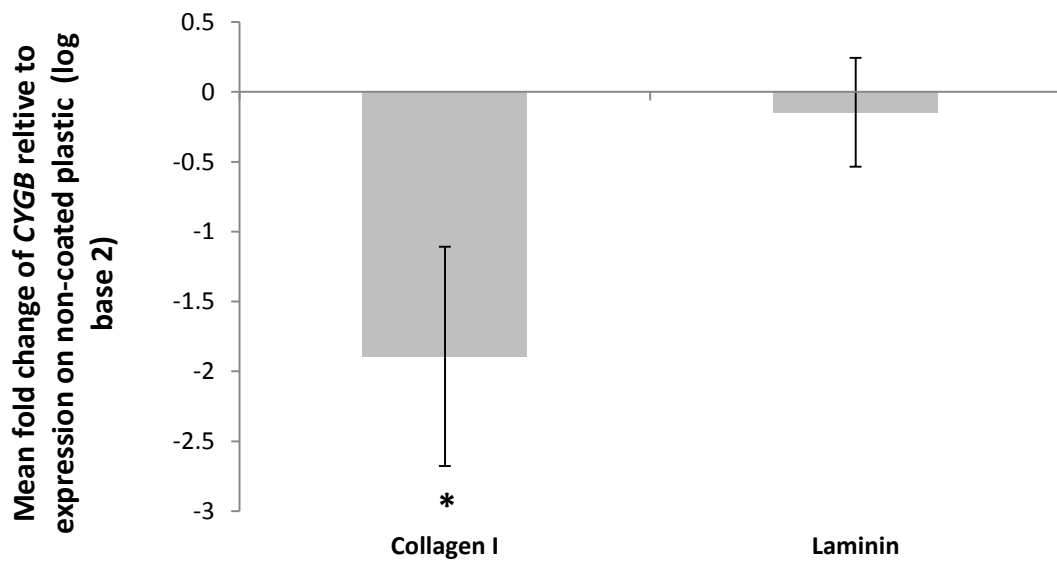


Figure 5.3: Mean expression (+/- SEM) expression of *CYGB* in LX-2 cells cultured on collagen I and laminin proteins analysed by RT-qPCR calibrated to expression on non-coated flasks. * denotes significance at $p=0.05$ according to Kruskal Wallance compared with expression on a non-coated control. N=3.

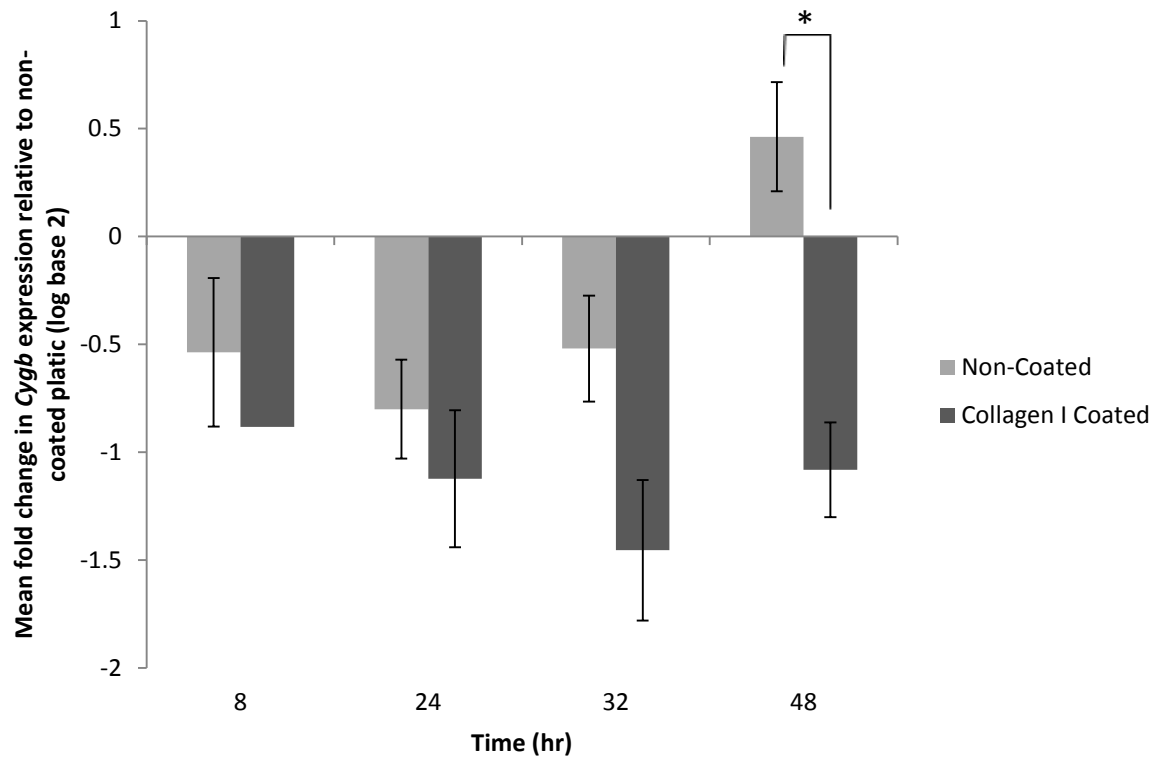


Figure 5.4: Mean (+/- SEM) expression of *Cygb* across a passage (48hr) on non-coated and collagen I coated flasks relative to 0hr time point on a confluent non-coated plastic. * denotes significance at $p < 0.05$ compared with expression on non-coated plastic according to Mann-Whitney test. N=3.

5.2.3 Surface coated collagen is required for regulation of *Cygb*

The effects of the presence of collagen I on HSC-T6 cells were explored via response to different concentrations of collagen I either in solution in the media or coated onto a plate to investigate whether attachment to a collagen surface is required for regulation of *Cygb*. Figure 5.5 A and B indicate that cell attachment to collagen coated surfaces is necessary for an effect on *Cygb* expression to be observed. There was no effect of collagen I when diluted into the media on *Cygb* expression (Figure 5.5 A). When compared with cells cultured on commercial collagen I coated flasks (BD Biocoat®), *Cygb* was downregulated on the coated surface compared with all concentrations of collagen I in the media. Figure 5.5 B demonstrates that concentrations of collagen I greater than 6 and 10 $\mu\text{g}/\text{cm}^2$ coated on to the culture surface have an increased effect on *Cygb* expression in HSC-T6 cells. Significant down regulation ($p < 0.05$ one-way ANOVA with Tukey's post-hoc) of *Cygb* was observed in cells cultured on 0.4, 6 and 10 $\mu\text{g}/\text{cm}^2$ collagen I when compared with expression in cells cultured on non-coated plastic (fold change [log base 2] -0.3, -0.6 and -0.6, respectively) and there was downregulation of *Cygb* expression at all concentrations of collagen I when cells are grown on the matrix.

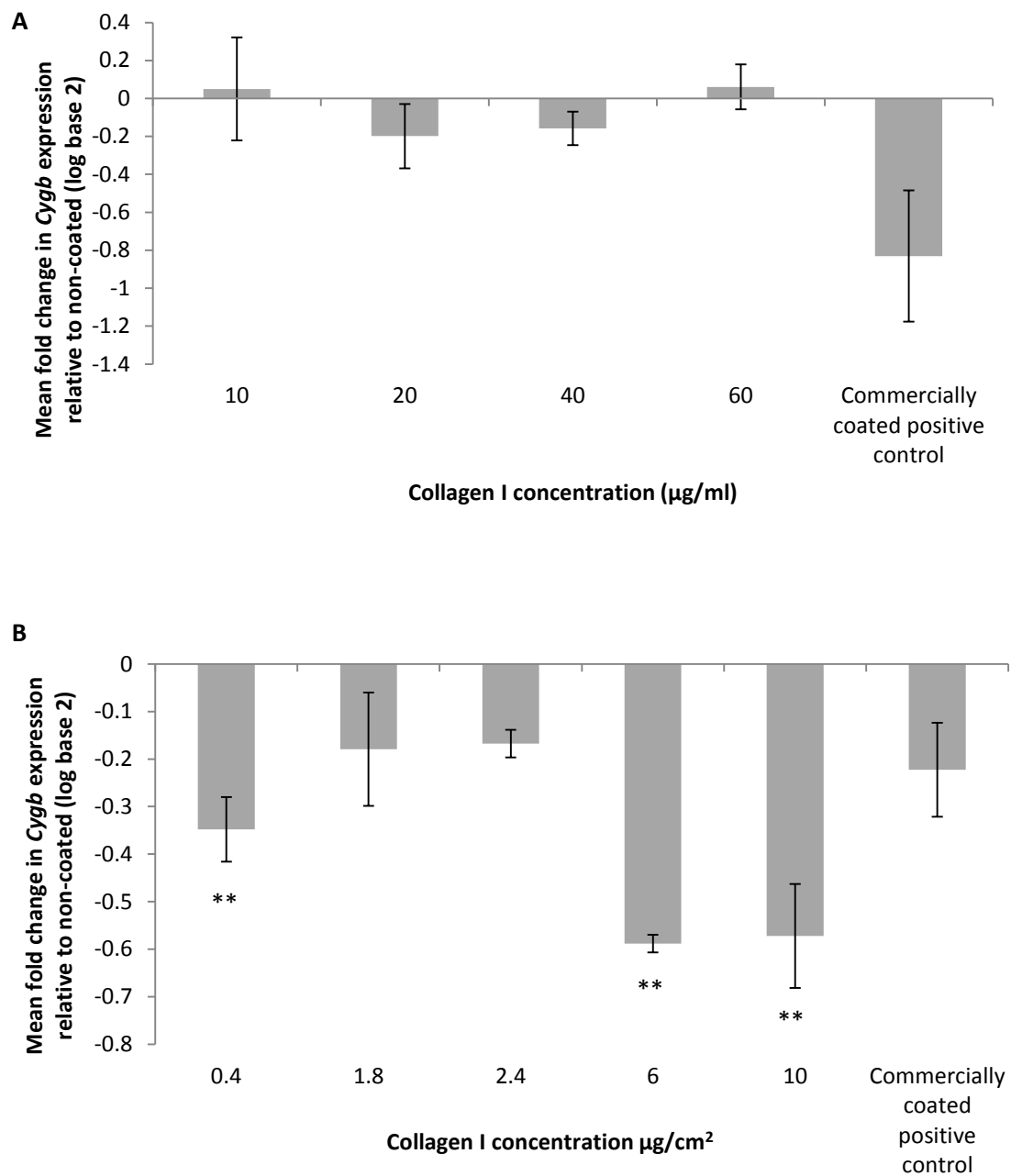


Figure 5.5: Mean (+/- SEM) expression of *Cygb* in HSC-T6 in the presence of collagen I 48 hrs after seeding. A) *Cygb* expression in cells cultured on non-coated plastic with collagen I diluted into the culture media relative to *Cygb* expression on non-coated plastic. B) Mean (+/- SEM) *Cygb* expression in cells cultured on collagen I coated plates at different concentration relative to *Cygb* expression on non-coated plastic. ** denotes significant difference ($p < 0.01$) from non-coated control according to one-way ANOVA with Tukey's post-hoc t test. Three repeats were conducted and relative expression averaged across the repeats. Positive control is a commercially bought collagen I coated plate from BD BioCoat®

5.2.4 Intracellular ROS in HSC-T6s cultured on collagen I, laminin and non-coated plastic

CYGB has been implicated in ROS scavenging (see section 1.1.6.2), and as *Cygb* expression was altered in HSC-T6 cells cultured on collagen I and laminin, levels of intracellular ROS were investigated in these cells (Figure 5.6). Although not statistically significant ($p > 0.05$, Kruskal-Wallace), the trend expected from the differences in *Cygb* is observed. Intracellular ROS is increased in HSC-T6 cells cultured on collagen I, where *Cygb* is downregulated, in line with the increase in intracellular ROS in the H₂O₂ treated positive control. Levels of intracellular ROS in cells cultured on laminin appear to be in line with cells cultured on non-coated plastic, and lower than ROS in the positive control cells or those cultured on collagen I.

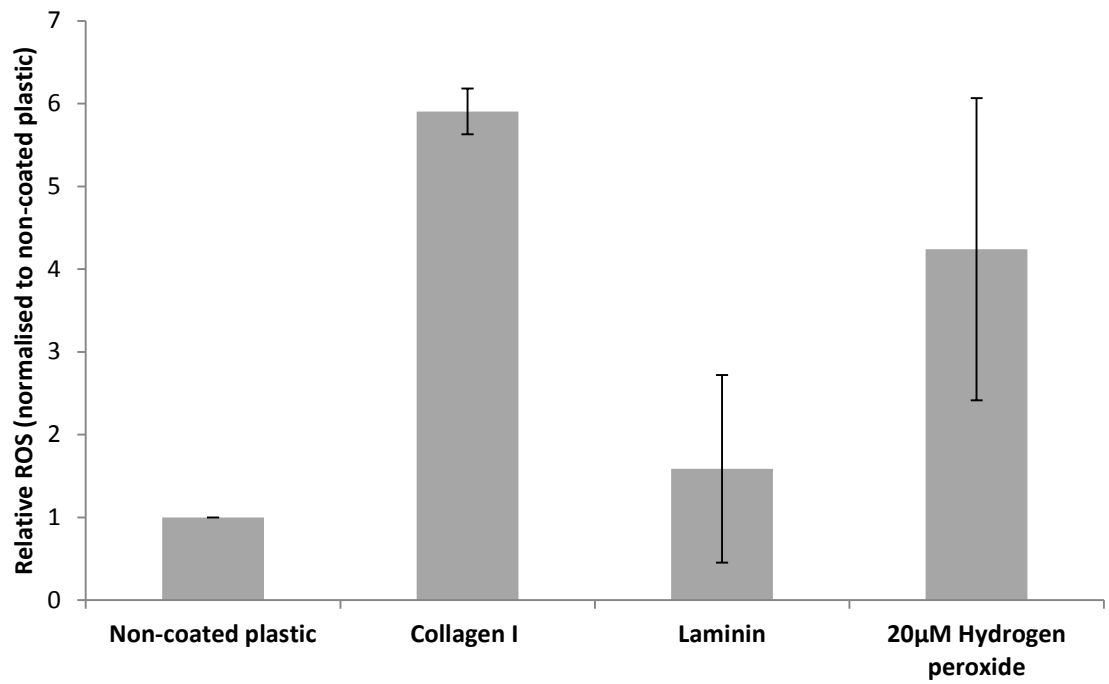


Figure 5.6: Mean (+/- SEM) relative levels of intracellular ROS in HSC-T6 cells cultured on non-coated plastic, collagen I laminin and cells treated with 20µM H₂O₂ for 1hr prior to analysis by fluorescence of H₂DCF-DA by flow cytometry. N=3.

5.3 Discussion

As well as effecting cell morphology as described in Chapter 4, different ECM proteins also regulate the expression of *Cygb* and stellate cell activation as assessed by α SMA expression. Work in this chapter has shown that HSC-T6s cultured on collagen I, collagen IV, fibronectin and gelatin, had an increased activation state as measured by α SMA. HSC-T6 cultured on laminin had decreased α SMA expression compared with expression on non-coated plastic, indicating a more quiescent phenotype. Therefore all ECM substrates had a significant effect on α SMA expression. It has been reported that far from acting simply as a mechanical cell scaffold, the ECM has an active role in modulation of cell behaviour (Martinez-Hernandez and Amenta, 1995). ECM proteins have various biological functions due to their ability to interact with other molecules such as other ECM proteins, cytokines and growth factors, signalling receptors and adhesion molecules. These functions are mediated by the specific domains present within each protein (Kim *et al.*, 2011). Cells such as HSCs also contribute to ECM remodelling and alter the balance of ECM proteins surrounding them, in turn changing the signals they receive (Wight and Potter-Perigo, 2011).

The ECM provides signals that help determine gene expression and cell fate of all cells (Streuli, 2009). The effect a variety of ECM proteins on HSC behaviour have been previously documented and are discussed in section 4.3. Work presented in this chapter demonstrates that modulation of the expression of activation markers and *Cygb* by ECM matrix, specifically collagen I in an HSC cell culture model. There is increasing research into fibrosis resolution and matrix degradation (Friedman, 2008c,

Ramachandran and Iredale, 2012), it is hypothesised that HSC may come into contact with a form of denatured collagen during the resolution process, which may be similar in structure to gelatin. In support of this hypothesis this study demonstrated that gelatin had a marked effect on activation state (α SMA expression), *Cygb* expression and proliferation of HSC-T6 cells, though the mechanism of action remains to be determined.

To our knowledge there have been no studies into whether ECM proteins affect the expression of *Cygb* in HSCs, this study has shown that RNA expression of *Cygb* is altered by culture matrix and that this is dependent on attachment to the matrix in the case of collagen I. The results presented here suggest that ECM proteins may signal to regulate *Cygb* gene expression within HSC, and the possible pathway involved is investigated in Chapter 6

Interestingly and unexpectedly, *Cygb* expression on collagen I was downregulated compared with expression on non-coated plastic, and a more marked but similar result was observed in HSC-T6s cultured on gelatin, whereas the opposite effect was seen in HSC-T6s grown on laminin. Although the observation that *Cygb* is downregulated on collagen I was unexpected in the context of the HSC activation, there is some support for the observation that *Cygb* RNA is downregulated by collagen I in vivo. Mann *et al.* (2008) reported an increase in *Cygb* RNA expression in CCl₄ treated mouse liver at 24hr, which was followed by an increase in collagen I α I expression at 48hr, however the 48hr time point, where collagen I α I is increased, *Cygb* RNA expression had

significantly decreased, to below that of normal liver levels, suggesting that collagen I deposition in a fibrotic liver could result in a reduction in *Cygb*.

Evidence suggesting that *Cygb* may be downregulated in fibrosis has also been reported by Cui *et al.* (2012), who reported that primary HSCs treated with arundic acid showed a marked increase in *Cygb* RNA and protein expression, associated with a decrease in α SMA RNA and protein expression, suggesting a more quiescent phenotype. Le *et al.*(2012) also presented evidence that *Cygb* may be anti-fibrotic, where *Cygb* knock-out mice showed increased hepatosteatosis when fed a choline-deficient amino-acid defined diet. These reports agree with our *in vitro* observations of HSC-T6 activation state and *Cygb* RNA expression. Western blot analysis of *Cygb* protein expression on laminin, collagen I and non-coated plastic confirmed the observation from RT-PCR, that *Cygb* expression is increased on laminin. Surprisingly, the indicated mass of the protein bands on the western blot were much larger than the reported weight of *Cygb* (21 kDa) at between 70-100 kDa. However, recent research by Tsujino *et al.* (2014) has shown that wild type CYGB can exist as a tetramer with two bands visible at approximately 75-80 kDa. Therefore, it seems plausible that CYGB exists in the tetrameric form in HSCs, and this may be related to its function in these cells as CYGB ligand binding affinity is affected by polymerization, each state showing different binding affinities for cyanide, with the monomer having the highest affinity, and in the ferrous state, affinities for CO also differ (Tsujino *et al.*, 2014). Furthermore, collagen I had the same suppressive effect on *CYGB* expression -LX-2 cells, but, unlike in HSC-T6s, laminin has no effect on *CYGB* expression this cell line, as

discussed in Chapter 4, this could be indicative of differences between the HSC-T6 and LX-2 cell lines. These differences could be due to differences in receptor expression, artefacts of cell immortalisation or species differences; further investigation is needed to elucidate the cause of the difference. Observation of the suppressive effect of collagen I on *Cygb* expression in both cell lines suggests that this is not specific to HSC-T6 cells and could therefore be related to true stellate cell biology.

Results showed that on both collagen I and non-coated plastic, *Cygb* expression is changed in a time dependant manner, with expression initially decreasing and remaining suppressed over 48hrs on collagen I but returning to initial levels on non-coated plastic, suggesting a signalling mechanism between collagen I and *Cygb* expression. The effects of collagen I on *Cygb* expression show that attachment of the cells to a basement matrix is required, and these effects are greater at higher concentrations of collagen I, again indicating a signalling through surface membrane receptors and the existence of 'outside-in signalling' between the ECM and *Cygb* gene regulation, whereby ECM composition effects *Cygb* RNA expression in both the HSC-T6 and LX-2 cell lines. Taken in context this may be important in the fibrotic process and the development of liver disease. Adherent cells require attachment to the ECM to advance through the cell cycle, changes in ECM composition on injury to the liver initiate positive and negative feedback pathways to regulate fibrosis. Primary amongst these changes are modifications in cell surface receptors, particularly integrins (Friedman, 2008b, Streuli, 2009). Activation of these receptors results in the formation of focal adhesions leading to a down-stream signalling cascade. HSCs have been shown

to express many ECM protein receptors, including several integrins and both discoidin domain receptors (Leitinger and Hohenester, 2007, Friedman, 2008c, Patsenker and Stichel, 2011). In Chapter 6 signalling from the ECM to *Cygb* in HSCs is investigated.

Chapter 6

Signalling between

ECM and *Cygb*

6.1 Introduction

Changes in ECM composition in the process of liver fibrosis are discussed in sections 1.2.3 and 1.2.4. These changes drive alterations in membrane receptors in HSC, particularly integrins, indicating the ECMs' role not only as a scaffold but as part of the cell-cell communication network via cell surface receptors (Benyon and Iredale, 2000, Bedossa and Paradis, 2003, Friedman, 2008c). An exhaustive review of integrin signalling is beyond the scope of this thesis; however a short overview of integrins, outside-in signalling and the downstream signalling cascades initiated from integrin activation are important for the context of this research. Integrins are transmembrane protein receptors, which mediate interactions between cells and their surrounding environment (Humphries, 2000, Patsenker and Stickel, 2011). Intercellular binding to ECM via integrins is one of the major influences on cell behaviour (Streuli, 2009). They were originally termed 'integrin' for their ability to integrate intracellular and extracellular responses (Hynes, 1987). Binding to ECM initiates the transmission of internal cell signals, termed 'outside-in signalling' and can provide instructions for gene expression (Clark and Brugge, 1995, Qin *et al.*, 2004, Streuli, 2009). HSC have been shown to express many cell surface receptors for ECM proteins including integrin subunits, which recognise many different ECM protein ligands and are discussed in section 6.1.3.

6.1.1 The structure of integrins

Integrins are non-covalently associated heterodimers composed of a large extracellular domain (700 – 1100 residues) and a short cytoplasmic domain (30 – 50 residues). The dimers are formed by the association of an α subunit of approximately 180 kDa and a β subunit of approximately 95 kDa, both of which are type I membrane glycoproteins. The extracellular domain of the integrin heterodimer comprises an asymmetric structure, formed of a globular 'head' on two flexible 'legs'. To date 18 α subunits and 8 β subunits, forming 24 heterodimers have been reported (Humphries, 2000, Arnaout, 2002, Stupack, 2007). Figure 6.1 illustrates the basic structure of an integrin.

6.1.2 Integrins, focal adhesions and focal adhesion kinase (FAK)

On activation, such as binding to ECM proteins, integrins cluster on the membrane plane, form focal adhesions and recruit non-receptor tyrosine kinase signalling molecules like focal adhesion kinase (FAK), which is one of several components that make up the focal adhesion, (Leitinger and Hohenester, 2007, Desgrosellier and Cheresch, 2010). On binding to an activated integrin, FAK itself becomes activated and autophosphorylates at tyrosine (Y) 397. Tyrosine phosphorylation is a key event in the formation of focal adhesions and FAK is a major signalling factor within them. Autophosphorylation of FAK Y397, which has been shown to be important in many of FAKs functions, initiates further phosphorylation events leading to an intracellular signalling cascade, Figure 6.2 depicts integrin clustering and focal adhesion formation,

leading to FAK phosphorylation and downstream intracellular signalling. FAK has been shown to be involved in cell migration and proliferation (Cary and Guan, 1999 Wozniak, 2004).

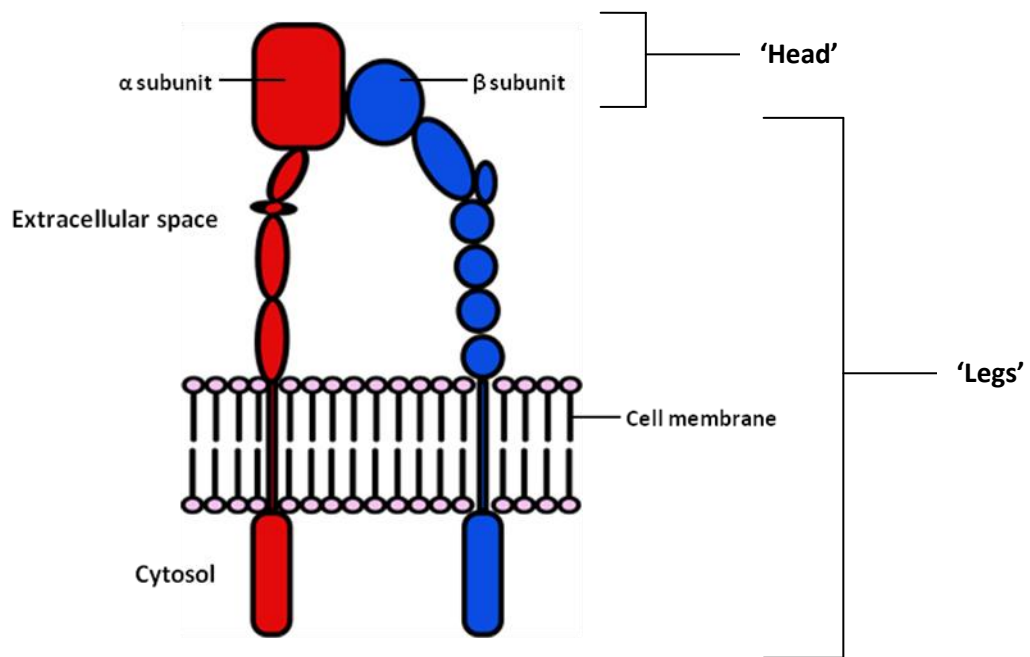


Figure 6.1: A simplified schematic of the structure of an integrin heterodimer showing the transmembrane region, the α and β subunits and the globular 'head' and flexible 'legs'.

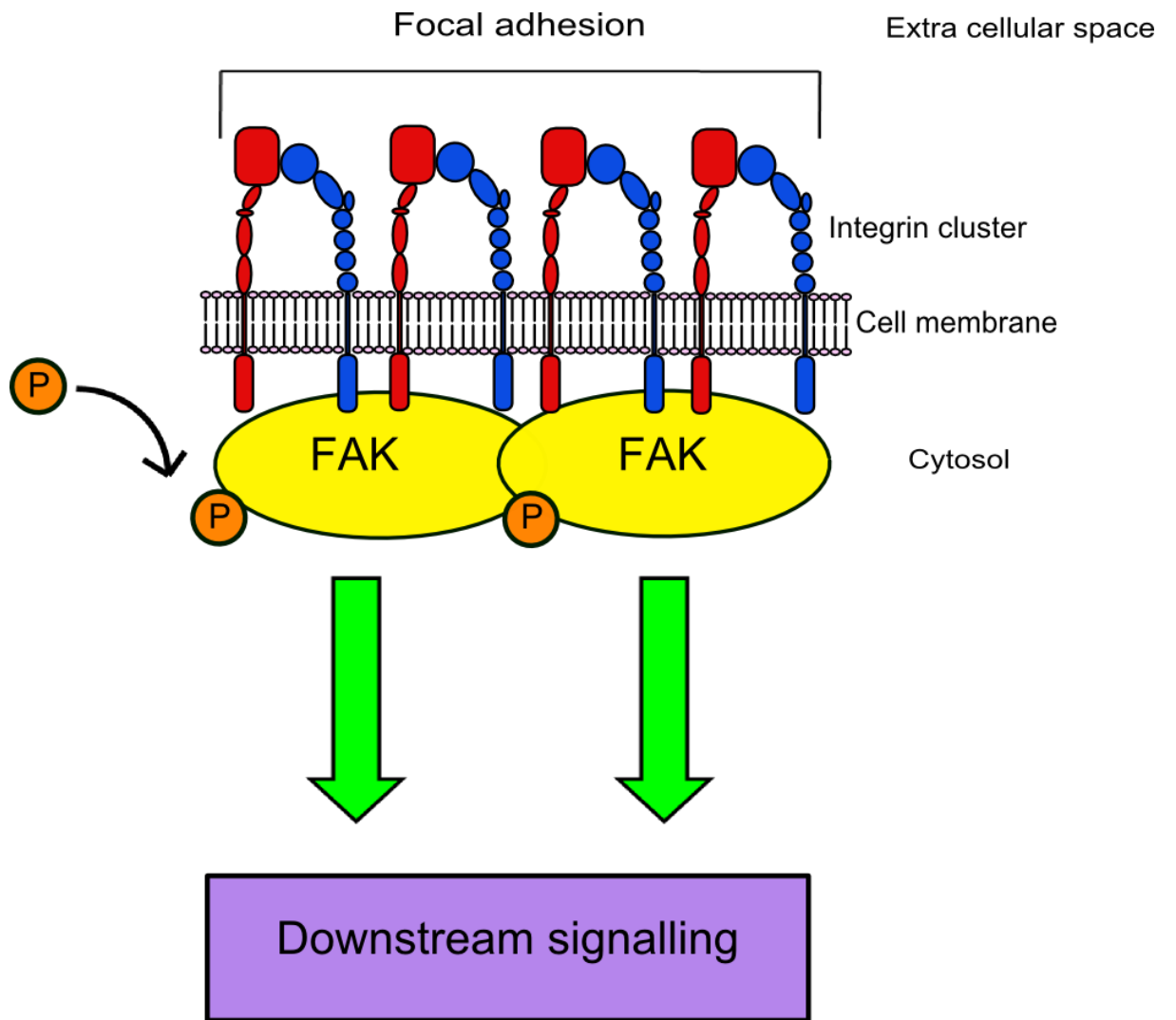


Figure 6.2: A simplified schematic of integrin clustering, focal adhesion formation and FAK autophosphorylation leading to downstream signalling.

6.1.3 Integrins associated with HSC

Table 6.1 gives summary detail of integrin subunits known to be expressed by HSCs.

Table 6.1: Integrin subunits associated with HSCs. References: Leitinger and Hohenester(2007), Friedman (2008b) and Patsenker and Stickel, (2011)

Receptor Subunit	Structure and Combinations	Ligands
Integrin beta 1 ($\beta 1$)	Forms heterodimers with integrin alpha subunits. In this instance, expression with regard to $\alpha 11$ and $\alpha 2$ is the focus.	When associated with $\alpha 11$, preferentially fibril forming collagens with specific sites for collagen I identified. When associated with $\alpha 2$, preferentially fibril-forming collagens, with specific sites for collagen I and III identified, but also laminin and fibronectin. When associated with $\alpha 5$, preferentially fibronectin, tenascin and collagens.
Integrin alpha 11 ($\alpha 11$)	Forms a heterodimer with integrin $\beta 1$ subunit.	See $\beta 1$
Integrin alpha 2 ($\alpha 2$)	Forms a heterodimer with integrin $\beta 1$ subunit.	See $\beta 1$
Integrin alpha 5 ($\alpha 5$)	Forms a heterodimer with integrin $\beta 1$ subunit.	See $\beta 1$
Integrin beta 3 ($\beta 3$)	Forms a heterodimer with integrin α_v subunit.	Interacts with collagen, fibronectin, vitronectin, fibrinogen and tenascin when associated with the α_v integrin subunit.
Integrin beta 4 ($\beta 4$)	Forms a heterodimer with integrin $\alpha 6$ subunit.	Evidence for interactions with fibronectin and laminin.
Integrin alpha 6 ($\alpha 6$)	Forms a heterodimer with integrin $\beta 4$ subunit.	

Attachment to ECM has been found to influence gene expression through integrin signalling (Miranti and Brugge, 2002, Streuli, 2009) and it has been previously reported that integrin activation can influence HSC behaviour. Zhou *et al.* (2004) found that antagonising the α_v integrin subunit inhibited the proliferation of primary rat HSCs and increased apoptosis in these cells. Inhibition of the β_1 subunit by a monoclonal antibody in human primary HSCs also reduced attachment to laminin, collagen I, collagen IV and fibronectin (Carloni *et al.*, 1996). HSCs also show *de novo* expression of $\alpha_8\beta_1$ on activation by CCl_4 or bile duct ligation in rats, and upregulation of $\alpha_v\beta_3$ on *in vitro* activation of rat and human primary HSC (Carloni *et al.*, 1996), suggesting an important role for integrins in the fibrotic process.

HSCs have also been shown to express discoidin domain receptors (DDR), which are collagen receptors that are distinct from integrins. DDR1 and DDR2 comprise a subfamily of receptor tyrosine kinases that have differing affinities for different collagens, DDR1 is activated by both fibrillar and non-fibrillar collagens, whereas DDR2 is only activated by fibrillar collagens such as collagen I and collagen III (Song *et al.*, 2011). Collagen I has been shown to stimulate DDR2 phosphorylation in HSC-T6 cells and culture on the basement membrane-like substrate matrigel reduced DDR2 expression in HSC-T6s compared with expression in cells cultured on collagen I. Over-expression of DDR2 in HSC-T6s also promoted cell proliferation and matrix metalloproteinase 2 expression (Olaso *et al.*, 2001). Thus, it is also feasible that DDRs could be involved in the changes in *Cygb* expression, morphology and proliferation that have been reported in chapters 3 and 4 of this thesis. The aims of the study reported in this chapter were to identify possible mechanisms of signal transduction

from ECM to *Cygb* through cell surface receptors and then downstream through intracellular signalling.

6.2 Results

6.2.1 Cell Surface ECM protein receptors are differently expressed in HSC-T6 cells cultured on different ECM proteins

Surface ECM protein receptors are differently expressed in HSC-T6 cells cultured on different ECM proteins. To investigate possible pathways for differential *Cygb* RNA expression in HSC-T6 cells, RT-PCR was undertaken on seven receptor sub-units for ECM proteins and also *DDR1* and *DDR2*. The receptors screened are detailed in Table 6.1. The rationale for receptor choice was based on receptors associated with ECM proteins effecting the most marked changes in *Cygb* RNA expression, collagen I, gelatin and laminin.

Figure 6.3 shows RT-PCR results for two of the receptors screened. Of the nine screened, these two integrin receptor subunits ($\alpha 2$ and $\beta 4$), showed significant ($p < 0.05$) differences in expression in HSC-T6s cultured on laminin, collagen I and gelatin, using receptor expression in cells cultured on non-coated plastic as the reference. These differences mirror the differences in *Cygb* and α SMA expression observed on these surfaces. The $\alpha 2$ subunit preferentially binds with fibrillar collagens such as collagen I when associated with the $\beta 1$ subunit. As indicated in Figure 6.3 A, $\alpha 2$ expression is significantly upregulated in cells cultured on collagen I and gelatin when

compared with expression on laminin. The opposite is true for the $\beta 4$ subunit, shown in Figure 6.3 B. This subunit is reported to associate with laminin (see Table 6.1). The other seven receptors screened showed no significant changes in expression (see appendix 4), except $\alpha 5$, which was significantly down regulated on collagen I ($p < 0.05$ one-way ANOVA with Tukey's post hoc t-test) compared with expression on non-coated plastic. However $\alpha 5$ showed no statistically significant difference in expression on laminin or gelatin (Figure 6.4).

6.2.2 ECM affects FAK phosphorylation in HSC-T6s

In support of a role for 'outside-in signalling' by ECM via integrin clustering, focal adhesion formation and autophosphorylation of FAK (pFAK) leading to downstream signalling was analysed. Figure 6.5 A-C show that levels of FAK (pY397) protein is greater in HSC-T6 cells cultured on collagen I than in those cells cultured on laminin or non-coated tissue culture plastic, as assessed by western blot analysis.

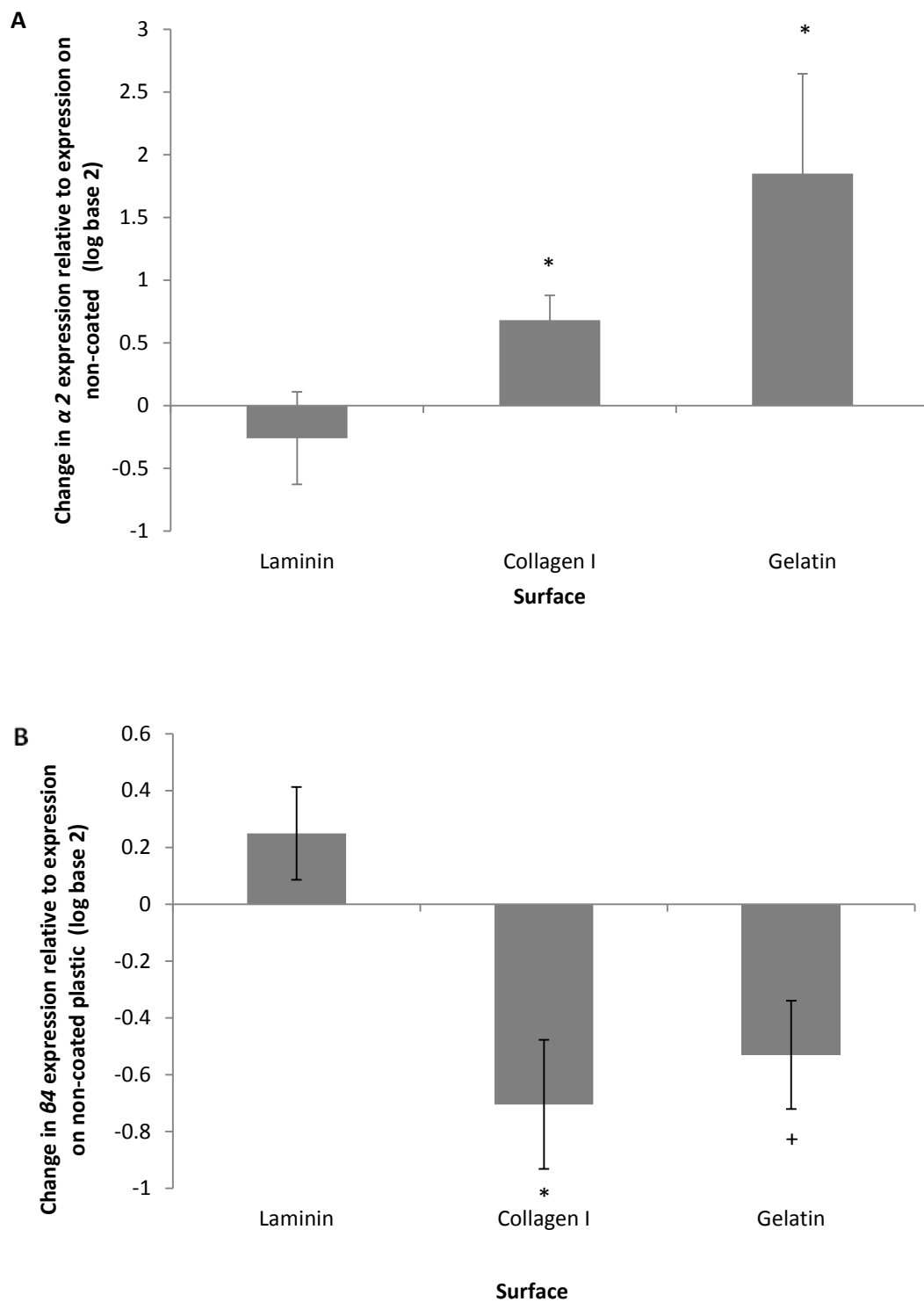


Figure 6.3: RT-PCR expression of A) $\alpha 2$ (N=5) and B) $\beta 4$ integrin subunit ECM receptors across laminin, collagen I and gelatin ECM proteins in HSC-T6 cells relative to the expression levels of those grown on non-coated T₂₅ culture flasks. * denotes significance at $p < 0.05$ according to one-way ANOVA with Tukey's post hoc t -test, + denotes significance at $p < 0.05$ according to t -test assuming equal variances, +/- SEM (N=3).

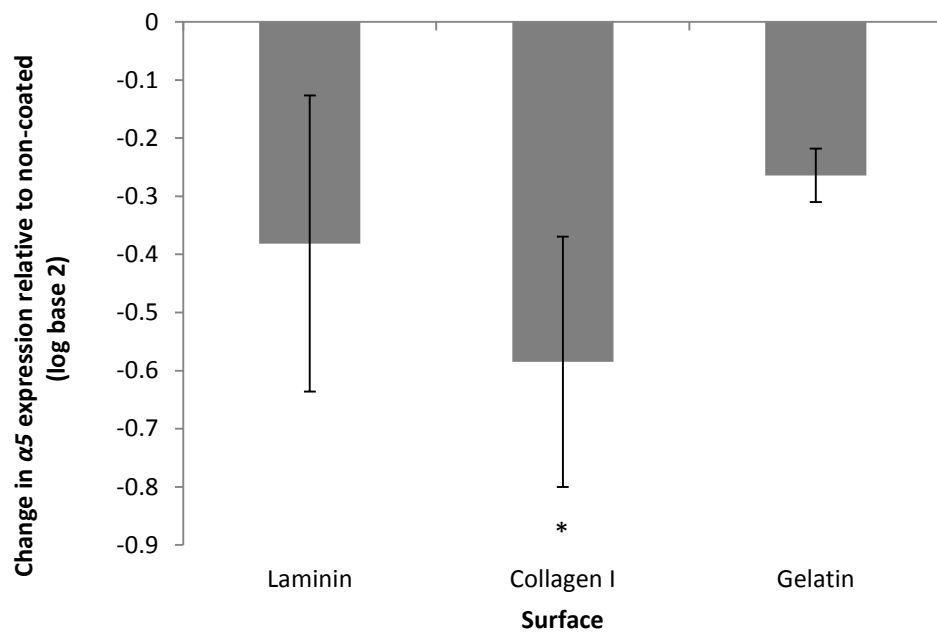


Figure 6.4: Expression data for $\alpha 5$ integrin subunit ECM receptor across laminin, collagen I and gelatin ECM proteins in HSC-T6 cells relative to the expression levels of those grown on non-coated T25 culture flasks. * denotes significance at $p < 0.05$ according to one-way ANOVA with Tukey's post hoc t -test, +/- SEM (N=2).

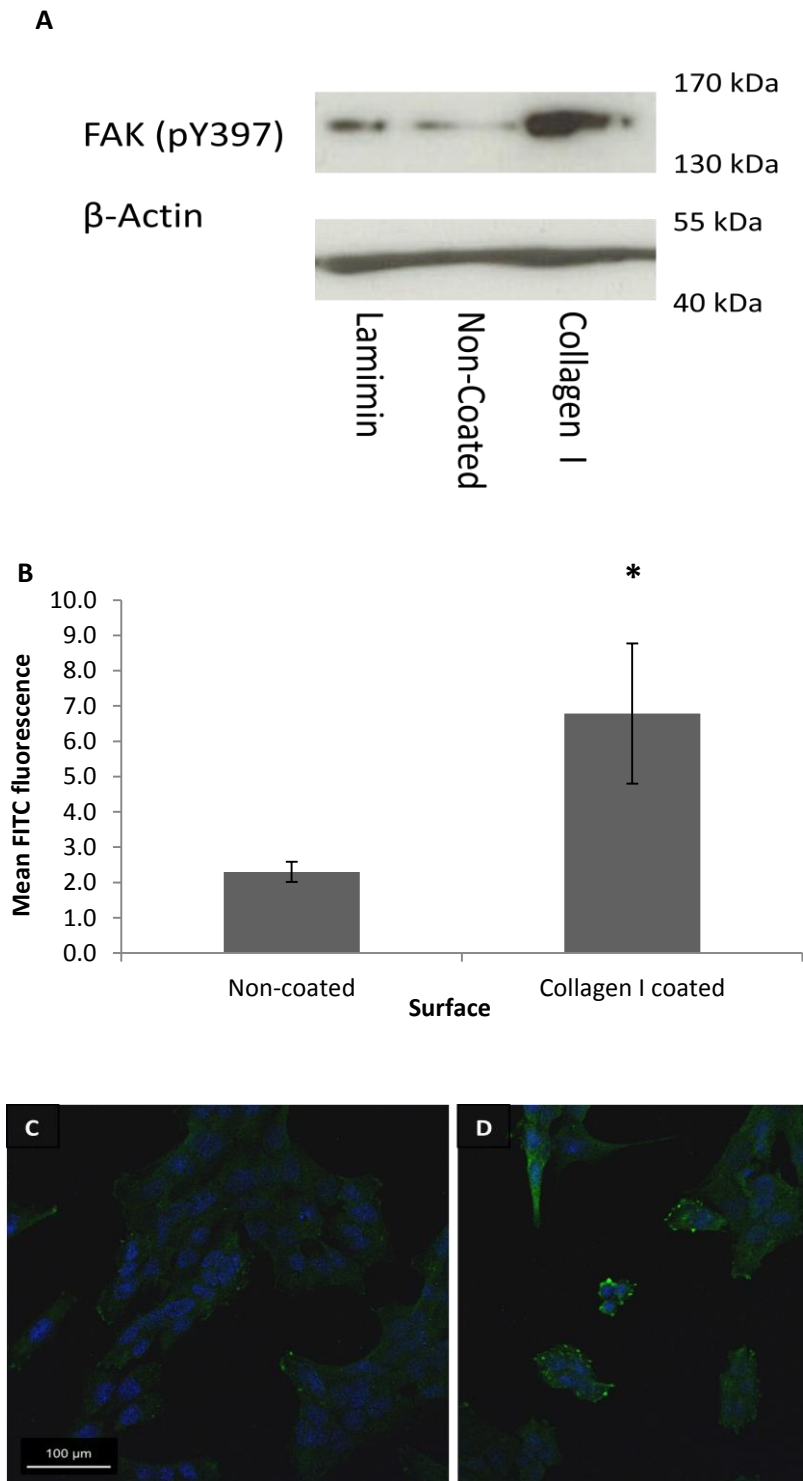


Figure 6.5: pFAK expression in HSC-T6 cells cultured on non-coated plastic and collagen I A) Western blot for levels of phosphorylated FAK Y397 in cells cultured on laminin, non-coated tissue culture plastic and collagen I with β -Actin loading control. B) Mean FITC fluorescence \pm SEM (N=3) in HSC-T6 cells cultured on non-coated plastic and collagen I, analysed by flow cytometry, $p < 0.05$ according to one-way ANOVA with Tukey's post hoc t -test C) and D) Confocal image of cells cultured on glass and collagen I respectively and probed for expression of phosphorylated FAK Y397 (N=3).

6.2.3 RNAi of FAK was unsuccessful and had no effect on *Cygb* expression in HSC-T6 cells.

To investigate whether reduction of *FAK* expression would reconstitute *Cygb* expression in HSC-T6 when cultured on collagen I, RNAi of *FAK* was undertaken. After initial optimisation (appendix 5) RNAi of *FAK* expression in HSC-T6s cultured on non-coated plastic and collagen I was carried out, followed by RT-PCR analysis of both *FAK* and *Cygb* expression. As Figure 6.6 shows, RNAi of *FAK* only achieved an approximately 25% reduction in *FAK* expression in cells cultured on non-coated plastic (Figure 6.6 A) and no reduction in *FAK* expression in cells cultured collagen I (Figure 6.6 B). Unsurprisingly, there was no effect of *FAK* RNAi treatment on *Cygb* expression in these cells either, and the non-targeting control RNAi treatment (NT2 and NT4), appear to have off-target effects on *Cygb* expression in cells cultured on non-coated plastic (Figure 6.7).

6.2.4 Inhibition of FAK with FAK Inhibitor 14

As an alternative approach to RNAi, to further investigate the effects of FAK autophosphorylation and the downstream signalling resulting from this autophosphorylation on *Cygb* expression, inhibition of FAK phosphorylation by FAK Inhibitor 14 (FAKI) was optimised in HSC-T6 cells. FAKI has been shown to inhibit autophosphorylation of FAK Y397 in the BT474 breast cancer cell line (Xu *et al.*, 2005), and, therefore, might also inhibit autophosphorylation in HSC-T6s. Initially an MTT test was conducted on cells cultured on non-coated tissue culture plastic, with concentrations of FAK I between 0 and 100 μ M as suggested in the literature (Xu *et al.*, 2005). The second lowest concentration of FAK I (10 μ M) proved toxic to HSC-T6 cells. Furthermore, the lowest

concentration (1 μ m) caused approximately 30% cell death when initially tested (Figure 6.8 A). A second MTT assay was conducted with a lower concentration range between 0 and 1 μ M on non-coated plastic and collagen I. Figure 6.8 B shows the results of the second MTT assay, for cells cultured on collagen I only the highest concentration of FAKI (1 μ M) had significant effect on cell viability, where as a significant effect was observed for both 0.5 μ M and 1 μ M in cells cultured on non-coated plastic.

Initial western blot analysis was conducted on cells treated for 24 hrs (recommended in the literature, Golubovskaya *et al.*(2008)) and 48 hrs. Although the 24 hr treatment showed a good response to FAKI with increasing concentrations inhibiting FAK pY397 expression in cells cultured on both surfaces, the 48 hr treatment showed a lack of inhibition, suggesting the treatment is unsuitable for 48 hr periods (appendix 6). As previously stated in section 5.2.2, *Cygb* RNA expression in HSC-T6 cells cultured on non-coated plastic and collagen I differs at the 48hr time point. Thus, it is important that the FAKI treatment is effective at this point, to investigate if inhibiting FAK effects *Cygb* expression in these cells. To this end, two treatment regimes were conducted, where HSC-T6 cells were either cultured for 24hrs then treated with FAKI for 24hrs, or treated for 24hrs then cultured for a further 24hrs in inhibitor-free media. Figure 6.9 shows that FAKI effects FAK Y397 phosphorylation through the cultured for 24hr then treated for 24hr regimen by flow cytometry (Figure 6.9 A) and confocal microscopy (Figure 6.9 B). A visible decrease in phosphorylated FAK is detected in HSC-T6 cells treated with FAK in a concentration dependant manner by both analysis methods (Figure 6.9).

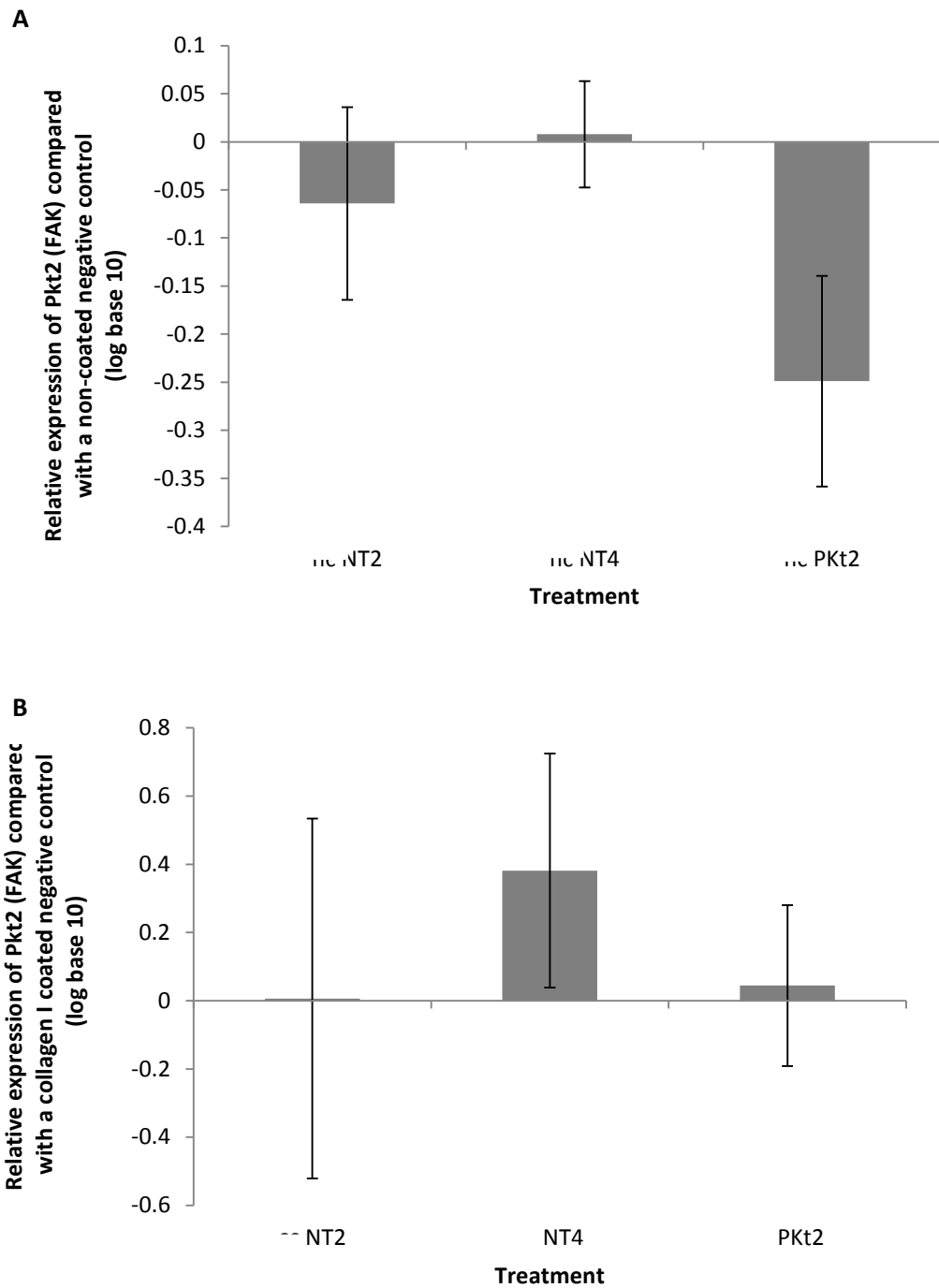


Figure 6.6: FAK expression after RNAi treatment with PKt2 (FAK) in HSC-T6 cells seeded at 100,000 cells/ml, cultured for 48 hrs with 24 hrs RNAi on **A)** non-coated plastic and **B)** collagen I, then analysed for *PKt2* expression by RT-PCR. Abbreviations: NT2 = non-targeting siRNA cocktail 2, NT4 = non-targeting siRNA cocktail 4. +/- SEM (N=3).

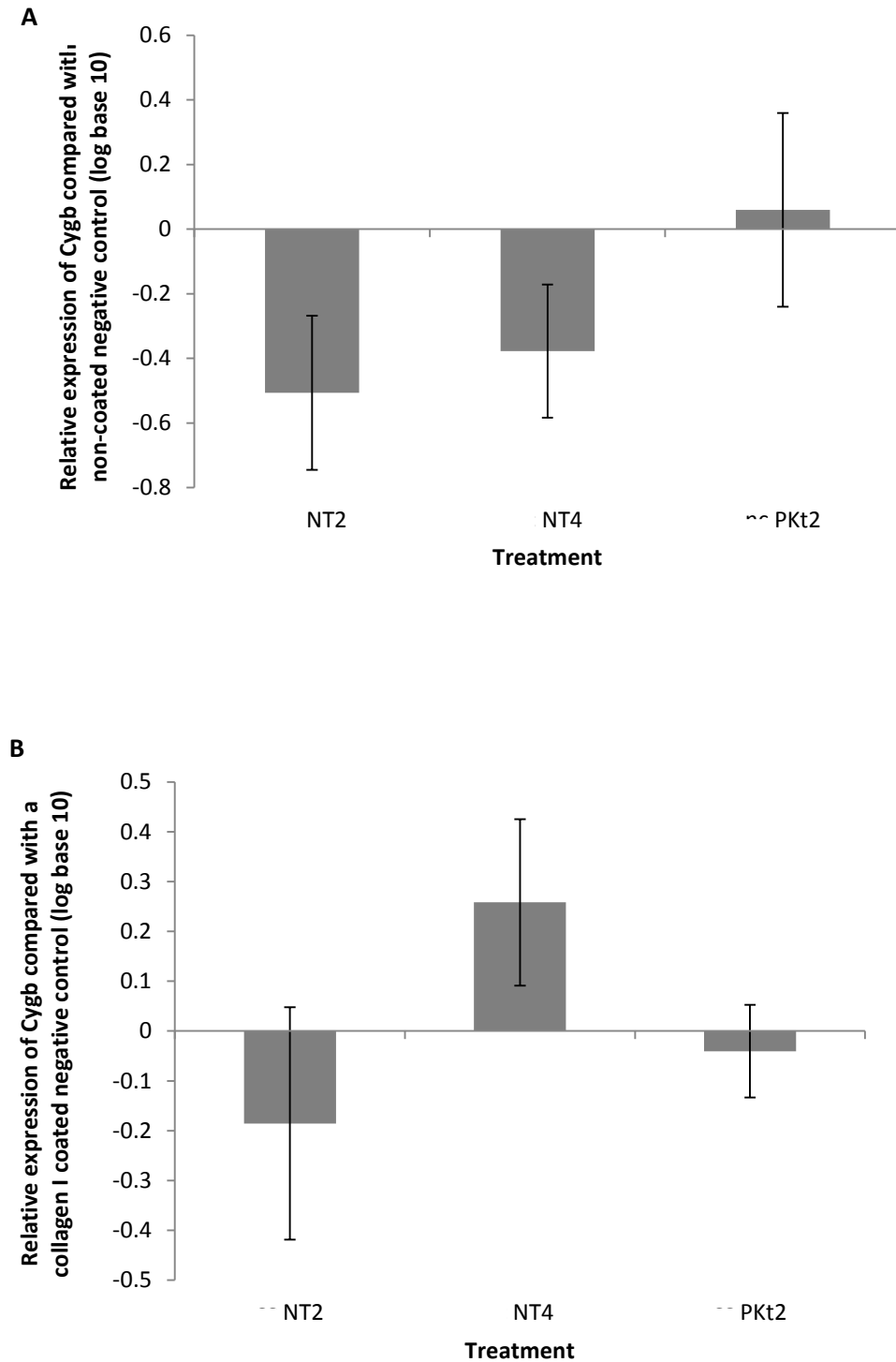


Figure 6.7: *Cygb* expression after RNAi treatment with *PKt2* (*FAK*) in HSC-T6 cells seeded at 100,000 cells/ml, cultured for 48 hrs with 24 hrs RNAi on **A)** non-coated plastic and **B)** collagen I then analysed for *Cygb* expression by RT-PCR. Abbreviations: NT2 = non-targeting siRNA cocktail 2, NT4 = non-targeting siRNA cocktail 4. =+/- SEM (N=3).

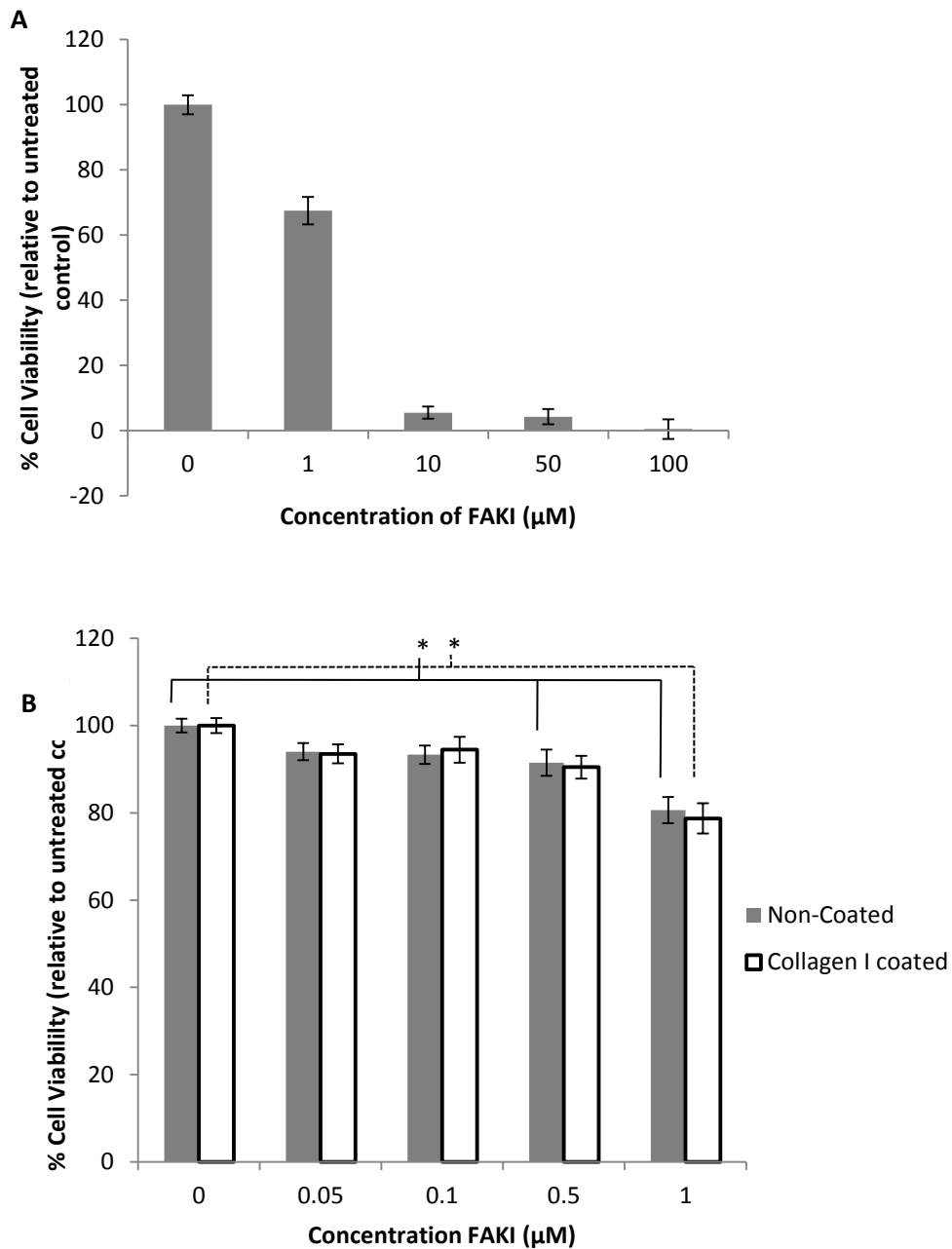


Figure 6.8: Results of MTT viability assay for HSC-T6 treated for 48hrs with FAKI. Cells were seeded at 100,000 cells/ml and immediately treated with FAKI. MTT assay was undertaken at 48 hrs of culture and cell viability normalised to a percentage of the untreated control cells. A) Viability of HSC-T6 cells cultured on non-coated plastic and treated with FAKI concentrations between 0 and 100 μM for 48 hrs. B) Viability of HSC-T6 cells cultured on non-coated plastic and collagen I and treated with FAKI concentrations between 0 and 1 μM for 48 hrs. +/- SEM (N=3)

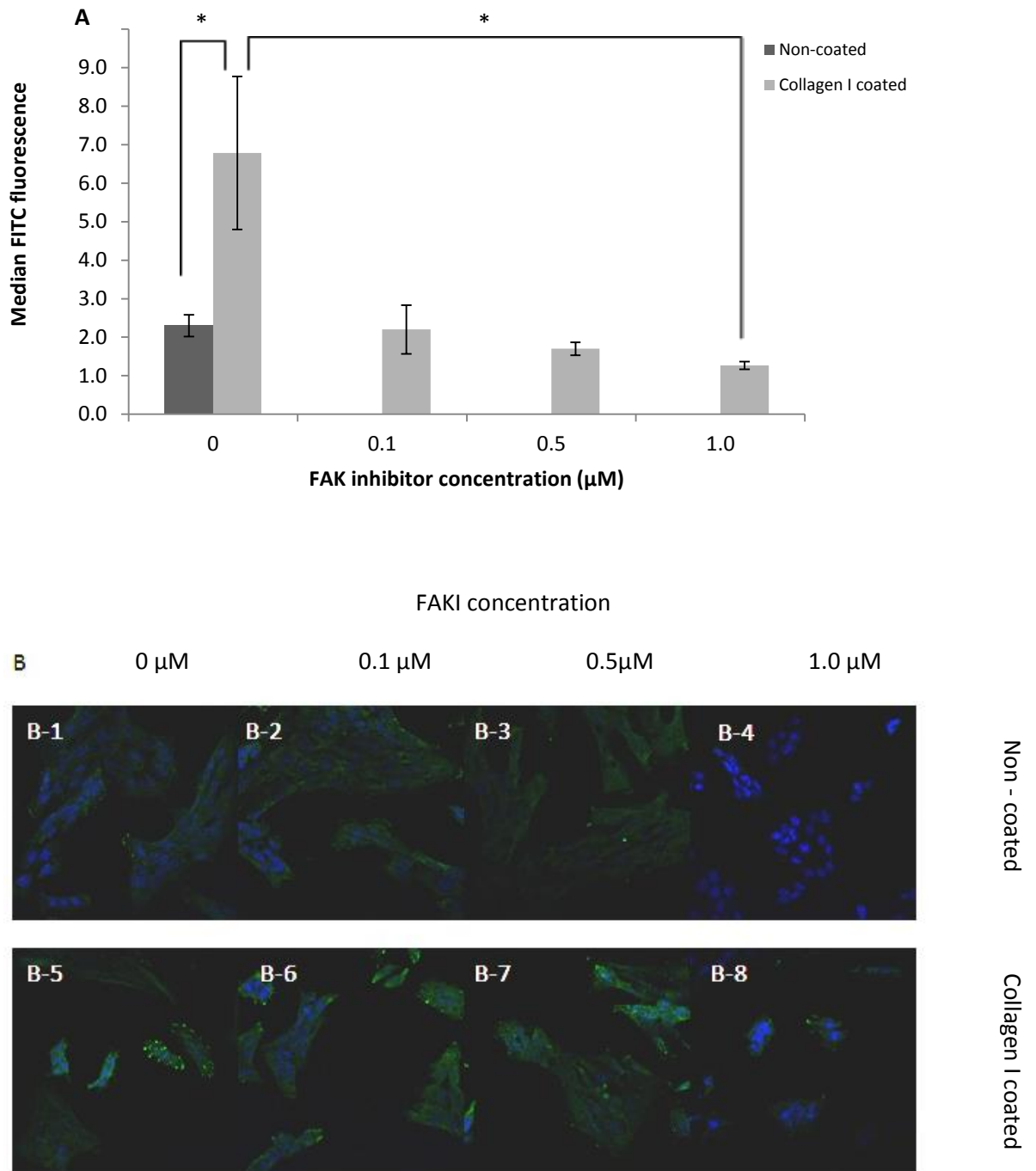


Figure 6.9: Results of pFAK inhibition in HSC-T6 cells A) Median (+/- SEM) fluorescence of FAK pY397 analysed by flow cytometry in cells treated with different concentrations FAKI. Cells were seeded at 100,000 cells/ml cultured for 24hrs prior to 24hrs of treatment with FAKI then probed for FAK pY397. B) Confocal Microscopy of cells probed for FAK pY397 cultured on non-coated (B-1-4) or collagen I coated (B-5-8) coverslips. Cells were either untreated (B-1 and B-5) or treated with 0.1µM (B-2 and B-6), 0.5 µM (B-3 and B-7) or 1.0µM (B-4 and B-8) FAKI 14.

6.2.5 The effect of FAKI on Cygb expression is inconclusive

To investigate the effect of blocking FAK autophosphorylation with FAKI on Cygb expression in HSC-T6 cells, western blot and RT-PCR analysis of Cygb expression in HSC-T6 cells treated for 24 hrs FAKI was undertaken. Figure 6.10 shows the results of these analyses; western blot suggests a possible increase in Cygb protein expression in HSC-T6 cells treated with FAKI (Figure 6.10 A), where as RT-PCR shows no clear effect and the error bars are large, reducing confidence in the result obtained (Figure 6.10 B), there is no statistically significant difference between any treatment or from the or negative control. These results give no conclusive evidence for or against FAK autophosphorylation being involved in the signalling cascade from ECM to Cygb expression in HSC-T6 cells.

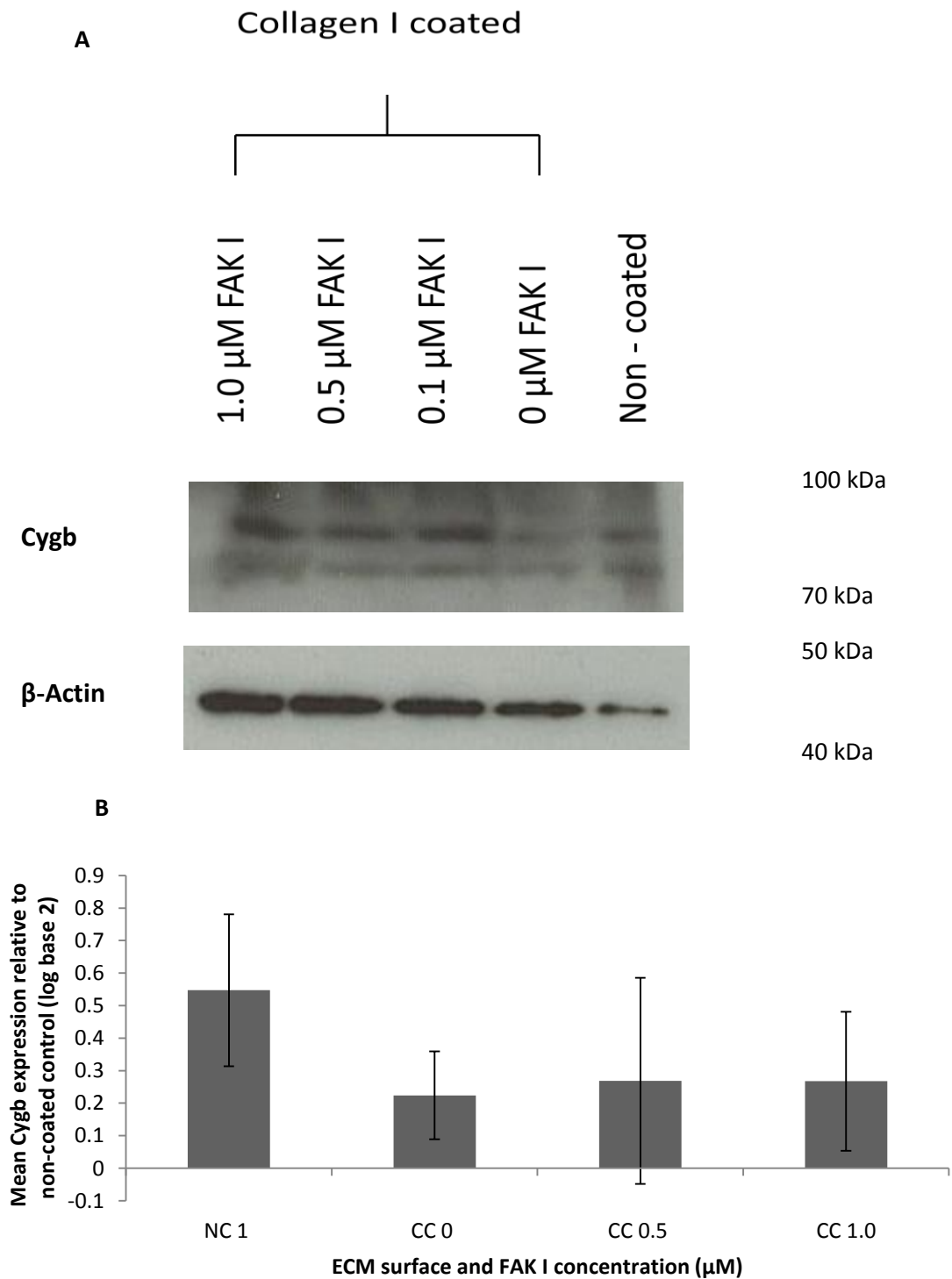


Figure 6.10: The effect of pFAK inhibition on Cygb expression in HSC-T6s A) Western blot for Cygb in HSC-T6 cultured on non-coated plastic or collagen I and treated with different concentrations of focal adhesion kinase inhibitor 14 (FAKI) with a β -Actin loading control. B) RT-PCR of HSC-T6 cultured on non-coated plastic or collagen I and treated with different concentrations of focal adhesion kinase inhibitor 14 (FAKI), N of at least 3 for all treatments.

6.3 Discussion

This study reports different expression of integrin subunit RNA in HSC-T6 cells cultured on laminin, collagen I and gelatin. It has been previously reported that ECM protein receptors can be up-regulated upon HSC activation, particularly integrins. For example $\alpha 5 \beta 1$ integrin expression has been shown to increase on activation of primary rat HSCs and upon its binding to fibronectin, where there is an accumulation of signalling proteins and the aggregation of the receptors initiates the ERK (Extracellular signal-regulated kinase) and JNK signalling pathways (Milliano and Luxon, 2003). Zhou *et al.* (2004) also reported an increase in the αv and $\beta 3$ subunits in HSCs cultured on collagen I and vitronectin, and that disruption of these receptor subunits resulted in inhibition of proliferation and induced apoptosis in these cells. It has also been documented that ECM protein receptors play a role in HSC behaviour. Yang *et al.* (2008) reported that LX-2 migratory behaviour towards collagen I was altered in the presence of $\alpha 1$ - and $\alpha 2$ -blocking antibodies indicating these receptors have a role in HSC function. Olsen (2012) observed that cellular fibronectin containing the alternatively spliced extra domain A (EIIIA), which is upregulated during the wound healing process, increased motility in primary rat HSC and that this process required the $\alpha 9 \beta 1$ integrin. Priya and Sudhakaran (2008) also observed altered HSC behaviour mediated through integrin signalling. They reported an increase in apoptosis in HSCs maintained on collagen I when treated with curcumin in the presence of an anti- $\alpha 2 \beta 1$ antibody when compared with those treated with curcumin with no antibody present, suggesting integrins also control apoptotic pathways. Activation of HSCs can also be mediated through receptor

activation; Zvibel *et al.* (2010) reported that L-thyroxine, a synthetic thyroid hormone identical to the thyroid hormone-thyroxine, induced activation of primary rat HSCs and this could be reversed by antibody blocking of the $\beta 3$ integrin subunit. In this study we observed differences in expression in the $\alpha 2$ and $\beta 4$ subunits on collagen I, gelatin and laminin, as well as $\alpha 5$ on collagen I, and it is possible that integrins containing these subunits could be involved in a signalling cascade, which goes on to influence *Cygb* expression in HSC-T6s, as *Cygb* is also differently expressed at the RNA and protein level on different ECM surfaces in these cells (Chapter 5). The results of the receptor screen in this study show no significant difference or biological trend in DDR receptor expression. DDRs do not recognise gelatin as the triple helix of collagen is required for DDR activation (Vogel *et al.*, 2006). It is therefore unlikely that *Cygb* expression is mediated through a DDR signalling pathway as our observations indicate that expression of *Cygb* RNA in HSC-T6 cells is effected by gelatin, along with collagen I and laminin. Thus, it is more likely that *Cygb* RNA expression is modulated via an integrin signalling pathway. The observed difference in cell morphology (in HSC-T6 cells) proliferation and activation state reported in Chapter 4 are also likely to be regulated through integrins, as other authors have reported changes in cell behaviour associated with integrin expression and activation, which is discussed above; however, not all relevant receptors for ECM proteins in HSC have been screened in this study, and although alterations in three of the five integrin subunits screened were observed, integrin subunit blocking experiments were not performed, therefore we cannot conclude directly that these subunits are responsible for the observed effects on HSC-

T6s. The possibility remains that the receptor through which signal transduction is occurring has not yet been identified.

Whichever receptor ECM signals through in HSC-T6 cells, it is clear that HSC-T6s cultured on collagen I have increased FAK Y397 phosphorylation compared with those cultured on laminin and non-coated plastic. FAK is a critical mediator of integrin signalling as integrins have no intrinsic enzyme activity (Carver and Goldsmith, 2013) and Michael *et al.* (2009) showed that autophosphorylation of FAK at Y397 is important in adhesion strengthening and integrin binding rate, and FAK expression has a role in regulating integrin activation in human dermal fibroblasts. It has been shown that FAK is upregulated in an *in vivo* mouse model of liver fibrosis, and the distribution of FAK expression correlates with α SMA expression, a marker of activated HSC, in these fibrotic livers (Jiang *et al.*, 2004). Shen *et al.* (2006) demonstrated that FAK can mediate proliferation in primary rat HSCs and FAK silencing by short-hairpin RNA can reduce proliferation and induce apoptosis in HSC-T6 cells (An *et al.*, 2011). Rodriguez-Juan *et al.* (2009) reported similar observations in primary rat HSCs, where silencing of FAK by short-interfering RNA increased apoptosis in these cells, they also observed that blocking of the α 5 integrin subunit prevented FAK phosphorylation by binding of fibronectin, linking ECM binding to integrins to FAK phosphorylation in HSCs. The observation made in this study that there is an increase in phosphorylated FAK at Y397 in HSC-T6 cells cultured on collagen I, and these cells show increased proliferation and activation state, as analysed by ATRA uptake and α SMA RNA expression, is in line with the findings of others, namely that FAK expression and phosphorylation is an important event HSC activation and regulates processes in HSC that are associated

with their activation, such as increased proliferation and apoptosis (Chapters 4, 5 and 6) FAK has also been shown to be important in myofibroblast differentiation and activity in primary lung fibroblast in mice (Lagares *et al.*, 2012). HSC-T6 cultured on collagen I also have decreased *Cygb* expression, as does the human HSC cell line LX-2 (Chapter 5), and FAK phosphorylation could have a role in the control of *Cygb* expression in these cells.

In this investigation, silencing of *de novo* FAK expression by RNAi was not achieved, unlike in the study conducted by An *et al.* (2011), and therefore no effect on HSC-T6 behaviour or *Cygb* expression was observed. Further optimisation of this technique needs to be undertaken in order to effectively silence FAK expression, for this study to discover if inhibiting new FAK synthesis effects *Cygb* expression and establish a signalling mechanism. But it might not be that *de novo* FAK expression is the most important event in ECM signalling to *Cygb*, phosphorylation of FAK already present in the cell could have a more important role in the signalling mechanism. Inhibition of FAK phosphorylation by FAKI has been shown to effect cell behaviour in several previous studies. Golubovskaya *et al.* (2008) showed that treatment with FAKI inhibited cell attachment, caused cell detachment and reduced cell viability in BT474 breast cancer cells, Hochwald *et al.* (2009) found similar results in the pancreatic cancer cell lines Panc-1 and Miapaca-2 as did Beierle *et al.* (2010) in neuroblastoma cell lines, indicating FAKI has anti-tumour activity. Anti-angiogenic activity of FAKI has also been observed in human umbilical vein endothelial cells (HUVEC), where FAKI treatment impaired HUVEC viability induced apoptosis, impaired cell migration and blocked FAK autophosphorylation (Cabrita *et al.*, 2011). This study reports decreased cell viability

and inhibition of FAK phosphorylation in HSC-T6s at concentrations below 1 μ M, this is much lower than the concentrations required for inhibition of phosphorylation in HUVECs (5 μ M) (Cabrita *et al.*, 2011) and the cancer cell lines studied (10 μ M) (Xu *et al.*, 2005, Hochwald *et al.*, 2009, Beierle *et al.*, 2010), suggesting that HSC-T6s could be more sensitive to this treatment than endothelial cells or cancer cells.

Unfortunately investigation of the effects of inhibition of FAK phosphorylation on *Cygb* expression by western blot and RT-PCR proved inconclusive. RT-PCR analysis showed no effect of FAKI on *Cygb* expression in either cells cultured on non-coated plastic or collagen I; however western blot suggests that *Cygb* protein expression is reconstituted by FAKI treatment. Confusingly, there is also no effect of culture on collagen I on *Cygb* in these cells, this could be caused by the effects of continuous cell culture on cell phenotype, incorrect coating of collagen I on tissue culture plates or collagen I stocks being beyond their use-by date. It is also possible that the FAKI stocks had gone-off due to too many freeze-thaw cycles, hence no effect on *Cygb* was observed as potency might have been lost. In contrast, western blot analysis of *Cygb* protein expression seems to indicate a recapitulation of expression in HSC-T6s treated with FAKI, implying a signalling link between FAK phosphorylation and *Cygb* expression, therefore further experiments are required resolve this issue. It has not been possible to establish this link with certainty over the course of this investigation, however the findings of this study and the implications of discovering a link between ECM signalling to *Cygb* expression in HSCs, possibly occurring through FAK phosphorylation is discussed in Chapter 7.

Chapter 7

General Discussion

7.1 General Discussion

Chronic liver disease is of increasing concern in the UK and Europe, accounting for 2% of deaths in England, with a rise of 25% in deaths in England between 2001 and 2009. In Europe; liver cirrhosis is the cause of around 170,000 deaths, and liver cancer 47,000 deaths, per annum and 29 million people suffer from a chronic liver condition, which is comparable with other diseases that have a high degree of public and media attention, such as breast cancer (Effiong *et al.*, 2012, Blachier *et al.*, 2013). All chronic liver diseases can induce fibrosis in the liver, ultimately leading to cirrhosis, and the recently discovered globin, Cygb has been implicated within the fibrotic process in fibrosing diseases (Kristensen *et al.*, 2000, Nakatani *et al.*, 2004, Schmidt *et al.*, 2004, Zion *et al.*, 2009, Mimura *et al.*, 2010, He *et al.*, 2011, Cui *et al.*, 2012, Singh *et al.*, 2013). Within liver disease it is widely accepted that HSCs are the major effectors of hepatic fibrogenesis and HSC activation is the dominant profibrotic pathway (Friedman, 2008b, Friedman, 2008c). Cygb expression in the liver has been reported to be specific to HSCs, however this observation is disputed, with some reports of expression in hepatocytes (Kawada *et al.*, 2001, Geuens *et al.*, 2003, Yang *et al.*, 2011, Motoyama *et al.*, 2014). Whatever its cellular expression, there are many reports that Cygb is upregulated in liver disease, both in murine models and in diseased human liver (Kristensen *et al.*, 2000, Schmidt *et al.*, 2004, He *et al.*, 2011, Cui *et al.*, 2012, Motoyama *et al.*, 2014). Data presented in this thesis confirm this observation in murine models of liver disease and in human liver tissue from different disease aetiologies, staining for CYGB was also observed in hepatocytes in both normal and

diseased tissue, but was more strongly associated with fibrotic regions, where HSCs accumulate, than hepatocytes in the diseased samples (Chapter 3).

One of the key changes in the liver during chronic injury is the accumulation and change in composition of ECM (Benyon and Iredale, 2000) and HSC are critical mediators in this process (Friedman, 2008b). Many studies have shown that ECM can affect HSC behaviour via outside-in signalling (Davis, 1988, Friedman et al., 1989, Gaca et al., 2003, Friedman, 2008c, Yang et al., 2008). Presented in Chapters 3 and 4 of this study is further evidence that different ECM proteins can effect HSC morphology, proliferation and activation state, with collagen I, an important component of the hepatic scar, conferring a more activated phenotype on HSCs, and laminin, a major constituent of ECM in a normal liver, promoting a more quiescent phenotype. Also presented in Chapter 5 is the novel observation that *Cygb* expression in HSCs at the RNA and protein level is effected by ECM. Surprisingly, *Cygb* expression was down regulated in HSCs, which had a more activated phenotype, contrary to several previous reports of *Cygb* upregulation in activated HSCs (Kristensen *et al.*, 2000, Kawada *et al.*, 2001). However, consistent with our data, more recent research has suggested that *Cygb* has an antifibrotic effect, Thuy *et al.* (2011) found increased tumorigenesis (which is related to hepatotoxicity and subsequent increase in fibrosis) in DEN treated *Cygb* knockout mice, and Cui *et al.* (2012) found that arundic acid attenuated fibrosis, and observed a corresponding increase in *Cygb* expression. Therefore, our observation that activated HSCs have reduced *Cygb* expression is entirely consistent with these more recent reports.

Signalling from the ECM to cells occurs via cell surface ECM receptors, predominantly integrins (Benyon and Iredale, 2000, Bedossa and Paradis, 2003), integrin signalling through cell attachment to ECM has been found to influence gene expression and behaviour (Carloni et al., 1996, Miranti and Brugge, 2002), (Zhou et al., 2004), (Streuli, 2009). Data presented in this report show differential expression of integrin subunits in cells cultured on different ECM proteins, this observation is in agreement with findings from Zhou *et al.* (2004) who also reported differential expression of integrin subunits in HSCs on different ECM proteins. Transduction of the signal from ECM through integrins occurs through integrin clustering and activation, the formation of focal adhesions and the autophosphorylation of FAK (Leitinger, 2003, Desgrosellier and Cheresch, 2010). Chapter 6 of this study presents data that shows increased FAK phosphorylation in HSC-T6 cells cultured on collagen I compared with those cultured on non-coated plastic or laminin. HSCs cultured on collagen I have a more activated phenotype (Chapters 3 and 4) and the observation that these cells have increased pFAK Y397 is in line with the observations of others who have observed an upregulation of pFAK in fibrotic livers (Jiang *et al.*, 2004) and that FAK can mediate stellate cell behaviour (Shen JG *et al.*, 2006, Rodriguez-Juan *et al.*, 2009, An *et al.*, 2011).

We were unable to directly confirm a link between FAK Y397 phosphorylation and *Cygb* expression in this report (Chapter 6). However a link between FAK signalling and *Cygb* expression is feasible and this is the subject of on-going research in our laboratory. There are several known signalling pathways mediated through FAK phosphorylation that could impact *Cygb* expression through effecting transcription

factor expression and activity, some of which have binding sites in the promoter region of the *Cygb* gene, for example, NFAT, AP-1 and HIF-1 are known to positively regulate *Cygb* transcription under hypoxic conditions (Singh *et al.*, 2009), some of these pathways are depicted in Figure 7.1. FAK phosphorylation also modulates ROS generation through activation of the RAC-1 (Ras-related C3 botulinum toxin substrate-1), a member of the Rho GTPase family. RAC-1 activation increases intracellular ROS, and as discussed in section 1.1.6.2, *Cygb* might have a role in ROS scavenging, or as part of a signalling cascade involving ROS modulation, therefore *Cygb* could be involved in the RAC-1 pathway, affecting levels of intracellular ROS. Nimnual *et al.* (2003) demonstrated that a RAC-mediated increase in intracellular ROS in the rat embryonic fibroblast cell line, REF52, caused downregulation of Rho GTPase. Early in the research into *Cygb*, Nakatani *et al.* (2004) speculated that *Cygb* overexpression in the NIH3T3 mouse fibroblast cell line could induce the activation of Rho owing to the observed formation of actin stress fibres and focal contacts, for which Rho activation is critical (Ridley and Hall, 1992), in these cells. Rho activation has also been shown to inhibit migration in NIH3T3 cells (Olivo *et al.*, 2000). HSC-T6 cells cultured on laminin show increased *Cygb* expression and decreased proliferation, and the opposite is true for HSC-T6 cells cultured on collagen I, which is in line with observations of impaired cell migration in *Cygb* overexpressing cells made by Nakatani *et al.* (2004). RAC and Rho GTPases are known to be critical for signal transduction from extracellular sources to cytoskeletal rearrangement (Etienne-Manneville and Hall, 2002). An increase in RAC results in an increase in ROS, which, in turn, causes increased spreading and migration, in contrast, an increase in Rho induces increased contractility and adhesion, and Rho

can be negatively regulated by RAC, as was shown by Nimnual *et al.* (2003). Data presented in Chapter 5 of this thesis show that HSC-T6 cells cultured on collagen I have increased intracellular ROS, and these cells have decreased *Cygb* expression. Cells cultured on laminin, where *Cygb* is increased, do not have increased levels of intracellular ROS, therefore, redox regulation of this pathway could be influenced by cellular levels of *Cygb*, which might regulate ROS and have a regulatory role in the RAC signalling pathway, this is depicted in Figure 7.2 A and B. Other work in our laboratory has also suggested a role for *CYGB* in the motility of cancer cells, with *CYGB* overexpression in head and neck cancer cell lines reducing cell motility and intracellular ROS levels (Dr. Hodges, personal communication), which is further evidence for a potential role for *CYGB* in this signalling pathway.

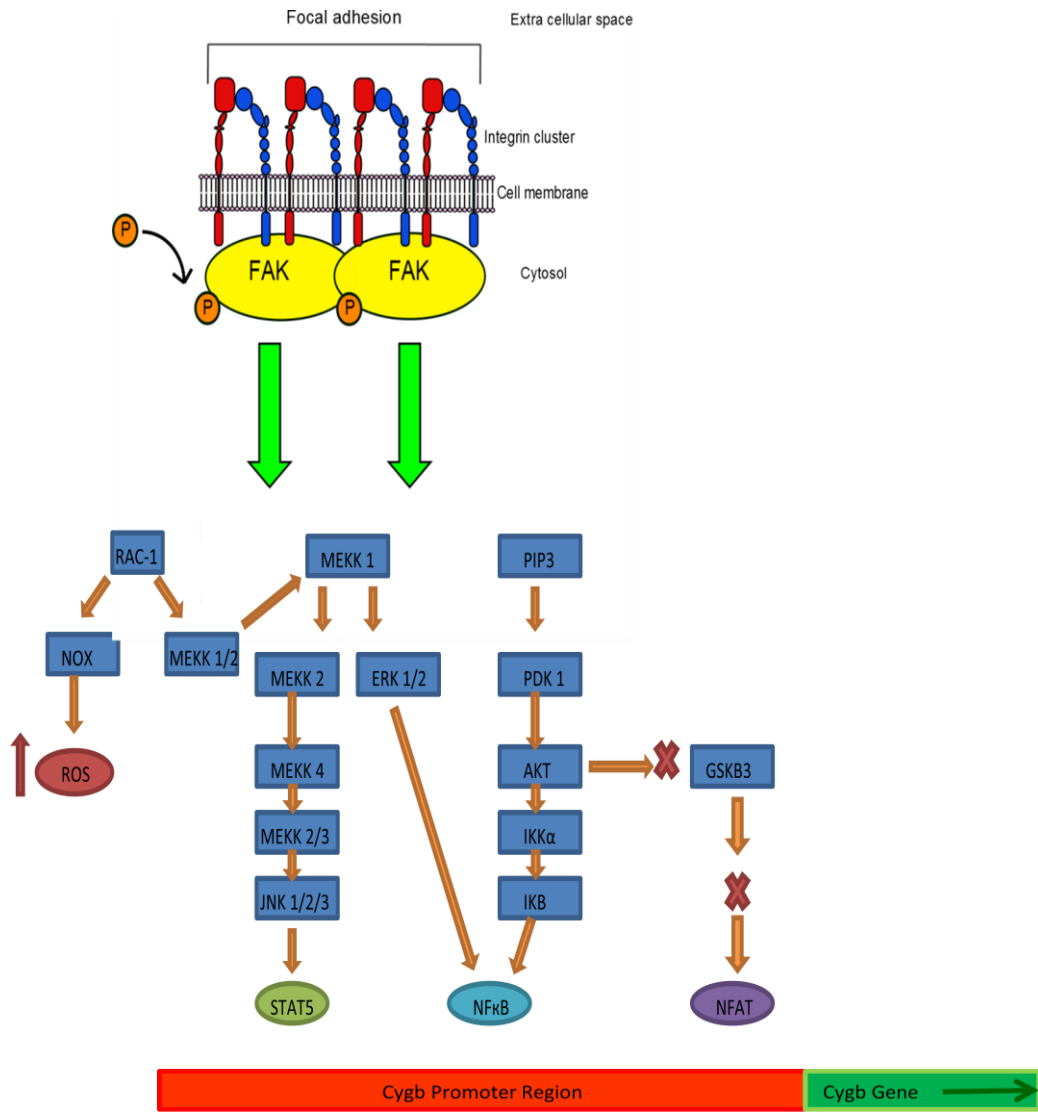


Figure 7.1: Signalling pathways from focal adhesion kinase (FAK) phosphorylation (P) to transcription factors known to have binding motifs present in the *CYGB* promoter region, and also effecting reactive oxygen species (ROS) generation. NFAT binding to the *CYGB* is known to promote *CYGB* transcription (Singh *et al.*, 2009)

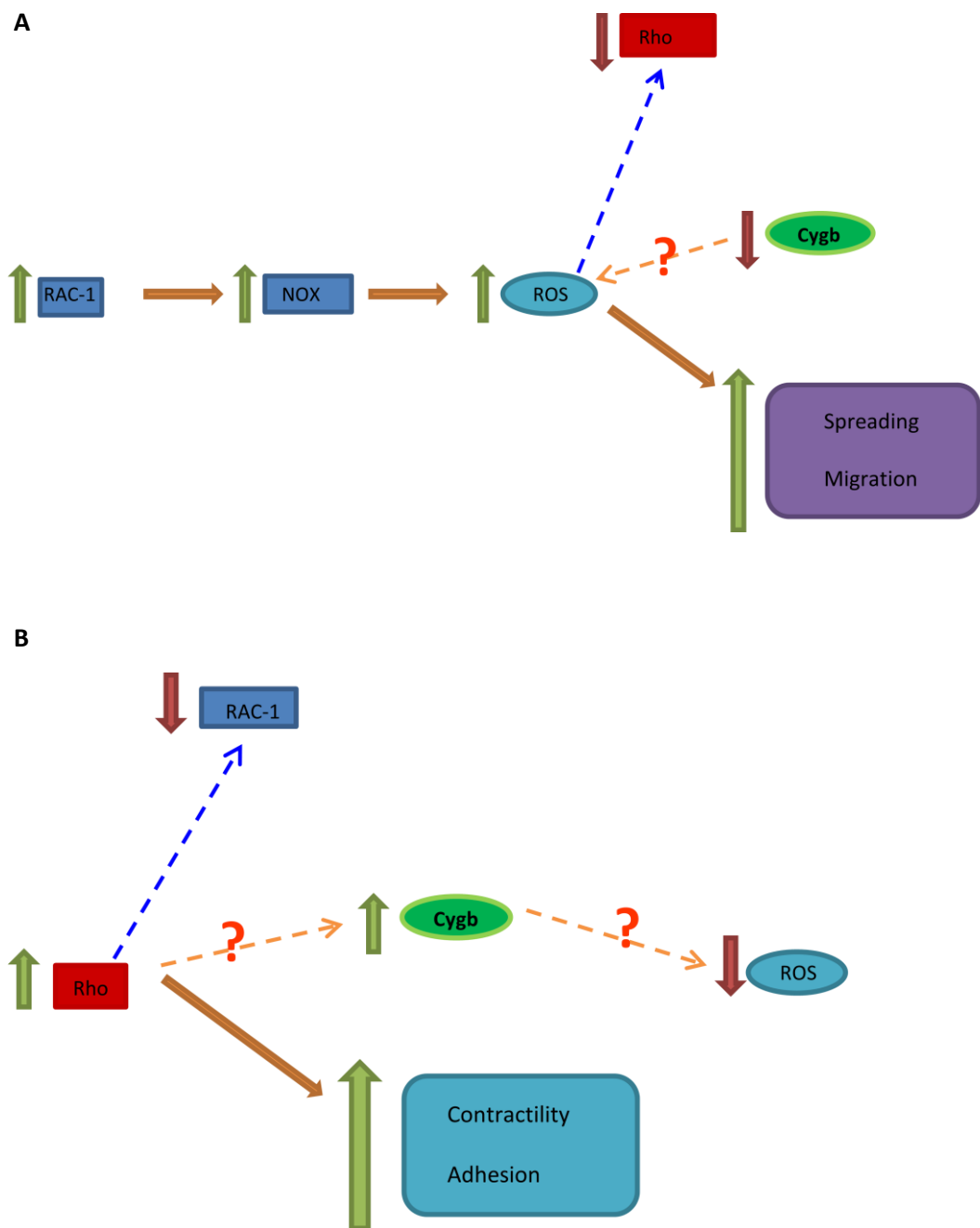


Figure 7.2: Possible signalling pathways linking A) RAC-1 activation and ROS (reaction oxygen species) generation and Rho downregulation and increased cell spreading and migration and B) Rho activation and RAC-1 downregulation and increased cell contractility and adhesion, indicating possible regulation of these pathways by Cygb.

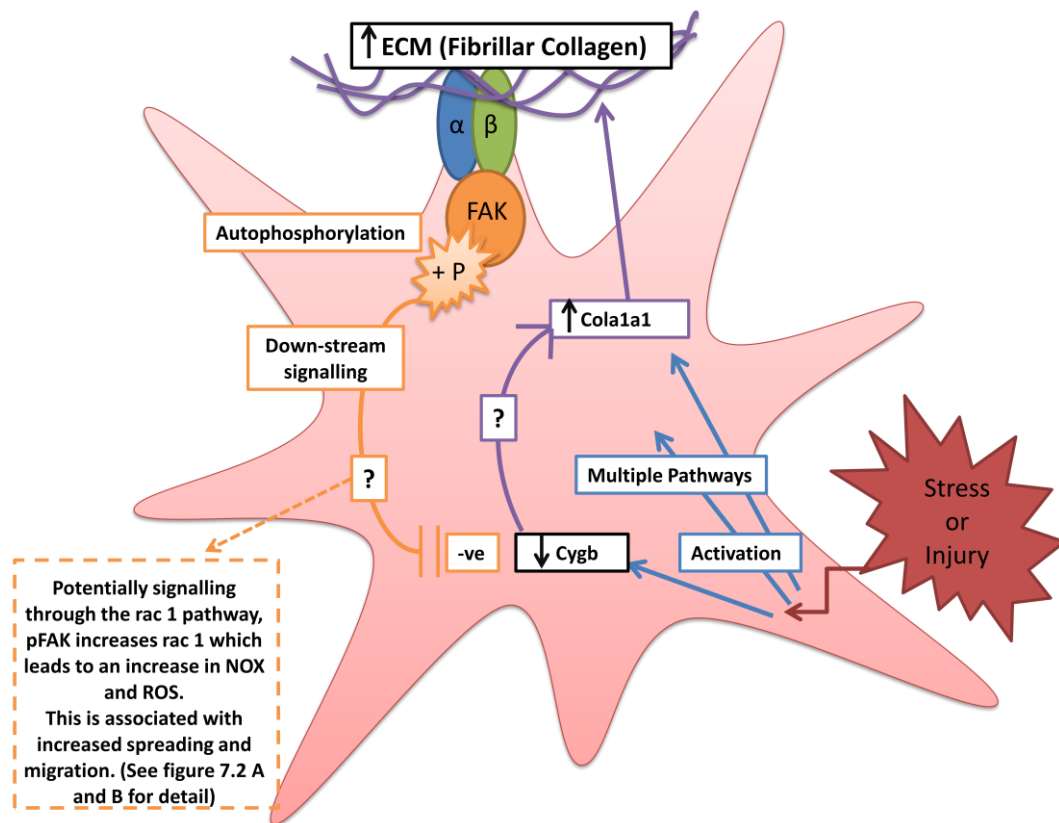


Figure 7.3: Possible signalling pathway between ECM and Cygb expression through integrin activation, FAK phosphorylation to Cygb expression, impacting on cell behaviour and possibly going through the RAC signalling pathway.

Thus, *Cygb* could have a role in modulating intracellular ROS, in turn affecting the RAC/Rho signalling pathway and impacting on cell migration and adhesion, a diagram presenting the overall hypothesis of ECM signalling through integrin activation and FAK phosphorylation to *Cygb* expression, HSC activation and cell proliferation is depicted in Figure 7.3. Work in our laboratory is continuing to investigate this signalling pathway and establish the link between ECM and *Cygb* expression.

7.2 Future work

The most important aspect of future work on this project is the confirmation of a direct link between ECM signalling and *Cygb* gene expression, which was explored in Chapter 6. Differential integrin expression in HSC-T6 cells cultured on different ECM proteins was observed. To discover if signalling from ECM to *Cygb* occurs through integrins, and to establish the start of the signalling cascade, expression of all integrin subunits would need to be undertaken. To find out which integrin subunit or subunits are pivotal in signal transduction to *Cygb* expression, blocking or knockdown experiments also need to be conducted, looking at the effect of blocking integrins on *Cygb* expression.

The most important observation in Chapter 6 is the difference in FAK pY397 expression between HSC-T6 cells cultured on collagen I and those cultured on laminin or non-coated plastic, leading to hypothesis that signalling from ECM to *Cygb* is dependent on FAK phosphorylation. However, confirmation of this link was not established in this investigation, therefore, work is continuing to see whether FAK phosphorylation impacts *Cygb* expression through pFAK inhibition experiments and RT-PCR analysis of *Cygb* expression. Investigations by others in our laboratory are also focusing on the link between

Rho kinase, CYGB expression and cell behaviour in terms of attachment and proliferation, to determine if CYGB is indeed involved in the signalling pathways outlined in Figure 7.2.

Other important aspects, which were outside the scope of the current study, are the observations of the reciprocal nature of *Cygb* and α SMA gene expression and the finding that laminin has the opposite effect to collagen I. Further investigations into the effects of laminin along the lines of those carried out in Chapter 5 on collagen I, such as a time course of expression and influence of attachment to the surface would be interesting. Also, increased levels of pFAK were not observed in HSC-T6 cells cultured on laminin, therefore no potential signal transduction mechanism has been identified in this circumstance. Further investigation into signalling from laminin to *Cygb* expression should be undertaken, to establish if it is a different mechanism from collagen I, or whether the two pathways overlap in HSC-T6 cells. Also, differences between ECM receptor signalling in the HSC-T6 cell line and the LX-2 cell line, and differences in this signalling pathway between rat and human HSCs should be further investigated, as laminin has no effect on *Cygb* expression in LX-2 cells, this difference is important as it has implications for the translation of this research from *in vitro* models into *in vivo models* and also studies in human tissue.

Investigations into the effects of gelatin should be undertaken, to establish how this protein, which is not known as a biological ECM substrate, is having an influence which is greater than collagen I on HSC-T6 cells. Experiments similar to those carried out on HSC-T6 cells cultured on collagen I should be done to discover if signalling from gelatin occurs along the same pathway as collagen I.

Finally repetition of all experiments should be conducted in primary HSCs. Due to lack of resources, investigations into the effect of ECM on *Cygb* in primary stellate cells were

difficult to conduct and were often unsuccessful, but the major limitation of this project is that the model has not been confirmed in primary cells, and therefore it is not known whether the data presented here are an artefact cell immortalisation or a real effect that translates to primary cells. This is important for the implications of these findings on future research.

In summary, reported in this thesis is the novel observation that *Cygb* expression in an *in vitro* model of HSC can be modulated by ECM. This discovery could have important implications for the understanding of the progression of liver fibrosis, and provide a new target for the treatment and reversal of liver fibrosis.

Chapter 8

References

- AN, J., ZHENG, L., XIE, S., DUN, Z., HAO, L., YAO, D., SHIH, D. Q. & ZHANG, X. 2011. Down-regulation of focal adhesion kinase by short hairpin RNA increased apoptosis of rat hepatic stellate cells. *APMIS*, 119, 319-329.
- ANANIA, F. A., POTTER, J. J., RENNIE-TANKERSLEY, L. & MEZEY, E. 1995. Effects of acetaldehyde on nuclear protein binding to the nuclear factor I consensus sequence in the alpha 2(I) collagen promoter. *Hepatology*, 21, 1640-8.
- ARNAOUT, M. A. 2002. Integrin structure: new twists and turns in dynamic cell adhesion. *Immunological Reviews*, 186, 1-1.
- ARREDONDO-PETER, R., HARGROVE, M. S., MORAN, J. F., SARATH, G. & KLUCAS, R. V. 1998. Plant Hemoglobins. *Plant Physiology*, 118, 1121-1125.
- ARTHUR, M. J. P. 2000. *Fibrogenesis II. Metalloproteinases and their inhibitors in liver fibrosis*.
- ASAHINA, K., KAWADA, N., KRISTENSEN, D. B., NAKATANI, K., SEKI, S., SHIOKAWA, M., TATENO, C., OBARA, M. & YOSHIZATO, K. 2002. Characterization of human stellate cell activation-associated protein and its expression in human liver. *Biochimica Et Biophysica Acta-Genes Structure and Expression*, 1577, 471-475.
- ASCENZI, P., BOCEDI, A., DE SANCTIS, D., PESCE, A., BOLOGNESI, M., MARDEN, M. C., DEWILDE, S., MOENS, L., HANKELN, T. & BURMESTER, T. 2004. Neuroglobin and cytoglobin: Two new entries in the hemoglobin superfamily*. *Biochem Mol Biol Educ*, 32, 305-13.
- ASCENZI, P., MARINO, M., POLTICELLI, F., COLETTA, M., GIOIA, M., MARINI, S., PESCE, A., NARDINI, M., BOLOGNESI, M., REEDER, B. J. & WILSON, M. T. 2013. Non-covalent and covalent modifications modulate the reactivity of monomeric mammalian globins. *Biochim Biophys Acta*, 1834, 1750-6.
- ASTUDILLO, L., BERNAD, S., DERRIEN, V., SEBBAN, P. & MIKSOVSKA, J. 2013. Reduction of the internal disulfide bond between Cys 38 and 83 switches the ligand migration pathway in cytoglobin. *J Inorg Biochem*, 129, 23-9.
- AWENIUS, C., HANKELN, T. & BURMESTER, T. 2001. Neuroglobins from the zebrafish *Danio rerio* and the pufferfish *Tetraodon nigroviridis*. *Biochemical and Biophysical Research Communications*, 287, 418-421.
- BASHFORD, D., CHOTHIA, C. & LESK, A. M. 1987. DETERMINANTS OF A PROTEIN FOLD - UNIQUE FEATURES OF THE GLOBIN AMINO-ACID-SEQUENCES. *Journal of Molecular Biology*, 196, 199-216.
- BATALLER, R. & BRENNER, D. A. 2005. Liver fibrosis. *Journal of Clinical Investigation*, 115, 209-218.
- BEAUSSIER, M., WENDUM, D., SCHIFFER, E., DUMONT, S., REY, C., LIENHART, A. & HOUSSET, C. 2007. Prominent contribution of portal mesenchymal cells to liver fibrosis in ischemic and obstructive cholestatic injuries. *Laboratory Investigation*, 87, 292-303.
- BEDOSSA, P. & PARADIS, V. 2003. Liver extracellular matrix in health and disease. *J Pathol*, 200, 504-15.
- BEIERLE, E. A., MA, X., STEWART, J., NYBERG, C., TRUJILLO, A., CANCE, W. G. & GOLUBOVSKAYA, V. M. 2010. Inhibition of focal adhesion kinase decreases tumor growth in human neuroblastoma. *Cell Cycle*, 9, 1005-15.
- BELLENTANI, S., SCAGLIONI, F., MARINO, M. & BEDOGNI, G. 2010. Epidemiology of Non-Alcoholic Fatty Liver Disease. *Digestive Diseases*, 28, 155-161.
- BENTON, M. J. 1990. PHYLOGENY OF THE MAJOR TETRAPOD GROUPS - MORPHOLOGICAL DATA AND DIVERGENCE DATES. *Journal of Molecular Evolution*, 30, 409-424.
- BENYON, R. C. & IREDALE, J. P. 2000. Is liver fibrosis reversible? *Gut*, 46, 443-446.
- BLACHIER, M., LELEU, H., PECK-RADOSAVLJEVIC, M., VALLA, D. C. & ROUDOT-THORAVAL, F. 2013. The burden of liver disease in Europe: A review of available epidemiological data. *Journal of Hepatology*, 58, 593-608.
- BORKHAM-KAMPHORST, E., KOVALENKO, E., VAN ROEYEN, C. R. C., GASSLER, N., BOMBLE, M., OSTENDORF, T., FLOEGE, J., GRESSNER, A. M. & WEISKIRCHEN, R. 2008. Platelet-derived

- growth factor isoform expression in carbon tetrachloride-induced chronic liver injury. *Laboratory Investigation*, 88, 1090-1100.
- BRADFORD, M. 1976. A rapid and sensitive method for the quantitation of microgram quantities of protein utilizing the principle of protein-dye binding. *Anal Biochem*, 72, 248-54.
- BREITKOPF, K., GODOY, P., CIUCLAN, L., SINGER, M. V. & DOOLEY, S. 2006. TGF-beta/Smad signaling in the injured liver. *Zeitschrift Fur Gastroenterologie*, 44, 57-66.
- BRUNORI, M. 1999. Hemoglobin is an honorary enzyme. *Trends in Biochemical Sciences*, 24, 158-161.
- BUNN, H. F. & FORGET, B. G. 1986. Hemoglobin: Molecular Genetic and Clinical Aspects. Philadelphia, PA: Saunders Company.
- BURMESTER, T., EBNER, B., WEICH, B. & HANKELN, T. 2002. Cytoglobin: A novel globin type ubiquitously expressed in vertebrate tissues. *Molecular Biology and Evolution*, 19, 416-421.
- BURMESTER, T., GERLACH, F. & HANKELN, T. 2007. Regulation and role of neuroglobin and cytoglobin under hypoxia. In: ROACH, R. C., WAGNER, P. D. & HACKETT, P. H. (eds.) *Hypoxia and the Circulation*. Berlin: Springer-Verlag Berlin.
- BURMESTER, T., HABERKAMP, M., MITZ, S., ROESNER, A., SCHMIDT, M., EBNER, B., GERLACH, F., FUCHS, C. & HANKELN, T. 2004. Neuroglobin and cytoglobin: Genes, proteins and evolution. *Iubmb Life*, 56, 703-707.
- BURMESTER, T. & HANKELN, T. 2014. Function and evolution of vertebrate globins. *Acta Physiol (Oxf)*, 211, 501-14.
- BURMESTER, T., WEICH, B., REINHARDT, S. & HANKELN, T. 2000. A vertebrate globin expressed in the brain. *Nature*, 407, 520-523.
- CABRITA, M. A., JONES, L. M., QUIZI, J. L., SABOURIN, L. A., MCKAY, B. C. & ADDISON, C. L. 2011. Focal adhesion kinase inhibitors are potent anti-angiogenic agents. *Mol Oncol*, 5, 517-26.
- CANBAY, A., HIGUCHI, H., BRONK, S. F., TANIAI, M., SEBO, T. J. & GORES, G. J. 2002. Fas enhances fibrogenesis in the bile duct ligated mouse: A link between apoptosis and fibrosis. *Gastroenterology*, 123, 1323-1330.
- CARLONI, V., ROMANELLI, R. G., PINZANI, M., LAFFI, G. & GENTILINI, P. 1996. Expression and function of integrin receptors for collagen and laminin in cultured human hepatic stellate cells. *Gastroenterology*, 110, 1127-1136.
- CARVER, W. & GOLDSMITH, E. C. 2013. Regulation of Tissue Fibrosis by the Biomechanical Environment. *Biomed Research International*.
- CARY, L. A. & GUAN, J. L. 1999. Focal adhesion kinase in integrin-mediated signaling. *Front Biosci*, 4, D102-13.
- CERNARO, V., LACQUANITI, A., DONATO, V., FAZIO, M. R., BUEMI, A. & BUEMI, M. 2012. Fibrosis, regeneration and cancer: what is the link? *Nephrol Dial Transplant*, 27, 21-7.
- CHEN, A., BENO, D. W. & DAVIS, B. H. 1996. Suppression of stellate cell type I collagen gene expression involves AP-2 transmodulation of nuclear factor-1-dependent gene transcription. *J Biol Chem*, 271, 25994-8.
- CHEN, H., ZHAO, X. & MENG, T. 2014. Expression and biological role of cytoglobin in human ovarian cancer. *Tumour Biol*.
- CHUANG, S. C., LA VECCHIA, C. & BOFFETTA, P. 2009. Liver cancer: Descriptive epidemiology and risk factors other than HBV and HCV infection. *Cancer Letters*, 286, 9-14.
- CLARK, E. A. & BRUGGE, J. S. 1995. INTEGRINS AND SIGNAL-TRANSDUCTION PATHWAYS - THE ROAD TAKEN. *Science*, 268, 233-239.
- CUI, W. H., WANG, M., MAEGAWA, H., TERANISHI, Y. & KAWADA, N. 2012. Inhibition of the activation of hepatic stellate cells by arundic acid via the induction of cytoglobin. *Biochemical and Biophysical Research Communications*, 425, 642-648.

- DAVIS, B. H. 1988. Transforming growth factor beta responsiveness is modulated by the extracellular collagen matrix during hepatic ito cell culture. *J Cell Physiol*, 136, 547-53.
- DAVIS, B. H., KRAMER, R. T. & DAVIDSON, N. O. 1990. RETINOIC ACID MODULATES RAT ITO CELL-PROLIFERATION, COLLAGEN, AND TRANSFORMING GROWTH-FACTOR-BETA PRODUCTION. *Journal of Clinical Investigation*, 86, 2062-2070.
- DE SANCTIS, D., DEWILDE, S., PESCE, A., MOENS, L., ASCENZI, P., HANKELN, T., BURMESTER, T. & BOLOGNESI, M. 2004. Crystal structure of cytoglobin: The fourth globin type discovered in man displays heme hexa-coordination. *Journal of Molecular Biology*, 336, 917-927.
- DESGROSELLIER, J. S. & CHERESH, D. A. 2010. Integrins in cancer: biological implications and therapeutic opportunities. *Nat Rev Cancer*, 10, 9-22.
- DICKERSON, R. E. & GEIS, I. 1983. Hemoglobin: Structure, Function, Evolution, and Pathology. Menlo Park, CA.: Benjamin/Cummings.
- DIXON, B. & POHAJDAK, B. 1992. DID THE ANCESTRAL GLOBIN GENE OF PLANTS AND ANIMALS CONTAIN ONLY 2 INTRONS. *Trends in Biochemical Sciences*, 17, 486-488.
- EFFIONG, K., OSINOWO, A. & PRING, A. 2012. Deaths from liver disease: Implications for end of life care in England. March 2012 ed.
- ELSHARKAWY, A. M., OAKLEY, F. & MANN, D. A. 2005. The role and regulation of hepatic stellate cell apoptosis in reversal of liver fibrosis. *Apoptosis*, 10, 927-39.
- EMARA, M., TURNER, A. R. & ALLALUNIS-TURNER, J. 2010. Hypoxic regulation of cytoglobin and neuroglobin expression in human normal and tumor tissues. *Cancer Cell Int*, 10, 33.
- ESTELLER, M. 2007. Epigenetic gene silencing in cancer: the DNA hypermethylome. *Human Molecular Genetics*, 16, R50-R59.
- ETIENNE-MANNEVILLE, S. & HALL, A. 2002. Rho GTPases in cell biology. *Nature*, 420, 629-35.
- FAGO, A., HUNDAHL, C., MALTE, H. & WEBER, R. E. 2004. Functional properties of neuroglobin and cytoglobin. Insights into the ancestral physiological roles of globins. *IUBMB Life*, 56, 689-96.
- FORDEL, E., GEUENS, E., DEWILDE, S., ROTTIERS, P., CARMELIET, P., GROOTEN, J. & MOENS, L. 2004. Cytoglobin expression is upregulated in all tissues upon hypoxia: an in vitro and in vivo study by quantitative real-time PCR. *Biochemical and Biophysical Research Communications*, 319, 342-348.
- FORDEL, E., THIJIS, L., MOENS, L. & DEWILDE, S. 2007. Neuroglobin and cytoglobin expression in mice - Evidence for a correlation with reactive oxygen species scavenging. *Febs Journal*, 274, 1312-1317.
- FORREST, E. & REED, E. 2011. Alcohol and the liver. *Medicine*, 39, 532-535.
- FRIEDMAN, S. L. 2003. Liver fibrosis - from bench to bedside. *Journal of Hepatology*, 38, S38-S53.
- FRIEDMAN, S. L. 2008a. Hepatic fibrosis-Overview. *Toxicology*, 254, 120-129.
- FRIEDMAN, S. L. 2008b. Hepatic stellate cells: Protean, multifunctional, and enigmatic cells of the liver. *Physiological Reviews*, 88, 125-172.
- FRIEDMAN, S. L. 2008c. Mechanisms of hepatic fibrogenesis. *Gastroenterology*, 134, 1655-1669.
- FRIEDMAN, S. L., LALAZAR, A., WONG, L., BLANER, W. S., VOGEL, S. & THEISS, G. 1997. HSC-T6 cells, an immortalized rat hepatic stellate cell line. *Hepatology*, 26, 839-839.
- FRIEDMAN, S. L., ROCKEY, D. C., MCGUIRE, R. F., MAHER, J. J., BOYLES, J. K. & YAMASAKI, G. 1992. ISOLATED HEPATIC LIPOCYTES AND KUPFFER CELLS FROM NORMAL HUMAN LIVER - MORPHOLOGICAL AND FUNCTIONAL-CHARACTERISTICS IN PRIMARY CULTURE. *Hepatology*, 15, 234-243.
- FRIEDMAN, S. L., ROLL, F. J., BOYLES, J., ARENSON, D. M. & BISSELL, D. M. 1989. MAINTENANCE OF DIFFERENTIATED PHENOTYPE OF CULTURED RAT HEPATIC LIPOCYTES BY BASEMENT-MEMBRANE MATRIX. *Journal of Biological Chemistry*, 264, 10756-10762.
- FUJITA, Y., KOINUMA, S., DE VELASCO, M. A., BOLZ, J., TOGASHI, Y., TERASHIMA, M., HAYASHI, H., MATSUO, T. & NISHIO, K. 2014. Melanoma transition is frequently accompanied by a loss of cytoglobin expression in melanocytes: a novel expression site of cytoglobin. *PLoS One*, 9, e94772.

- GABELE, E., BRENNER, D. A. & RIPPE, R. A. 2003. Liver fibrosis: signals leading to the amplification of the fibrogenic hepatic stellate cell. *Front Biosci*, 8, d69-77.
- GACA, M. D., ZHOU, X., ISSA, R., KIRIELLA, K., IREDALE, J. P. & BENYON, R. C. 2003. Basement membrane-like matrix inhibits proliferation and collagen synthesis by activated rat hepatic stellate cells: evidence for matrix-dependent deactivation of stellate cells. *Matrix Biol*, 22, 229-39.
- GARDNER, A. M., COOK, M. R. & GARDNER, P. R. 2010. Nitric-oxide dioxygenase function of human cytoglobin with cellular reductants and in rat hepatocytes. *J Biol Chem*, 285, 23850-7.
- GENIN, O., RECHAVI, G., NAGLER, A., BEN-ITZHAK, O., NAZEMI, K. J. & PINES, M. 2008. Myofibroblasts in pulmonary and brain metastases of alveolar soft-part sarcoma: a novel target for treatment? *Neoplasia*, 10, 940-8.
- GEUENS, E., BROUNS, I., FLAMEZ, D., DEWILDE, S., TIMMERMANS, J. P. & MOENS, L. 2003. A globin in the nucleus! *J Biol Chem*, 278, 30417-20.
- GIAMPIERI, M. P., JEZEQUEL, A. M. & ORLANDI, F. 1981. THE LIPOCYTES IN NORMAL HUMAN-LIVER - A QUANTITATIVE STUDY. *Digestion*, 22, 165-&.
- GOLUBOVSKAYA, V. M., NYBERG, C., ZHENG, M., KWEH, F., MAGIS, A., OSTROV, D. & CANCE, W. G. 2008. A Small Molecule Inhibitor, 1,2,4,5-Benzenetetraamine Tetrahydrochloride, Targeting the Y397 Site of Focal Adhesion Kinase Decreases Tumor Growth. *Journal of Medicinal Chemistry*, 51, 7405-7416.
- GOODMAN, M., CZELUSNIAK, J., KOOP, B. F., TAGLE, D. A. & SLIGHTOM, J. L. 1987. GLOBINS - A CASE-STUDY IN MOLECULAR PHYLOGENY. *Cold Spring Harbor Symposia on Quantitative Biology*, 52, 875-890.
- GRESSNER, A. M., WEISKIRCHEN, R., BREITKOPF, K. & DOOLEY, S. 2002. Roles of TGF-beta in hepatic fibrosis. *Frontiers in Bioscience*, 7, D793-D807.
- GUO, X., PHILIPSEN, S. & TAN-UN, K.-C. 2006. Characterization of human cytoglobin gene promoter region. *Biochimica et Biophysica Acta (BBA) - Gene Structure and Expression*, 1759, 208-215.
- GUO, X., PHILIPSEN, S. & TAN-UN, K.-C. 2007. Study of the hypoxia-dependent regulation of human CYGB gene. *Biochemical and Biophysical Research Communications*, 364, 145-150.
- HALLIGAN, K. E., JOURD'HEUIL, F. L. & JOURD'HEUIL, D. 2009. Cytoglobin Is Expressed in the Vasculature and Regulates Cell Respiration and Proliferation via Nitric Oxide Dioxygenation. *Journal of Biological Chemistry*, 284, 8539-8547.
- HAMDANE, D., KIGER, L., DEWILDE, S., GREEN, B. N., PESCE, A., UZAN, J., BURMESTER, T., HANKELN, T., BOLOGNESI, M., MOENS, L. & MARDEN, M. C. 2003. The redox state of the cell regulates the ligand binding affinity of human neuroglobin and cytoglobin. *Journal of Biological Chemistry*, 278, 51713-51721.
- HANKELN, T., EBNER, B., FUCHS, C., GERLACH, F., HABERKAMP, M., LAUFS, T. L., ROESNER, A., SCHMIDT, M., WEICH, B., WYSTUB, S., SAALER-REINHARDT, S., REUSS, S., BOLOGNESI, M., DE SANCTIS, D., MARDEN, M. C., KIGER, L., MOENS, L., DEWILDE, S., NEVO, E., AVIVI, A., WEBER, R. E., FAGO, A. & BURMESTER, T. 2005. Neuroglobin and cytoglobin in search of their role in the vertebrate globin family. *J Inorg Biochem*, 99, 110-9.
- HARDISON, R. 1998. Hemoglobins from bacteria to man: Evolution of different patterns of gene expression. *Journal of Experimental Biology*, 201, 1099-1117.
- HARDISON, R. C. 1996. A brief history of hemoglobins: Plant, animal, protist, and bacteria. *Proceedings of the National Academy of Sciences of the United States of America*, 93, 5675-5679.
- HARGROVE, M. S. 2000. A flash photolysis method to characterize hexacoordinate hemoglobin kinetics. *Biophysical Journal*, 79, 2733-2738.
- HAZRA, S., XIONG, S. G., WANG, J. H., RIPPE, R. A., CHATTERJEE, V. K. K. & TSUKAMOTO, H. 2004. Peroxisome proliferator-activated receptor gamma induces a phenotypic switch from activated to quiescent hepatic stellate cells. *Journal of Biological Chemistry*, 279, 11392-11401.

- HE, X., LV, R. Y., WANG, K., HUANG, X. F., WU, W. T., YIN, L. F. & LIU, Y. 2011. Cytochrome Exhibits Anti-Fibrosis Activity on Liver In Vivo and In Vitro. *Protein Journal*, 30, 437-446.
- HEDLEY-WHYTE, E. T., GOLDMAN, J. E., NEDERGAARD, M., FRIEDMAN, A., HAN, X. N., SCHMIDT, R. E. & POWERS, J. M. 2009. Hyaline Protoplasmic Astrocytopathy of Neocortex. *Journal of Neuropathology and Experimental Neurology*, 68, 136-147.
- HEROLD, S., FAGO, A., WEBER, R. E., DEWILDE, S. & MOENS, L. 2004. Reactivity studies of the Fe(III) and Fe(II)NO forms of human neuroglobin reveal a potential role against oxidative stress. *J Biol Chem*, 279, 22841-7.
- HOCHWALD, S. N., NYBERG, C., ZHENG, M., ZHENG, D., WOOD, C., MASSOLL, N. A., MAGIS, A., OSTROV, D., CANCE, W. G. & GOLUBOVSKAYA, V. M. 2009. A novel small molecule inhibitor of FAK decreases growth of human pancreatic cancer. *Cell Cycle*, 8, 2435-43.
- HOCKEL, M., SCHLENGER, K., ARAL, B., MITZE, M., SCHAFFER, U. & VAUPEL, P. 1996. Association between tumor hypoxia and malignant progression in advanced cancer of the uterine cervix. *Cancer Res*, 56, 4509-15.
- HOCKEL, M. & VAUPEL, P. 2001. Tumor hypoxia: definitions and current clinical, biologic, and molecular aspects. *J Natl Cancer Inst*, 93, 266-76.
- HODGES, N. J., INNOCENT, N., DHANDA, S. & GRAHAM, M. 2008. Cellular protection from oxidative DNA damage by over-expression of the novel globin cytochrome in vitro. *Mutagenesis*, 23, 293-298.
- HUANG, G. C., ZHANG, J. S. & TANG, Q. Q. 2004. Involvement of C/EBP-alpha gene in in vitro activation of rat hepatic stellate cells. *Biochem Biophys Res Commun*, 324, 1309-18.
- HUMPHRIES, M. J. 2000. Integrin structure. *Biochem Soc Trans*, 28, 311-39.
- HVITVED, A. N., TRENT, J. T., PREMIER, S. A. & HARGROVE, M. S. 2001. Ligand binding and hexacoordination in Synechocystis hemoglobin. *Journal of Biological Chemistry*, 276, 34714-34721.
- HYNES, R. O. 1987. Integrins: a family of cell surface receptors. *Cell*, 48, 549-54.
- IKEDA, K., WAKAHARA, T., WANG, Y. Q., KADOYA, H., KAWADA, N. & KANEDA, K. 1999. In vitro migratory potential of rat quiescent hepatic stellate cells and its augmentation by cell activation. *Hepatology*, 29, 1760-1767.
- INAGAKI, Y. & OKAZAKI, I. 2007. Emerging insights into transforming growth factor beta Smad signal in hepatic fibrogenesis. *Gut*, 56, 284-292.
- IREDALE, J. P., BENYON, R. C., PICKERING, J., MCCULLEN, M., NORTHROP, M., PAWLEY, S., HOVELL, C. & ARTHUR, M. J. 1998. Mechanisms of spontaneous resolution of rat liver fibrosis. Hepatic stellate cell apoptosis and reduced hepatic expression of metalloproteinase inhibitors. *J Clin Invest*, 102, 538-49.
- ISHIDA, M., UEHA, T. & SAGAMI, I. 2008. Effects of mutations in the heme domain on the transcriptional activity and DNA-binding activity of NPAS2. *Biochem Biophys Res Commun*, 368, 292-7.
- ISSA, R., ZHOU, X., CONSTANDINOU, C. M., FALLOWFIELD, J., MILLWARD-SADLER, H., GACA, M. D., SANDS, E., SULIMAN, I., TRIM, N., KNORR, A., ARTHUR, M. J., BENYON, R. C. & IREDALE, J. P. 2004. Spontaneous recovery from micronodular cirrhosis: evidence for incomplete resolution associated with matrix cross-linking. *Gastroenterology*, 126, 1795-808.
- ITOH, R., FUJITA, K., MU, A., KIM, D. H., TAI, T. T., SAGAMI, I. & TAKETANI, S. 2013. Imaging of heme/hemeproteins in nucleus of the living cells expressing heme-binding nuclear receptors. *FEBS Lett*, 587, 2131-6.
- JEZEQUEL, A. M., BONAZZI, P., NOVELLI, G., VENTURINI, C. & ORLANDI, F. 1984. EARLY STRUCTURAL AND FUNCTIONAL-CHANGES IN LIVER OF RATS TREATED WITH A SINGLE DOSE OF VALPROIC ACID. *Hepatology*, 4, 1159-1166.
- JIANG, H. Q., ZHANG, X. L., LIU, L. & YANG, C. C. 2004. Relationship between focal adhesion kinase and hepatic stellate cell proliferation during rat hepatic fibrogenesis. *World J Gastroenterol*, 10, 3001-5.

- KAKAR, S., HOFFMAN, F. G., STORZ, J. F., FABIAN, M. & HARGROVE, M. S. 2010. Structure and reactivity of hexacoordinate hemoglobins. *Biophys Chem*, 152, 1-14.
- KAWADA, N., KRISTENSEN, D. B., ASAHINA, K., NAKATANI, K., MINAMIYAMA, Y., SEKI, S. & YOSHIZATO, K. 2001. Characterization of a stellate cell activation-associated protein (STAP) with peroxidase activity found in rat hepatic stellate cells (vol 276, pg 25318, 2001). *Journal of Biological Chemistry*, 276, 47744-47745.
- KAWADA, N. & LE, T. T. 2011. CYTOGLOBIN AS A NOVEL TUMOR SUPPRESSOR IN THE LIVER. *Hepatology*, 54, 757A-757A.
- KENT, G., GAY, S., INOUE, T., BAHU, R., MINICK, O. T. & POPPER, H. 1976. VITAMIN-A-CONTAINING LIPOCYTES AND FORMATION OF TYPE-3 COLLAGEN IN LIVER-INJURY. *Proceedings of the National Academy of Sciences of the United States of America*, 73, 3719-3722.
- KHEDMAT, H. & TAHERI, S. 2011. Non-alcoholic steatohepatitis: An update in pathophysiology, diagnosis and therapy. *Hepatitis Monthly*, 11, 74-85.
- KIM, S. H., TURNBULL, J. & GUIMOND, S. 2011. Extracellular matrix and cell signalling: the dynamic cooperation of integrin, proteoglycan and growth factor receptor. *Journal of Endocrinology*, 209, 139-151.
- KIMURA, M. 1987. Molecular evolutionary clock and the neutral theory. *J Mol Evol*, 26, 24-33.
- KINNMAN, N., FRANCOZ, C., BARBU, W., WENDUM, D., REY, C., HULTCRANTZ, R., POUPON, R. & HOUSSET, C. 2003. The myofibroblastic conversion of peribiliary fibrogenic cells distinct from hepatic stellate cells is stimulated by platelet-derived growth factor during liver fibrogenesis. *Laboratory Investigation*, 83, 163-173.
- KINNMAN, N., HULTCRANTZ, R., BARBU, V., REY, C., WENDUM, D., POUPON, R. & HOUSSET, C. 2000. PDGF-mediated chemoattraction of hepatic stellate cells by bile duct segments in cholestatic liver injury. *Laboratory Investigation*, 80, 697-707.
- KISSELEVA, T., CONG, M., PAIK, Y., SCHOLTEN, D., JIANG, C. Y., BENNER, C., IWASAKO, K., MOORE-MORRIS, T., SCOTT, B., TSUKAMOTO, H., EVANS, S. M., DILLMANN, W., GLASS, C. K. & BRENNER, D. A. 2012. Myofibroblasts revert to an inactive phenotype during regression of liver fibrosis. *Proceedings of the National Academy of Sciences of the United States of America*, 109, 9448-9453.
- KNITTEL, T., KOBOLD, D., DUDAS, J., SAILE, B. & RAMADORI, G. 1999. Role of the Ets-1 transcription factor during activation of rat hepatic stellate cells in culture. *Am J Pathol*, 155, 1841-8.
- KRISTENSEN, D. B., KAWADA, N., IMAMURA, K., MIYAMOTO, Y., TATENO, C., SEKI, S., KUROKI, T. & YOSHIZATO, K. 2000. Proteome analysis of rat hepatic stellate cells. *Hepatology*, 32, 268-277.
- KRIZHANOVSKY, V., YON, M., DICKINS, R. A., HEARN, S., SIMON, J., MIETHING, C., YEE, H., ZENDER, L. & LOWE, S. W. 2008. Senescence of activated stellate cells limits liver fibrosis (vol 134, pg 657, 2008). *Cell*, 135, 190-190.
- LAGARES, D., BUSNADIEGO, O., GARCIA-FERNANDEZ, R. A., KAPOOR, M., LIU, S., CARTER, D. E., ABRAHAM, D., SHI-WEN, X., CARREIRA, P., FONTAINE, B. A., SHEA, B. S., TAGER, A. M., LEASK, A., LAMAS, S. & RODRIGUEZ-PASCUAL, F. 2012. Inhibition of focal adhesion kinase prevents experimental lung fibrosis and myofibroblast formation. *Arthritis Rheum*, 64, 1653-64.
- LE, T. T., SUOH, M., MATSUMOTO, Y., SHIMADA, M., HIRANO, Y., MOTOYAMA, H., HAI, H., YOSHIZATO, K. & KAWADA, N. 2012. Cytochrome deficiency promotes liver fibrosis and liver cancer development in mice with steatohepatitis throughout activating oxidative stress pathway. *Hepatology*, 56, 865A-865A.
- LECHAUVE, C., CHAUVIERRE, C., DEWILDE, S., MOENS, L., GREEN, B. N., MARDEN, M. C., CELIER, C. & KIGER, L. 2010. Cytochrome conformations and disulfide bond formation. *Febs j*, 277, 2696-704.
- LEITINGER, B. 2003. Molecular analysis of collagen binding by the human discoidin domain receptors, DDR1 and DDR2 - Identification of collagen binding sites in DDR2. *Journal of Biological Chemistry*, 278, 16761-16769.
- LEITINGER, B. & HOHENESTER, E. 2007. Mammalian collagen receptors. *Matrix Biology*, 26, 146-155.

- LI, D., CHEN, X. Q., LI, W. J., YANG, Y. H., WANG, J. Z. & YU, A. C. 2007. Cytochrome up-regulated by hydrogen peroxide plays a protective role in oxidative stress. *Neurochem Res*, 32, 1375-80.
- LI, T., EHEIM, A. L., KLEIN, S., USCHNER, F. E., SMITH, A. C., BRANDON-WARNER, E., GHOSH, S., BONKOVSKY, H. L., TREBICKA, J. & SCHRUM, L. W. 2014. Novel role of nuclear receptor Rev-erb α in hepatic stellate cell activation: potential therapeutic target for liver injury. *Hepatology*, 59, 2383-96.
- LIN, X. Z., HORNG, M. H., SUN, Y. N., SHIESH, S. C., CHOW, N. H. & GUO, X. Z. 1998. Computer morphometry for quantitative measurement of liver fibrosis: Comparison with Knodell's score, colorimetry and conventional description reports. *Journal of Gastroenterology and Hepatology*, 13, 75-80.
- MAKINO, M., SAWAI, H., SHIRO, Y. & SUGIMOTO, H. 2011. Crystal structure of the carbon monoxide complex of human cytochrome. *Proteins-Structure Function and Bioinformatics*, 79, 1143-1153.
- MAKINO, M., SUGIMOTO, H., SAWAI, H., KAWADA, N., YOSHIKATO, K. & SHIRO, Y. 2006. High-resolution structure of human cytochrome: identification of extra N- and C-termini and a new dimerization mode. *Acta Crystallographica Section D*, 62, 671-677.
- MAN, K. N., PHILIPSEN, S. & TAN-UN, K. C. 2008. Localization and expression pattern of cytochrome in carbon tetrachloride-induced liver fibrosis. *Toxicol Lett*, 183, 36-44.
- MANCINI, M. L. & SONIS, S. T. 2014. Mechanisms of cellular fibrosis associated with cancer regimen-related toxicities. *Front Pharmacol*, 5, 51.
- MANN, J. & MANN, D. A. 2009. Transcriptional regulation of hepatic stellate cells. *Adv Drug Deliv Rev*, 61, 497-512.
- MARTINEZ-HERNANDEZ, A. 1984. The hepatic extracellular matrix. I. Electron immunohistochemical studies in normal rat liver. *Laboratory investigation; a journal of technical methods and pathology*, 51, 57-74.
- MARTINEZ-HERNANDEZ, A. & AMENTA, P. S. 1995. The extracellular matrix in hepatic regeneration. *FASEB J*, 9, 1401-10.
- MCLYSAGHT, A., HOKAMP, K. & WOLFE, K. H. 2002. Extensive genomic duplication during early chordate evolution. *Nat Genet*, 31, 200-4.
- MCRONALD, F. E., LILOGLOU, T., XINARIANOS, G., HILL, L., ROWBOTTOM, L., LANGAN, J. E., ELLIS, A., SHAW, J. M., FIELD, J. K. & RISK, J. M. 2006. Down-regulation of the cytochrome gene, located on 17q25, in tylosis with oesophageal cancer (TOC): evidence for trans-allele repression. *Hum Mol Genet*, 15, 1271-7.
- MCRONALD, F. E., RISK, J. M. & HODGES, N. J. 2012. Protection from intracellular oxidative stress by cytochrome in normal and cancerous oesophageal cells. *PLoS One*, 7, e30587.
- MEDERACKE, I., HSU, C. C., TROEGER, J. S., HUEBENER, P., MU, X., DAPITO, D. H., PRADERE, J.-P. & SCHWABE, R. F. 2013. Fate tracing reveals hepatic stellate cells as dominant contributors to liver fibrosis independent of its aetiology. *Nat Commun*, 4.
- MERX, M. W., FLÖGEL, U., STUMPE, T., GÖDECKE, A., DECKING, U. K. M. & SCHRADER, J. 2001. Myoglobin facilitates oxygen diffusion. *The FASEB Journal*.
- MICHAEL, K. E., DUMBAULD, D. W., BURNS, K. L., HANKS, S. K. & GARCIA, A. J. 2009. Focal adhesion kinase modulates cell adhesion strengthening via integrin activation. *Mol Biol Cell*, 20, 2508-19.
- MILLIANO, M. T. & LUXON, B. A. 2003. Initial signaling of the fibronectin receptor (α 5) β 1 integrin in hepatic stellate cells is independent of tyrosine phosphorylation. *Journal of Hepatology*, 39, 32-37.
- MIMURA, I., NANGAKU, M., NISHI, H., INAGI, R., TANAKA, T. & FUJITA, T. 2010. Cytochrome, a novel globin, plays an antifibrotic role in the kidney. *American Journal of Physiology-Renal Physiology*, 299, F1120-F1133.

- MINNING, D. M., GOW, A. J., BONAVENTURA, J., BRAUN, R., DEWHIRST, M., GOLDBERG, D. E. & STAMLER, J. S. 1999. Ascaris haemoglobin is a nitric oxide-activated 'deoxygenase'. *Nature*, 401, 497-502.
- MIRANTI, C. K. & BRUGGE, J. S. 2002. Sensing the environment: a historical perspective on integrin signal transduction. *Nature Cell Biology*, 4, E83-E90.
- MOTOYAMA, H., KOMIYA, T., THUY, L. T. T., TAMORI, A., ENOMOTO, M., MORIKAWA, H., IWAI, S., UCHIDA-KOBAYASHI, S., FUJII, H., HAGIHARA, A., KAWAMURA, E., MURAKAMI, Y., YOSHIZATO, K. & KAWADA, N. 2014. Cytoglobin is expressed in hepatic stellate cells, but not in myofibroblasts, in normal and fibrotic human liver. *Lab Invest*, 94, 192-207.
- MURPHY, F. R., ISSA, R., ZHOU, X., RATNARAJAH, S., NAGASE, H., ARTHUR, M. J., BENYON, C. & IREDALE, J. P. 2002. Inhibition of apoptosis of activated hepatic stellate cells by tissue inhibitor of metalloproteinase-1 is mediated via effects on matrix metalloproteinase inhibition: implications for reversibility of liver fibrosis. *J Biol Chem*, 277, 11069-76.
- MURZIN, A. G., BRENNER, S. E., HUBBARD, T. & CHOTHIA, C. 1995. SCOP - A STRUCTURAL CLASSIFICATION OF PROTEINS DATABASE FOR THE INVESTIGATION OF SEQUENCES AND STRUCTURES. *Journal of Molecular Biology*, 247, 536-540.
- MYLLYHARJU, J. & KIVIRIKKO, K. I. 1999. Identification of a novel proline-rich peptide-binding domain in prolyl 4-hydroxylase. *Embo j*, 18, 306-12.
- NAGABABU, E. & RIFKIND, J. M. 2004. Heme degradation by reactive oxygen species. *Antioxid Redox Signal*, 6, 967-78.
- NAKATANI, K., OKUYAMA, H., SHIMAHARA, Y., SAEKI, S., KIM, D. H., NAKAJIMA, Y., SEKI, S., KAWADA, N. & YOSHIZATO, K. 2004. Cytoglobin/STAP, its unique localization in splanchnic fibroblast-like cells and function in organ fibrogenesis. *Laboratory Investigation*, 84, 91-101.
- NARMADA, B. C., KANG, Y., VENKATRAMAN, L., PENG, Q., SAKBAN, R. B., NUGRAHA, B., JIANG, X., BUNTE, R. M., SO, P. T., TUCKER-KELLOGG, L., MAO, H. Q. & YU, H. 2013. Hepatic stellate cell-targeted delivery of hepatocyte growth factor transgene via bile duct infusion enhances its expression at fibrotic foci to regress dimethylnitrosamine-induced liver fibrosis. *Hum Gene Ther*, 24, 508-19.
- NEUWALD, A. F., LIU, J. S., LIPMAN, D. J. & LAWRENCE, C. E. 1997. Extracting protein alignment models from the sequence database. *Nucleic Acids Research*, 25, 1665-1677.
- NIETO, N., FRIEDMAN, S. L. & CEDERBAUM, A. 2002. Stimulation and proliferation of primary rat hepatic stellate cells by cytochrome P450 2E1-derived reactive oxygen species. *Hepatology*, 35, 62-73.
- NIMNUAL, A. S., TAYLOR, L. J. & BAR-SAGI, D. 2003. Redox-dependent downregulation of Rho by Rac. *Nat Cell Biol*, 5, 236-41.
- OHATA, M., LIN, M., SATRE, M. & TSUKAMOTO, H. 1997. Diminished retinoic acid signaling in hepatic stellate cells in cholestatic liver fibrosis. *American Journal of Physiology-Gastrointestinal and Liver Physiology*, 272, G589-G596.
- OKANOUE, T., BURBIGE, E. J. & FRENCH, S. W. 1983. THE ROLE OF THE ITO CELL IN PERIVENULAR AND INTRALOBULAR FIBROSIS IN ALCOHOLIC HEPATITIS. *Archives of Pathology & Laboratory Medicine*, 107, 459-463.
- OLASO, E., IKEDA, K., ENG, F. J., XU, L. M., WANG, L. H., LIN, H. C. & FRIEDMAN, S. L. 2001. DDR2 receptor promotes MMP-2-mediated proliferation and invasion by hepatic stellate cells. *Journal of Clinical Investigation*, 108, 1369-1378.
- OLEKSIEWICZ, U., LILOGLOU, T., TASOPOULOU, K. M., DASKOULIDOU, N., BRYAN, J., GOSNEY, J. R., FIELD, J. K. & XINARIANOS, G. 2013. Cytoglobin has bimodal: tumour suppressor and oncogene functions in lung cancer cell lines. *Hum Mol Genet*, 22, 3207-17.
- OLIVO, C., VANNI, C., MANCINI, P., SILENGO, L., TORRISI, M. R., TARONE, G., DEFILIPPI, P. & EVA, A. 2000. Distinct involvement of cdc42 and RhoA GTPases in actin organization and cell shape in untransformed and Dbl oncogene transformed NIH3T3 cells. *Oncogene*, 19, 1428-36.

- OLSEN, A. L., SACKEY, B. K., MARCINKIEWICZ, C., BOETTIGER, D. & WELLS, R. G. 2012. Fibronectin extra domain-A promotes hepatic stellate cell motility but not differentiation into myofibroblasts. *Gastroenterology*, 142, 928-937.e3.
- OSTOJIC, J., GROZDANIC, S., SYED, N. A., HARGROVE, M. S., TRENT, J. T., 3RD, KUEHN, M. H., KARDON, R. H., KWON, Y. H. & SAKAGUCHI, D. S. 2008. Neuroglobin and cytoglobin distribution in the anterior eye segment: a comparative immunohistochemical study. *J Histochem Cytochem*, 56, 863-72.
- PARES, A., CABALLERIA, J., BRUGUERA, M., TORRES, M. & RODES, J. 1986. Histological course of alcoholic hepatitis. Influence of abstinence, sex and extent of hepatic damage. *J Hepatol*, 2, 33-42.
- PATSENKER, E. & STICKEL, F. 2011. Role of integrins in fibrosing liver diseases. *American Journal of Physiology-Gastrointestinal and Liver Physiology*, 301, G425-G434.
- PELLICORO, A., RAMACHANDRAN, P. & IREDALE, J. P. 2012. Reversibility of liver fibrosis. *Fibrogenesis Tissue Repair*, 5, S26.
- PESCE, A., BOLOGNESI, M., BOCEDI, A., ASCENZI, P., DEWILDE, S., MOENS, L., HANKELN, T. & BURMESTER, T. 2002. Neuroglobin and cytoglobin - Fresh blood for the vertebrate globin family. *Embo Reports*, 3, 1146-1151.
- PETTA, S., MURATORE, C. & CRAXI, A. 2009. Non-alcoholic fatty liver disease pathogenesis: The present and the future. *Digestive and Liver Disease*, 41, 615-625.
- PFAFFL, M. W. 2001. A new mathematical model for relative quantification in real-time RT-PCR. *Nucleic Acids Res*, 29, e45.
- PIHLAJANIEMI, T., MYLLYLA, R. & KIVIRIKKO, K. I. 1991. Prolyl 4-hydroxylase and its role in collagen synthesis. *J Hepatol*, 13 Suppl 3, S2-7.
- PINZANI, M. 2002. PDGF and signal transduction in hepatic stellate cells. *Frontiers in Bioscience*, 7, D1720-D1726.
- POWELL, E. E., COOKSLEY, W. G. E., HANSON, R., SEARLE, J., HALLIDAY, J. W. & POWELL, L. W. 1990. THE NATURAL-HISTORY OF NONALCOHOLIC STEATOHEPATITIS - A FOLLOW-UP-STUDY OF 42 PATIENTS FOR UP TO 21 YEARS. *Hepatology*, 11, 74-80.
- POYNARD, T., MATHURIN, P., LAI, C. L., GUYADER, D., POUPON, R., TAINTURIER, M. H., MYERS, R. P., MUNTENAU, M., RATZIU, V., MANNS, M., VOGEL, A., CAPRON, F., CHEDID, A., BEDOSSA, P. & PANFIBROSIS, G. 2003. A comparison of fibrosis progression in chronic liver diseases. *Journal of Hepatology*, 38, 257-265.
- POYNARD, T., MCHUTCHISON, J., MANNS, M., TREPO, C., LINDSAY, K., GOODMAN, Z., LING, M. H. & ALBRECHT, J. 2002. Impact of pegylated interferon alfa-2b and ribavirin on liver fibrosis in patients with chronic hepatitis C. *Gastroenterology*, 122, 1303-13.
- PRIYA, S. & SUDHAKARAN, P. R. 2008. Cell survival, activation and apoptosis of hepatic stellate cells: modulation by extracellular matrix proteins. *Hepatology Research*, 38, 1221-1232.
- QIN, J., VINOGRADOVA, O. & PLOW, E. F. 2004. Integrin bidirectional signaling: a molecular view. *Plos Biology*, 2, 726-729.
- RAGHURAM, S., STAYROOK, K. R., HUANG, P., ROGERS, P. M., NOSIE, A. K., MCCLURE, D. B., BURRIS, L. L., KHORASANIZADEH, S., BURRIS, T. P. & RASTINEJAD, F. 2007. Identification of heme as the ligand for the orphan nuclear receptors REV-ERBalpha and REV-ERBbeta. *Nat Struct Mol Biol*, 14, 1207-13.
- RAMACHANDRAN, P. & IREDALE, J. P. 2012. Liver fibrosis: a bidirectional model of fibrogenesis and resolution. *QJM*.
- REEDER, B. J. 2010. The redox activity of hemoglobins: from physiologic functions to pathologic mechanisms. *Antioxid Redox Signal*, 13, 1087-123.
- REEDER, B. J., SVISTUNENKO, D. A. & WILSON, M. T. 2011. Lipid binding to cytoglobin leads to a change in haem co-ordination: a role for cytoglobin in lipid signalling of oxidative stress. *Biochemical Journal*, 434, 483-492.

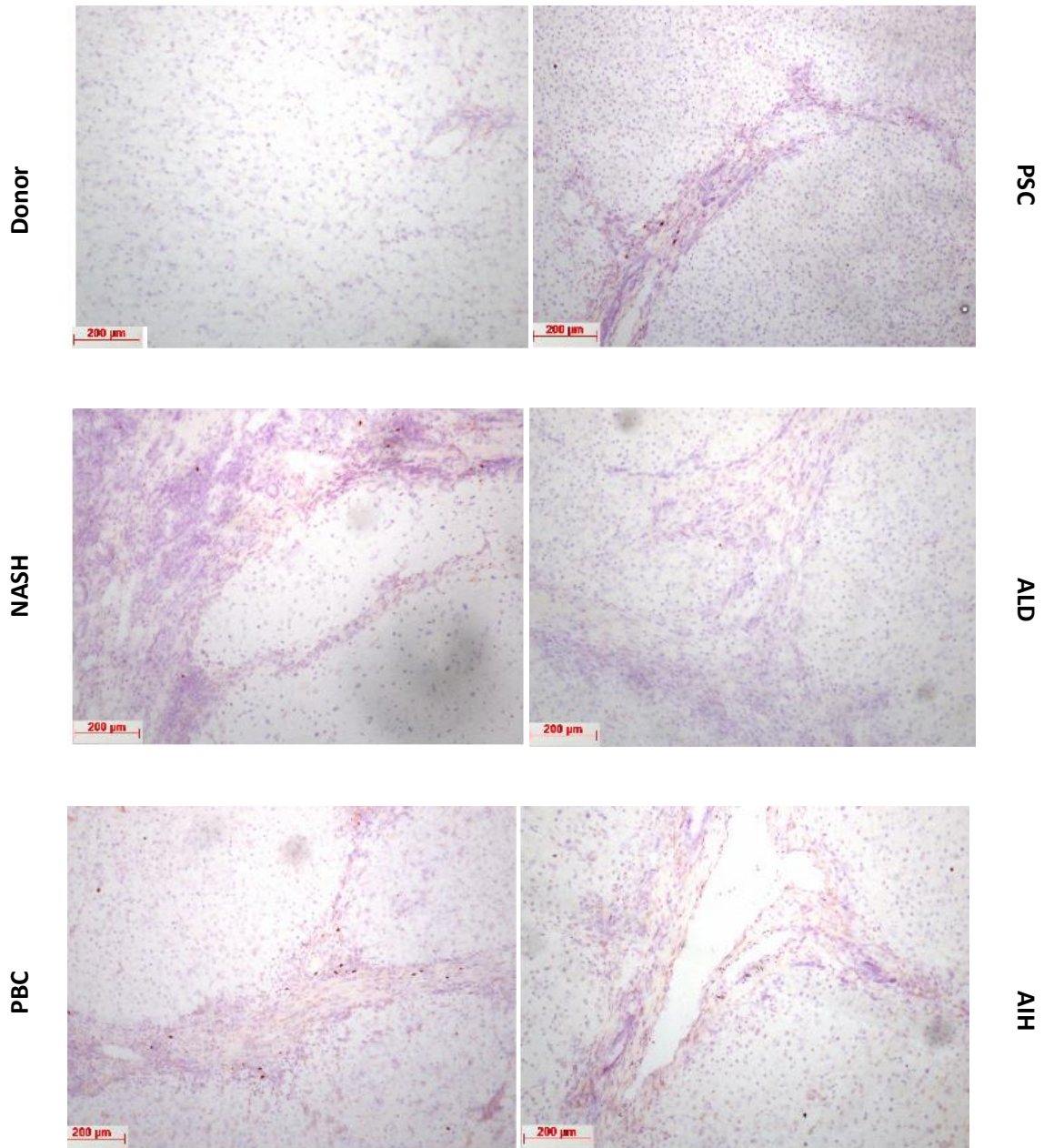
- REEVES, H. L. & FRIEDMAN, S. L. 2002. Activation of hepatic stellate cells - A key issue in liver fibrosis. *Frontiers in Bioscience-Landmark*, 7, D808-D826.
- REINHARDT, A. & HUBBARD, T. 1998. Using neural networks for prediction of the subcellular location of proteins. *Nucleic Acids Research*, 26, 2230-2236.
- REYNAERT, H., THOMPSON, M. G., THOMAS, T. & GEERTS, A. 2002. Hepatic stellate cells: role in microcirculation and pathophysiology of portal hypertension. *Gut*, 50, 571-581.
- RIDLEY, A. J. & HALL, A. 1992. The small GTP-binding protein rho regulates the assembly of focal adhesions and actin stress fibers in response to growth factors. *Cell*, 70, 389-99.
- RISK, J. M., MILLS, H. S., GARDE, J., DUNN, J. R., EVANS, K. E., HOLLSTEIN, M. & FIELD, J. K. 1999. The tylosis esophageal cancer (TOC) locus: more than just a familial cancer gene. *Dis Esophagus*, 12, 173-6.
- RODRIGUEZ-JUAN, C., DE LA TORRE, P., GARCIA-RUIZ, I., DIAZ-SANJUAN, T., MUNOZ-YAGUE, T., GOMEZ-IZQUIERDO, E., SOLIS-MUNOZ, P. & SOLIS-HERRUZO, J. A. 2009. Fibronectin increases survival of rat hepatic stellate cells--a novel profibrogenic mechanism of fibronectin. *Cell Physiol Biochem*, 24, 271-82.
- ROJKIND, M., DOMINGUEZ-ROSALES, J. A., NIETO, N. & GREENWEL, P. 2002. Role of hydrogen peroxide and oxidative stress in healing responses. *Cellular and Molecular Life Sciences*, 59, 1872-1891.
- SATO, T., KATO, R. & TYSON, C. A. 1995. REGULATION OF DIFFERENTIATED PHENOTYPE OF RAT HEPATIC LIPOCYTES BY RETINOIDS IN PRIMARY CULTURE. *Experimental Cell Research*, 217, 72-83.
- SCHMIDT, M., GERLACH, F., AVIVI, A., LAUFS, T., WYSTUB, S., SIMPSON, J. C., NEVO, E., SAALER-REINHARDT, S., REUSS, S., HANKELN, T. & BURMESTER, T. 2004. Cytoglobin is a respiratory protein in connective tissue and neurons, which is up-regulated by hypoxia. *Journal of Biological Chemistry*, 279, 8063-8069.
- SCOTT, N. L. & LECOMTE, J. T. J. 2000. Cloning, expression, purification, and preliminary characterization of a putative hemoglobin from the cyanobacterium *Synechocystis* sp PCC 6803. *Protein Science*, 9, 587-597.
- SENOO, H. 2004. Structure and function of hepatic stellate cells. *Medical Electron Microscopy*, 37, 3-15.
- SHAW, R. J., HALL, G. L., WOOLGAR, J. A., LOWE, D., ROGERS, S. N., FIELD, J. K., LILOGLOU, T. & RISK, J. M. 2007. Quantitative methylation analysis of resection margins and lymph nodes in oral squamous cell carcinoma. *British Journal of Oral & Maxillofacial Surgery*, 45, 617-622.
- SHAW, R. J., HOBKIRK, A. J., NIKOLAIDIS, G., WOOLGAR, J. A., TRIANTAFYLLOU, A., BROWN, J. S., LILOGLOU, T. & RISK, J. M. 2013. Molecular staging of surgical margins in oral squamous cell carcinoma using promoter methylation of p16(INK4A), cytoglobin, E-cadherin, and TMEFF2. *Ann Surg Oncol*, 20, 2796-802.
- SHAW, R. J., OMAR, M. M., ROKADIYA, S., KOGERA, F. A., LOWE, D., HALL, G. L., WOOLGAR, J. A., HOMER, J., LILOGLOU, T., FIELD, J. K. & RISK, J. M. 2009. Cytoglobin is upregulated by tumour hypoxia and silenced by promoter hypermethylation in head and neck cancer. *Br J Cancer*, 101, 139-44.
- SHE, H. Y., XIONG, S. G., HAZRA, S. & TSUKAMOTO, H. 2005. Adipogenic transcriptional regulation of hepatic stellate cells. *Journal of Biological Chemistry*, 280, 4959-4967.
- SHEN JG, ZHANG XL, HUO XX & J., W. 2006. BASIC BIOLOGY. *Journal of Gastroenterology and Hepatology*, 21, A367-A380.
- SHIGEMATSU, A., ADACHI, Y., MATSUBARA, J., MUKAIDE, H., KOIKE-KIRIYAMA, N., MINAMINO, K., SHI, M., YANAI, S., IMAMURA, M., TAKETANI, S. & IKEHARA, S. 2008. Analyses of expression of cytoglobin by immunohistochemical studies in human tissues. *Hemoglobin*, 32, 287-96.
- SHIVAPURKAR, N., STASTNY, V., OKUMURA, N., GIRARD, L., XIE, Y., PRINSEN, C., THUNNISSEN, F. B., WISTUBA, II, CZERNIAK, B., FRENKEL, E., ROTH, J. A., LILOGLOU, T., XINARIANOS, G., FIELD, J.

- K., MINNA, J. D. & GAZDAR, A. F. 2008. Cytooglobin, the newest member of the globin family, functions as a tumor suppressor gene. *Cancer Res*, 68, 7448-56.
- SINGH, S., CANSECO, D., GRINSFELDER, D., BOCK-MARQUETTE, I., COLLINS, S. C., RUIZ-LOZANO, P., ROTHERMEL, B. A. & MAMMEN, P. P. 2013. Cytooglobin: A Novel Epicardial Regulator of Epithelial to Mesenchymal Transition (EMT) Within the Ischemic Heart. *Circulation*, 128.
- SINGH, S., CANSECO, D. C., MANDA, S. M., SHELTON, J. M., CHIRUMAMILLA, R. R., GOETSCH, S. C., YE, Q., GERARD, R. D., SCHNEIDER, J. W., RICHARDSON, J. A., ROTHERMEL, B. A. & MAMMEN, P. P. 2014. Cytooglobin modulates myogenic progenitor cell viability and muscle regeneration. *Proc Natl Acad Sci U S A*, 111, E129-38.
- SINGH, S., MANDA, S. M., SIKDER, D., BIRRER, M. J., ROTHERMEL, B. A., GARRY, D. J. & MAMMEN, P. P. A. 2009. Calcineurin Activates Cytooglobin Transcription in Hypoxic Myocytes. *Journal of Biological Chemistry*, 284, 10409-10421.
- SMAGGHE, B. J., HALDER, P. & HARGROVE, M. S. 2008. Measurement of distal histidine coordination equilibrium and kinetics in hexacoordinate hemoglobins. In: POOLE, R. K. (ed.) *Globins and Other Nitric Oxide-Reactive Proteins, Pt A*.
- SONG, S., SHACKEL, N. A., WANG, X. M., AJAMI, K., MCCAUGHAN, G. W. & GORRELL, M. D. 2011. Discoidin domain receptor 1: isoform expression and potential functions in cirrhotic human liver. *Am J Pathol*, 178, 1134-44.
- STICKEL, F. & SEITZ, H. K. 2010. Alcoholic steatohepatitis. *Best Practice & Research Clinical Gastroenterology*, 24, 683-693.
- STREULI, C. H. 2009. Integrins and cell-fate determination. *Journal of Cell Science*, 122, 171-177.
- STUPACK, D. G. 2007. The biology of integrins. *Oncology (Williston Park)*, 21, 6-12.
- TAKAHASHI, Y., TAKAHASHI, S., SHIGA, Y., YOSHIMI, T. & MIURA, T. 2000. Hypoxic induction of prolyl 4-hydroxylase alpha (I) in cultured cells. *J Biol Chem*, 275, 14139-46.
- TERGAONKAR, V. 2006. NFkappaB pathway: a good signaling paradigm and therapeutic target. *Int J Biochem Cell Biol*, 38, 1647-53.
- THUY LE, T. T., MORITA, T., YOSHIDA, K., WAKASA, K., IIZUKA, M., OGAWA, T., MORI, M., SEKIYA, Y., MOMEN, S., MOTOYAMA, H., IKEDA, K., YOSHIZATO, K. & KAWADA, N. 2011. Promotion of liver and lung tumorigenesis in DEN-treated cytooglobin-deficient mice. *Am J Pathol*, 179, 1050-60.
- TIAN, S. F., YANG, H. H., XIAO, D. P., HUANG, Y. J., HE, G. Y., MA, H. R., XIA, F. & SHI, X. C. 2013. Mechanisms of neuroprotection from hypoxia-ischemia (HI) brain injury by up-regulation of cytooglobin (CYGB) in a neonatal rat model. *J Biol Chem*, 288, 15988-6003.
- TRENT, J. T. & HARGROVE, M. S. 2002. A ubiquitously expressed human hexacoordinate hemoglobin. *Journal of Biological Chemistry*, 277, 19538-19545.
- TRENT, J. T., WATTS, R. A. & HARGROVE, M. S. 2001. Human neuroglobin, a hexacoordinate hemoglobin that reversibly binds oxygen. *Journal of Biological Chemistry*, 276, 30106-30110.
- TROEN, G., NILSSON, A., NORUM, K. R. & BLOMHOFF, R. 1994. CHARACTERIZATION OF LIVER STELLATE CELL RETINYL ESTER STORAGE. *Biochemical Journal*, 300, 793-798.
- TSUJINO, H., YAMASHITA, T., NOSE, A., KUKINO, K., SAWAI, H., SHIRO, Y. & UNO, T. 2014. Disulfide bonds regulate binding of exogenous ligand to human cytooglobin. *J Inorg Biochem*, 135, 20-7.
- VOGEL, S., PIANTEDOSI, R., FRANK, J., LALAZAR, A., ROCKEY, D. C., FRIEDMAN, S. L. & BLANER, W. S. 2000. An immortalized rat liver stellate cell line (HSC-T6): a new cell model for the study of retinoid metabolism in vitro. *Journal of Lipid Research*, 41, 882-893.
- VOGEL, W. F., ABDULHUSSEIN, R. & FORD, C. E. 2006. Sensing extracellular matrix: An update on discoidin domain receptor function. *Cellular Signalling*, 18, 1108-1116.
- WAKE, K. 1971. STERNZELLEN IN LIVER - PERISINUSOIDAL CELLS WITH SPECIAL REFERENCE TO STORAGE OF VITAMIN-A. *American Journal of Anatomy*, 132, 429-&.
- WALLACE, K., BURT, A. D. & WRIGHT, M. C. 2008. Liver fibrosis. *Biochemical Journal*, 411, 1-18.

- WANG, G. P. & XU, C. S. 2010. Reference gene selection for real-time RT-PCR in eight kinds of rat regenerating hepatic cells. *Mol Biotechnol*, 46, 49-57.
- WEINER, F. R., BLANER, W. S., CZAJA, M. J., SHAH, A. & GEERTS, A. 1992. ITO CELL EXPRESSION OF A NUCLEAR RETINOIC ACID RECEPTOR. *Hepatology*, 15, 336-342.
- WESTON, C. J., SHEPHERD, E. L., CLARIDGE, L. C., RANTAKARI, P., CURBISHLEY, S. M., TOMLINSON, J. W., HUBSCHER, S. G., REYNOLDS, G. M., AALTO, K., ANSTEE, Q. M., JALKANEN, S., SALMI, M., SMITH, D. J., DAY, C. P. & ADAMS, D. H. 2014. Vascular adhesion protein-1 promotes liver inflammation and drives hepatic fibrosis. *J Clin Invest*.
- WIGHT, T. N. & POTTER-PERIGO, S. 2011. The extracellular matrix: an active or passive player in fibrosis? *American Journal of Physiology-Gastrointestinal and Liver Physiology*, 301, G950-G955.
- WOJNAROWICZ, P. M., PROVENCHER, D. M., MES-MASSON, A. M. & TONIN, P. N. 2012. Chromosome 17q25 genes, RHBDF2 and CYGB, in ovarian cancer. *Int J Oncol*, 40, 1865-80.
- WYSTUB, S., EBNER, B., FUCHS, C., WEICH, B., BURMESTER, T. & HANKELN, T. 2004. Interspecies comparison of neuroglobin, cytoglobin and myoglobin: sequence evolution and candidate regulatory elements. *Cytogenet Genome Res*, 105, 65-78.
- XINARIANOS, G., MCRONALD, F. E., RISK, J. M., BOWERS, N. L., NIKOLAIDIS, G., FIELD, J. K. & LILOGLOU, T. 2006. Frequent genetic and epigenetic abnormalities contribute to the deregulation of cytoglobin in non-small cell lung cancer. *Hum Mol Genet*, 15, 2038-44.
- XU, L., HUI, A. Y., ALBANIS, E., ARTHUR, M. J., O'BYRNE, S. M., BLANER, W. S., MUKHERJEE, P., FRIEDMAN, S. L. & ENG, F. J. 2005. Human hepatic stellate cell lines, LX-1 and LX-2: new tools for analysis of hepatic fibrosis. *Gut*, 54, 142-151.
- XU, R., HARRISON, P. M., CHEN, M., LI, L., TSUI, T. Y., FUNG, P. C., CHEUNG, P. T., WANG, G., LI, H., DIAO, Y., KRISANSEN, G. W., XU, S. & FARZANEH, F. 2006. Cytoglobin overexpression protects against damage-induced fibrosis. *Mol Ther*, 13, 1093-100.
- YANG, C. Q., YANG, L., YANG, W. Z., ZHANG, Z., ZHANG, H., CHANG, Y. Z., YUAN, M. & CHEN, X. M. 2008. [Mechanism of hepatic stellate cell migration during liver fibrosis]. *Zhonghua Yi Xue Za Zhi*, 88, 119-22.
- YANG, J. D., SEOL, S. Y., LEEM, S. H., KIM, Y. H., SUN, Z. F., LEE, J. S., THORGEIRSSON, S. S., CHU, I. S., ROBERTS, L. R. & KANG, K. J. 2011. Genes Associated with Recurrence of Hepatocellular Carcinoma: Integrated Analysis by Gene Expression and Methylation Profiling. *Journal of Korean Medical Science*, 26, 1428-1438.
- YEN, E. H., SODEK, J. & MELCHER, A. H. 1979. The effect of oxygen partial pressure on protein synthesis and collagen hydroxylation by mature periodontal tissues maintained in organ cultures. *Biochem J*, 178, 605-12.
- YOKOI, Y., NAMIHISA, T., KURODA, H., KOMATSU, I., MIYAZAKI, A., WATANABE, S. & USUI, K. 1984. IMMUNOCYTOCHEMICAL DETECTION OF DESMIN IN FAT-STORING CELLS (ITO-CELLS). *Hepatology*, 4, 709-714.
- ZHOU, X. Y., MURPHY, F. R., GEH DU, N., ZHANG, J. L., IREDALE, J. P. & BENYON, R. C. 2004. Engagement of alpha(v)beta(3) integrin regulates proliferation and apoptosis of hepatic stellate cells. *Journal of Biological Chemistry*, 279, 23996-24006.
- ZION, O., GENIN, O., KAWADA, N., YOSHIZATO, K., ROFFE, S., NAGLER, A., IOVANNA, J. L., HALEVY, O. & PINES, M. 2009. Inhibition of transforming growth factor beta signaling by halofuginone as a modality for pancreas fibrosis prevention. *Pancreas*, 38, 427-35.
- ZVIBEL, I., ATIAS, D., PHILLIPS, A., HALPERN, Z. & OREN, R. 2010. Thyroid hormones induce activation of rat hepatic stellate cells through increased expression of p75 neurotrophin receptor and direct activation of Rho. *Lab Invest*, 90, 674-84.

Appendices

Appendix 1: Immunomatched controls for CYGB IHC

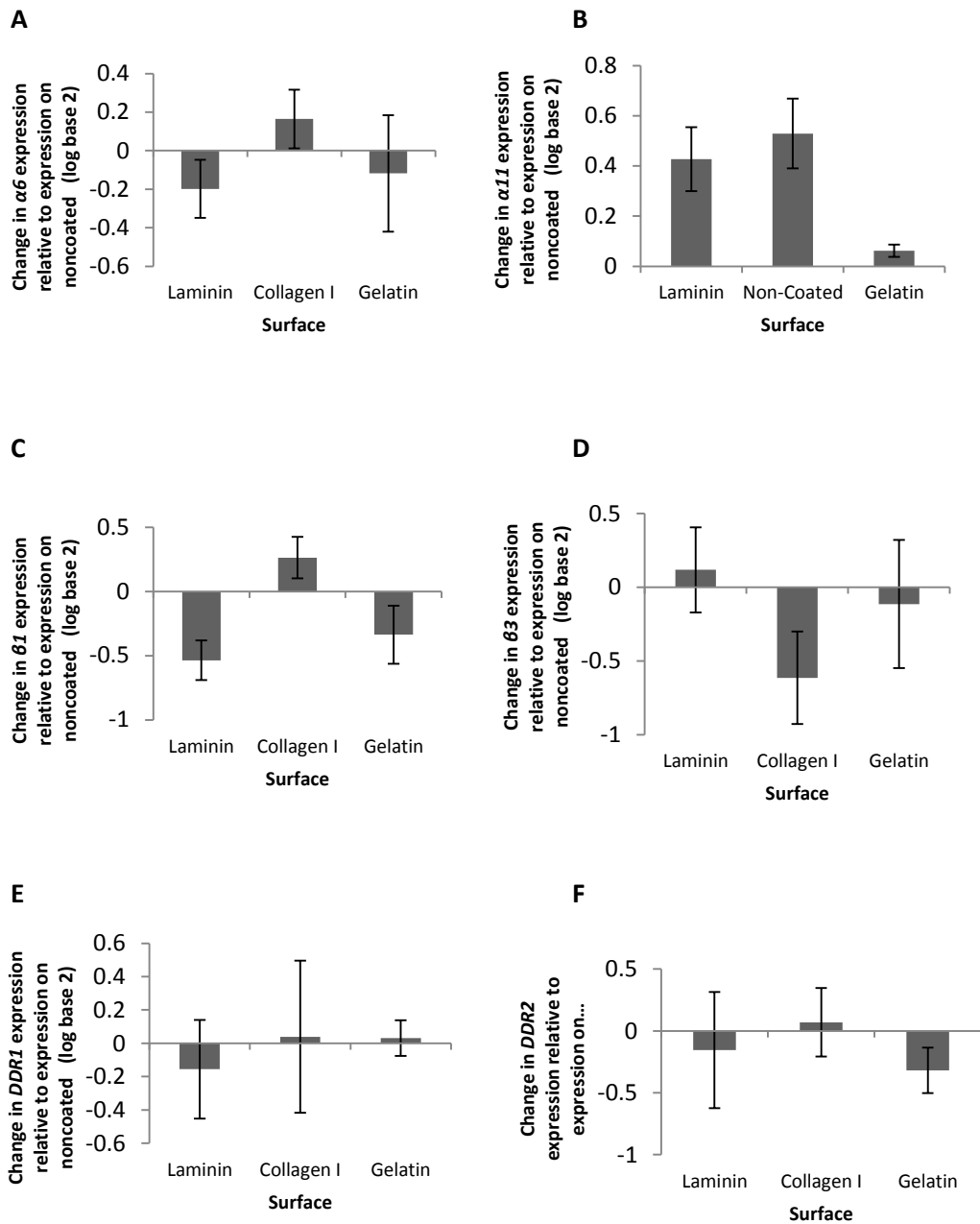


Appendix 1: Immunomatched controls for section staining for CYGB expression Abbreviations: NASH = non-alcoholic fatty liver disease, PBC = primary biliary cirrhosis, PSC = pulmonary sclerosing cholangitis, ALD = alcoholic liver disease, AIH = autoimmune hepatitis. N=1

Appendix 2: HSC-T6s grown on non-coated plastic, collagen I and laminin (see attached CD)

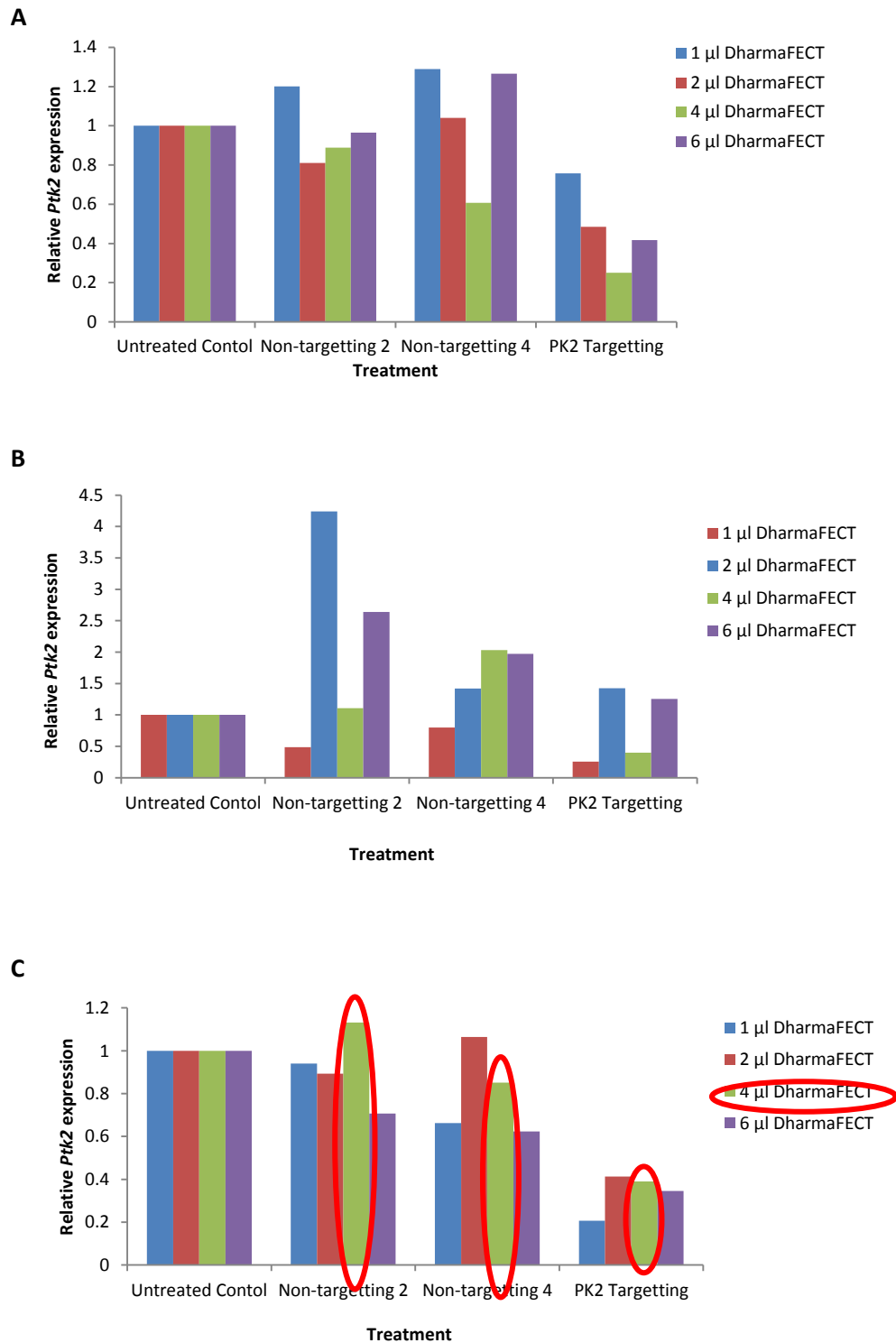
Appendix 3: LX-2s grown on non-coated plastic, collagen I and laminin (see attached CD)

Appendix 4: Results of non-significant ($p > 0.05$) ECM receptor expression by RT-PCR



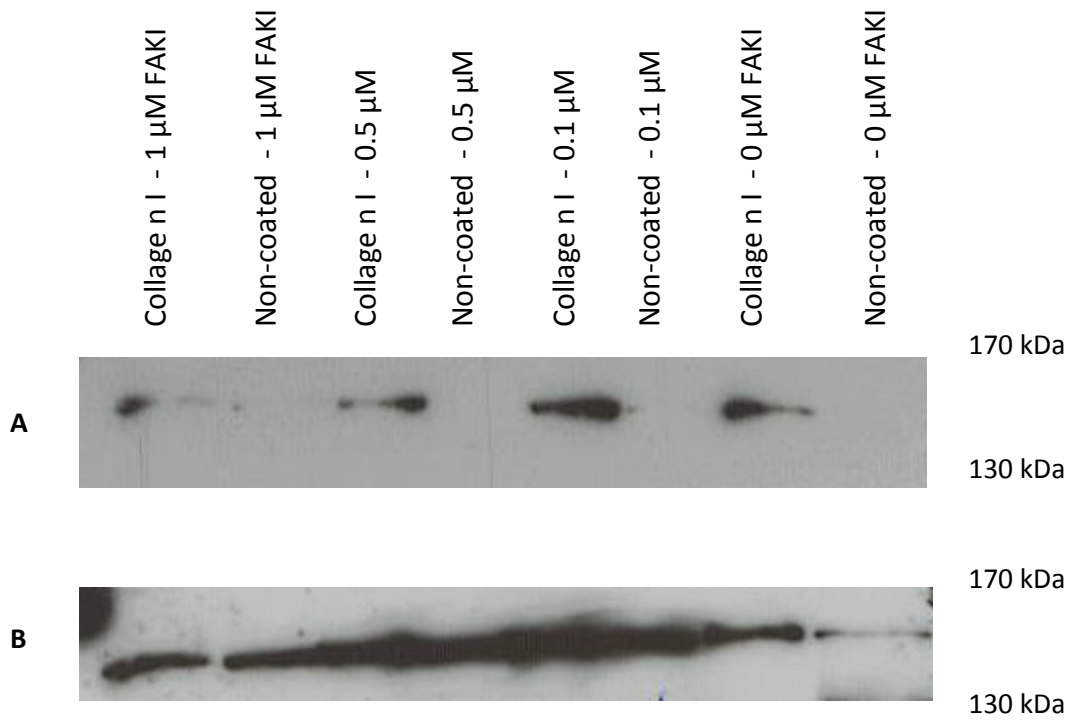
Appendix 4 : Expression of A) $\alpha 6$, B) $\alpha 11$, C) $\beta 1$, D) $\beta 3$, E) *DDR1* and F) *DDR2* integrin subunit ECM receptors across laminin, collagen I and gelatin ECM proteins in HSC-T6 cells relative to the expression levels of those grown on non-coated T₂₅ culture flasks. N=3

Appendix 5: Results of RNAi optimisation



Appendix 5: RNAi treatment of *Ptk2* (*FAK*) in HSC-T6 cells seeded at A) 50,000 cells/ml, B) 100,000 cells/ml and C) 200,000 cells/ml cultured for 48hrs on non-coated plastic with 24hrs RNAi then analysed for PKT2 expression by RT-PCR. N=1

Appendix 6: Western blot of FAK pY397 protein expression in HSC-T6s after 48hrs of treatment with FAKI



Appendix 6: Western blot for protein expression of phosphorylated FAK Y397 in cells cultured for 48hrs non-coated tissue culture plastic and collagen I and treated with FAKI for A) 24hrs and B) 48hrs.